DEVELOPMENT OF A NOVEL 3-FLUID NOZZLE FOR SPRAY-DRIED MICROENCAPSULATION OF QUERETIN IN ZEIN AND SODIUM CASEINATE

BY

SEAN R. KILKER

THESIS

Submitted in partial fulfillment of the requirements
for the degree of Master of Science in Food Science and Human Nutrition
with a concentration in Food Science
in the Graduate College of the
University of Illinois at Urbana-Champaign, 2020

Urbana, Illinois

Master's Committee:

Associate Professor Youngsoo Lee, Advisor
Professor Elvira de Mejia
Research Professor Graciela Wild Padua
Assistant Professor Yi-Cheng Wang

ABSTRACT

Microencapsulation is a powerful technology for stabilizing compounds of interest to the food industry that are difficult to incorporate into food matrices for a variety of reasons. Microfluidic assembly of microcapsules has recently been studied as a means for producing extremely uniform and small particles, which is beneficial for controlled release applications; however, it is difficult to scale this technology to meet the demands of the food industry. Spray-drying represents a much higher throughput option for microencapsulation, but requires additional processing steps to generate microcapsule suspensions and often suffers from large particle sizes with wide distributions.

This study proposes a novel 3-fluid nozzle technology that combines the fluid dynamic principles and single processing step found in microfluidic systems with the high throughput of spray-drying. Zein, the prolamin storage protein from corn, and quercetin, a polyphenolic flavonol compound with numerous health benefits, were chosen as a model system for this study. Zein nanoparticles ranging from 170 – 205 nm in size were successfully generated using a benchtop simulation of the proposed technology, with both total flow rate and initial zein concentration having a significant effect ($p < 0.05$) on resultant particle size and polydispersity index (PDI). Quercetin was successfully encapsulated in a zein/sodium caseinate system using spray drying with the novel 3-fluid nozzle. Contact time between the two phases for encapsulation was varied but found to have no significant effect on particle size, encapsulation efficiency, or antioxidant capacity; however, the spray-dried powders showed smaller particle sizes and narrow particle size distributions than what is typically seen in spray-drying

operations. Encapsulation efficiency of quercetin ranged from 70% to 80%, and samples exhibited around 80% of the antioxidant capacity of an unencapsulated quercetin control sample. The proposed nozzle technology could be useful for numerous encapsulation applications that require the narrower particle size distribution and high throughput for the food industry.

ACKNOWLEDGEMENTS

When I came to FSHN two years ago, I was nervous about being able to keep up with the pace of graduate school. Thanks to the support of countless individuals inside and out of the department, I am proud to present this work as the culmination of my time at the University of Illinois. I truly believe the FSHN department is one of the most welcoming and kindest groups of people I have ever had the privilege to work with.

I would like to thank my adviser, Dr. Youngsoo Lee, for agreeing to take me on as a student and for the countless hours he has spent helping me develop and refine my research. You truly care about each person in your lab group and have cultivated one of the best atmospheres for research and collaboration that I have ever seen. I would like to thank my advisory committee, Dr. de Mejia, Dr. Padua, and Dr. Wang, for their guidance throughout my research process and for the use of equipment in their respective labs. I would also like to thank Dr. Soo Lee and Dr. Schmidt for their help during lab meetings, SafeTraces for funding my research, and the Lee-Schmidt lab group for their kindness, friendship and support. I have never worked with a more talented and humbler group of individuals.

Finally, I would like to thank my partner, my family, and my friends for keeping me sane throughout the entire process of grad school. This work truly represents a collaborative effort between many individuals, and to anyone who assisted throughout my time as a graduate student, I cannot express my gratitude enough.

Table of Contents

CHAPTER 1: INTRODUCTION

1.1 Motivation

Microencapsulation is a promising technology for food formulation applications as it provides a means for relevant compounds to be incorporated into various food matrices while enhancing the stability, function, and/or sensory characteristics of the encapsulated material. Microfluidic processing is a newer technology that has very recently been used to generate uniform, nano-scale encapsulated materials [1]. While this strategy for encapsulation can create particles in a distribution that is more conducive to controlled-rate release kinetics, it is difficult to scale microfluidic production to the scale that would be needed by most food manufacturers.

A more conventional means of microencapsulation is spray-drying, a well-understood and scalable technology prevalent in industry for producing powdered products; however, as it relates to microencapsulation, spray-drying often requires an extra homogenization step to create the encapsulated system, and this step often results in large, widely-dispersed powder particles, which are inefficient and highly variable with regards to release kinetics.

A relatively unstudied technology within spray-drying setups, 3-fluid nozzles, have the potential to allow for encapsulated systems to be generated *in situ* while simultaneously capitalizing on the same laminar flow regime that governs microfluidic assembly of these particles. The **long-term goal** of this project is to develop and optimize a continuous microencapsulation process using a novel three-fluid nozzle within a spray dryer that allows for the tuning of particle size and particle size distribution by altering key process parameters. The **central hypothesis** is that by varying the total flow-rate and total contact time between the two phases used for

encapsulation will produce encapsulated particles with customizable particle size and narrow particle distributions) at significantly higher throughputs than are allowed in a microfluidic system.

Zein, the prolamin storage protein found in corn, will be used as the wall material in the model encapsulation system used in the study. Zein contains a high percentage of hydrophobic residues that give it both unique solubility characteristics in ethanol/water systems, as well as the capability to quickly self-assemble when precipitated. It has been widely studied in encapsulation systems with a wide variety of viable core materials with a range of applications [2] [3].

Quercetin, a polyphenol belonging to the flavonol subclass of flavonoid phytonutrient compounds, will be used as the core material in the model encapsulation system. Broadly, this class of compounds has been widely studied for their beneficial anti-oxidant and anti-inflammatory activity in humans [4] [5] . Quercetin has also been implicated as having an anti-oncogenic effect in the human colon; studies have shown regular ingestion of quercetin promotes apoptosis and cell-cycle arrest in nascent colon cancer tumors [6]. However, there are issues with quercetin as a food ingredient due to its low bioavailability as a result of minimal solubility in water, rapid degradation in the presence of both heat and light, and the bitter and astringent perception to food it imparts which further limits its application in food matrices [7] [8] [9].

1.2 Project Objectives

Objective 1

The first objective of this project was to evaluate the effect on particle size and polydispersity index (PDI) of the proposed three-fluid nozzle design by using a nozzle simulation chip with a modified inner-nozzle channel to generate zein particles suspensions The PDI of a powder sample is a direct measure of the range of particle sizes within that sample, with a higher PDI indicating there is a wider distribution. The *working hypothesis* for this objective is that modifying the inner-nozzle channel length of a three-fluid nozzle to mimic a microfluidic chip setup will allow for the assembly of zein particles with tunable particle size and a PDI of less than 0.2.

Objective 2

The second objective of this project is to encapsulate quercetin using spray drying with the novel three-fluid nozzle with varying contact times between continuous and dispersed phases, and to evaluate the effect of residence time and flow rate on the particle size, particle distribution, yield, encapsulation efficiency, and anti-oxidant activity of the encapsulated quercetin. The *working hypothesis* for this objective is that spray drying with longer contact time will allow for more complete zein self-assembly, which will mediate a narrower particle size distribution, higher quercetin loading, and higher antioxidant capacity than the particles produced with shorter residence time.

Scaling up the technology from the bench-top simulation trials is important to determine whether or not different fluid physics within the nozzle will affect the resultant powder size, or if it is limited to affecting only the aqueous particle suspensions. Ascertaining whether or not the quercetin is encapsulated and that its function has been

preserved is also critical for validating the technology for production of potential bioactive ingredients for food formulations.

1.3 Outline of Thesis

Chapter 2 is a literature review that provides further background on zein and its uses in other microencapsulated systems, quercetin and its health benefits, spray-drying and nozzle technology, microfluidic particle assembly, and potential surface-acting agents that could help mediate encapsulation.

Chapter 3 focuses on the design and testing of the nozzle-simulation chip used to generated initial zein particle suspensions and the implications this testing has on the proposed nozzle technology. A zein-in-ethanol dispersed phase, prepared from between 2-8% (w/w) zein, was fed into the chip with de-ionized water as the anti-solvent for precipitation and the resultant particles suspensions were studied for size and distribution. Total flow rates ranging from 2-8 mL/min were used with a constant 3:1 continuous to dispersed flow ratio.

Chapter 4 highlights the challenges related to scaling up from the nozzle simulation chip to the spray-dryer. Frequent clogging of the nozzle with zein agglomerate severely limited testing progress, and multiple solutions were tested considered. Different spray-drying parameters were tested, as well as several surface-acting agents and stock solution preparations. Sodium caseinate as a surfactant combined with acid-adjusted continuous and dispersed phases proved to be the most viable formulation for continuous spray-drying operations.

Chapter 5 reports on a set of directly scaled experiments from the nozzle simulation chip to the spray-dryer. Optimal throughput was considered when choosing

treatment groups; therefore, zein was prepared at 4% and 6% (w/w) and tested with total flow rates of 4 mL/min and 8 mL/min with contact times ranging from 5 – 20 seconds. Powder samples were analyzed for the effect of concentration and flow on size and distribution.

Chapter 6 reports the effect of different contact times and flow rates within the 3-fluid nozzle on encapsulated particles of quercetin within a zein/sodium caseinate matrix. Zein was prepared in 4% (w/w) stock solutions with constant 20:1 quercetin loading; sodium caseinate was loaded 1.25:1 with zein, with a 0.25:1 ratio within the dispersed phase and the remainder in the continuous phase. In addition to the physical properties of the powders, the powders were tested to verify that quercetin remained intact and capable of reducing free-radical concentrations.

Chapter 7 summarizes the research findings, overall implications for food manufacturers, and proposes the future supporting research.

1.4 References

[1] Y. Feng and Y. Lee, "Microfluidic fabrication of hollow protein microcapsules for rate-controlled release," *RSC Adv.,* vol. 7, no. 78, pp. 49455-49462, 24 10 2017.

[2] S. Quispe-Condori, D. A. Saldaña and F. Temelli, "Microencapsulation of flax oil with zein using spray and freeze drying," 2011.

[3] Q. Zhong, M. Jin, P. M. Davidson and S. Zivanovic, "Sustained release of lysozyme from zein microcapsules produced by a supercritical anti-solvent process," *Food Chemistry,* vol. 115, pp. 697-700.

[4] M. Lesjak, I. Beara, N. Simin, D. Pintać, T. Majkić, K. Bekvalac, D. Orčić and N. Mimica-Dukić, "Antioxidant and anti-inflammatory activities of quercetin and its derivatives," *Journal of Functional Foods,* vol. 40, pp. 68-75, 2018.

[5] M. Palma, P. Robert, F. Holgado, J. Velasco and G. Márquez-Ruiz, "Antioxidant Activity and Kinetics Studies of Quercetin, Epicatechin and Naringenin in Bulk Methyl Linoleate," *JAOCS, Journal of the American Oil Chemists' Society,* vol. 94, no. 9, pp. 1189-1196, 1 9 2017.

[6] S. G. Darband, M. Kaviani, B. Yousefi, S. Sadighparvar, F. G. Pakdel, J. A. Attari, I. Mohebbi, S. Naderi and M. Majidinia, *Quercetin: A functional dietary flavonoid with potential chemo-preventive properties in colorectal cancer,* vol. 233, Wiley-Liss Inc., 2018, pp. 6544-6560.

[7] Y. Guo and R. S. Bruno, "Endogenous and exogenous mediators of quercetin bioavailability," *Journal of Nutritional Biochemistry,* no. 26, pp. 201-210, 2015.

[8] A. Drewnowski and C. Gomez-Carneros, "Bitter taste, phytonutrients, and the consumer: a review," *The American Journal of Clinical Nutrition,* vol. 72, no. 6, pp. 1424-, 2000.

[9] S. Dall'acqua, G. Miolo, G. Innocenti and S. Caffieri, "The Photodegradation of Quercetin: Relation to Oxidation," *Molecules,* vol. 17, pp. 8898-8907, 2012.

CHAPTER 2: LITERATURE REVIEW

2.1 Introduction

There exists a broad spectrum of bioactive compounds of interest to food manufacturers; however, many of these compounds are not suitable for direct incorporation into food matrices due to various physical or chemical limitations. An emerging technology to bypass these limitations is microencapsulation, a process by which a compound of interest (the “core” material) is coated with or encased in a stable “shell” material to form a system of microcapsules that can adopt a number of different structures depending on the processing method used to create the system [1]. The resultant microcapsules can then be used in different food formulations to enhance the nutritional value or provide various intrinsic benefits to the end product, such as prolonged microbial resistance and oxidative stability.

Encapsulation of target nutritional compounds can be advantageous for food manufacturers looking to add value to existing food products or formulate new, more functional food systems. Bioactive compounds often do not offer a viable shelf-life length when incorporated in pure form, and many would impart negative sensory characteristics to the final food product. Microcapsules mitigate exposure to both oxidation and taste perception, as well as providing controlled release kinetics of the core material *in vivo*. Studies have also indicated that volatile flavors such as citrus may benefit from limited encapsulation in shelf-stable food systems. Numerous techniques exist to facilitate the assembly of encapsulated systems in either liquid emulsion or dry powder forms depending on the needs of the manufacturer.

2.2 Benefits of Encapsulation

A large body of research exists for numerous classes of compounds that benefit in some way from encapsulation within a stable shell matrix, either by enhancing shelf life, mitigating negative sensory properties, or offering increased bioavailability or controlled release. Table 2.1 provides a brief summary of encapsulation benefits and associated compounds.

2.2.1 Enhanced Shelf Life

Oxidative stress and photodegradation can limit the efficacy of volatile bioactive compounds in functional food systems. Polyunsaturated fatty acids in fish or flaxseed oil, as well as aromatic essential oils from plants and herbs have all been linked to beneficial health in humans, but suffer from increased susceptibility to oxidative attack due to their chemical structure. Studies have indicated numerous shell materials that mitigate the exposure of the oil compound to oxidation post-encapsulation [2, 3, 4, 5, 6]. Similarly, polyphenolic phytonutrient compounds such as anthocyanins, terpenes, and stilbenes are typically too volatile to incorporate as nutritional enhancing agents in food matrices as they are susceptible to both oxidation and photodegradation [7, 8, 9, 10, 11, 12]; much work has been done to stabilize these compounds so that their beneficial health effects can be realized in shelf-stable food systems.

2.2.2 Mitigation of Negative Sensory Properties

Many of the same polyphenolic compounds found in plants that are of interest to food manufacturers also have a characteristic bitter flavor that negatively impacts the sensory perception of the food product. Flavor-masking via encapsulation has been extensively studied as an application to increase consumer acceptance in novel functional food systems [13, 14, 15, 16, 17] .

Conversely, some desired flavor compounds are also associated with volatile compounds that are prone to oxidative degradation; this deterioration of the base flavor compound can either mute the perception of the flavor to the consumer and/or add an off flavor depending on the type and extent of oxidative stress. Encapsulating volatile flavor compounds such as citrus has been shown to positively increase the viable shelf life of products to which the flavor is incorporated before negative sensory effects are observed [18, 19, 20, 21].

2.2.3 Increased Bioavailability

Depending on the placement and extent of hydroxylation on the aromatic rings, many polyphenolic compounds exhibit limited solubility in water, negatively impacting the bioavailability of these compounds during human digestion. Coating these materials with amphiphilic compounds like proteins or modified starches can increase the partitioning of the core material into the water phase during digestion, increasing uptake and correspondingly bioavailability [22, 23, 24, 25, 26, 27]. Although many phytonutrient compounds can be consumed in their respective raw fruit and/or vegetable sources, encapsulation offers the unique opportunity to enhance the efficiency and therefore beneficial health impact of these compounds.

2.2.4 Controlled Release Kinetics

Of importance to the pharmaceutical industry for many years, the ability of a system with an active ingredient to dose the ingredient to humans post-consumption at a target location within the GI tract and/or with a slow time-release profile can be beneficial or even critical to apply the desired function of the active ingredient [28]. Pro- and prebiotic materials and some polyphenolic compounds specifically target

interactions within the human colon, but can be easily destroyed and/or absorbed during the digestive processes in both the stomach and small intestine.

Encapsulating these materials in a layer of shell material can facilitate survival of the core compound in its functional form through the harsh conditions of the stomach and enzymatic action of the small intestine [29, 30, 31, 32, 33]. By promoting an even distribution of particle sizes with a semi-porous microstructure, the core compound can be released slowly through diffusive processes as the shell-material limits the kinetics of release.

2.3 Encapsulation Technologies

There are a number of differing processes for assembling these encapsulated systems depending on the form of the desired product. Table 2.2 provides a concise summary of the different encapsulation methods as well as the tradeoffs associated with each method. Figures 2.1 gives examples of a microfluidics chip as well as two different channel arrangements that can be used.

2.3.1 Emulsion Method for Liquid Suspensions

Anti-solvent precipitation and emulsion encapsulation are commonly used to form suspensions of encapsulated particles for various core materials [34, 32, 35, 36]. Emulsions can either be created with the use of a high-shear mixer or a high-pressure homogenizer, as long as sufficient energy is imparted to the carrier fluid to disperse the encapsulated system into small droplets. The former technique is simpler and more scalable; however, due to the spatial variation of shear stress as a function of distance from the mixing element, the resultant emulsion can have a wide dispersion of particle sizes. The latter technique creates uniform emulsions but requires expensive and heavy equipment with relatively low throughput.

2.3.2 Drying Methods for Powdered Microcapsules

Dried powder encapsulated systems are most commonly created via freeze drying or spray drying [37, 38, 39, 40, 41, 42, 4, 43]. Freeze-drying has the advantage of exposing the core material to extremely mild temperatures and excels at processing heat-sensitive compounds. It is however extremely costly as the throughput of powder is much lower than what can be achieved with other encapsulation methods. Spray-drying as a technology is well-understood and ubiquitous in food processing for dried powders and its applications include microencapsulation of various compounds. It offers high throughput but frequently results in highly variable particle size distributions.

2.3.3 Microfluidic Assembly

Another emerging technology for encapsulated particle assembly is microfluidics [44, 45], which espouses large flow rates for fluid flow through micron-scale channels. Dominated by the laminar flow regime, microfluidic processing takes place on “chips” that can be fabricated with an arrangement of these micro-scale channels for a variety of applications, including biomaterials processing, micro-reactors, and “lab-on-a-chip” devices [46, 47, 48, 49, 50, 51, 52]. This methodology produces extremely uniform particles to a specific and tunable particle size, which is very attractive for core materials that are of interest in controlled-release applications. The only way to scale-up production with this method, however, is to add more microfluidic chips in parallel, which rapidly becomes unfeasible for economies of scale.

2.4 Spray-Drying Technology

Though the technology has existed for almost 150 years, spray-drying was not hugely popular with the food industry until the mid-1940’s, as the war effort caused dairy producers to adopt the technology *en masse* for the production of milk powder [53].

Although there are a multitude of variations on a traditional spray-drying configuration, the technology shared among them operates on the same underlying concept.

2.4.1 Equipment and Process Flow

A large, wide vessel is used as the drying chamber; air-handlers force or induce a draft through this drying chamber, while a steam or electrical element heats the incoming air flow. A liquid feedstock, usually with a set concentration of total solids, is pumped through a nozzle set into the main drying chamber and atomized into a fine mist. The high temperature of the inlet air combined with the massive increase of surface area as a result of atomization causes most of the solvent (usually water) to flash off almost immediately. The main drying chamber facilitates a long enough residence time of the particulate matter to dry completely, usually to a moisture content below 5%. Because of the high latent heat of vaporization of water, individual particles are not typically exposed to nearly as high a temperature as what is present at the inlet, and residence times are typically short in the main drying chamber; however, the heat load present can be an issue for thermolabile components.

The now cooled air moving through the dryer carries the dried powder through a at least one (and typically a series of) cyclone separator(s) that induce most of the powder particles to drop out into collection hoppers. Any fine particles remaining are filtered as the air is discharged out of the drying apparatus, usually through a roof stack. The air flow and inlet feed stock spray orientation can be set up as counter-current or co-current depending on the needs of the application [54, 55].

2.4.2 Important Process Parameters

Spray-drying is a highly dynamic process with several key parameters that can have a large effect on the physicochemical properties of the spray-dried powder. Temperature must be tightly controlled; typically, the outlet temperature held constant is a key indicator of final moisture content of the powder. The inlet temperature is typically controlled via a cascaded setpoint to the heating element via the outlet temperature sensor. It is also feasible to control the feed rate in the same manner in order to reduce the evaporative cooling load on a static heating element. Imprecise temperature control can lead to particles that differ with regards to surface moisture, which could encourage "stickiness" and potentially aggregation of the final powdered particulates.

Air velocity is also important as it pertains to particle retention and collection. The efficiency of the separation cyclones is directly associated with the velocity of the air moving through them. Too high of a velocity could lead to yield loss as more particles are discharged to the filtering apparatus than collected; whereas, too low of a velocity could expose fully dried powder in the drying chamber to undue levels of sensible heating, degrading the material being spray-dried

Similarly, atomizing air velocity, and specifically its ratio to the feed flow rate, is extremely important for final particle size considerations. As this ratio determines the extent of atomization at the nozzle/dryer interface, it is important that it be high enough to fully break the surface tension of the liquid feedstock into small enough droplets to be dried. Unduly high velocities typically result in unwanted spray-patterns out of the nozzle that could reduce yield loss [56].

2.4.3 Nozzle Technology

Of especially important consideration when designing a spray-drying operation is the selection of the nozzle used to atomize the liquid feedstock. Without appropriate atomization, there is not adequate surface area exposed to the heated air medium, and incomplete drying of the particulate material will occur. This can lead to issues with the material coating the inner drying chamber resulting in a catastrophic loss of yield, as well as nozzle plugging issues which would require a complete shut-down of the spray-dryer to address.

2.4.3.1 Hydraulic Nozzles

For applications with low total solids feedstock material, hydraulic atomizing nozzles can be used. These nozzles rely in creating sufficient backpressure within the nozzle assembly that the resulting pressure drop across the nozzle-tip/spray-dryer interface imparts significant energy into the fluid that it atomizes into a fine mist. Typically, a mechanical vortex or shear action is imparted *vis-à-vis* the nozzle geometry in order to aid in the break-up of the liquid particles. Plugging is the major issue with these nozzles, as well as having a relatively large resultant particle size unless pressures in excess of 1,000 psi are used, which typically requires a high capital investment in pumps that can handle this load.

2.4.3.2 Two-Fluid Air Atomized Nozzles

More common for industrial applications is the use of air-assisted atomization in a so-called “two-fluid nozzle”. The liquid feedstock (fluid 1) is pumped through a nozzle tip that is surrounded by a second orifice; hot, dry air (fluid 2) is compressed through this auxiliary orifice at a set pressure. Rather than relying on fluid pressure, a two-fluid nozzle uses this air stream to impart enough energy to the liquid feedstock to break up

the stream into small enough particles to be spray-dried. These handle higher solids feedstocks exceedingly well, as the nozzle tip for the feedstock can be machined much larger than that used in hydraulic nozzles.

Two-fluid nozzles are typically used with an emulsified feedstock of encapsulated material. This process typically requires an extra homogenization step prior to spray-drying that closely resembles or even mimics the emulsion method for encapsulation [57].

2.4.3.3 Three-Fluid Air Atomized Nozzles

A relatively new and unstudied nozzle technology that is gaining traction in the pharmaceutical space as a possible means of enhanced encapsulation potential is the three-fluid air atomized nozzle. With a setup almost identical to the two-fluid nozzle, this nozzle has a nested “inner fluid channel” within a larger “outer fluid channel”, which both are ejected through a tip surrounded by the atomizing air orifice. The underlying assumption is that the outer liquid feedstock (the shell material) will coat the outside of the inner liquid feedstock (the core material) as the particles are atomized, creating an encapsulated powder system. Very few studies within the food space have been conducted with this technology. Figure 2.2 shows a typical setup for both a 2-fluid and 3-fluid nozzle.

2.5 Microfluidic Assembly of Microcapsules

The technology of microfluidic processing has evolved rapidly in recent years and spawned several different areas of new research, one of which is the assembly of highly uniform and customizable encapsulated systems.

2.5.1 Governing Theory

The micron-scale channels used in microfluidic chips offer several advantages over traditional pumped-fluid systems. Viscous forces dominate at such a small scale over inertial forces, causing the flow regime throughout the length of the chip to remain laminar (Re < 2200) [58]. This allows for supreme control of diffusion within the fluid system, as random turbulent vortices are not present. Furthermore, all transport phenomena within the system takes place on exceedingly short time-scales due to the limited volume of liquid and dominant kinetic forces [58, 47]. Normally slow-to-respond key process parameters, such as temperature, are easily tuned dynamically in real time, mediating extremely precise process control that is simply not possible in macro-scale processing systems.

Channel layout and geometry is also eminently tunable, as most microfluidic chips are templated and manufactured as individual custom units. This customization allows for a broad range of applications within microfluidic processing including separation of liquid fractions, biomaterials processing, micro-reactions, and encapsulation [48, 46, 52].

2.5.2 Microencapsulation via Microfluidics

The precise control over flow-rates in separate channels as well as the capability to engineer different channel junctions allows for highly uniform microcapsules to be generated. Studies have indicated that polydispersity indices (PDI's) of significantly less than 0.2 (a threshold below which particle dispersions are said to be "mono-disperse") are achievable via microfluidic assembly [59, 60, 61, 62]. Research has also shown that the PDI of the microcapsules can also be tuned via the manipulation of a variety of process parameters, including flow rates, solids concentration of the feedstocks, and

the ratio of flow between the continuous and dispersed phases used to create the microcapsules [59, 60].

The most glaring downside of microfluidic encapsulation is the inability to easily scale to industrial levels of production. Because the channel dimensions cannot be enlarged without losing all of the precision control associated with microfluidic processing, the only means of scaling production is to add more microfluidic chips in parallel, which can rapidly become feasible if large production volumes are needed for formulations.

2.6 Model System

In order to test the proposed nozzle technology, a model system for encapsulation has been chosen in order to test not only the physical properties of the resultant spray-dried particles, but also the efficacy of the encapsulation. The wall material, zein, lends itself exceedingly well to the anti-solvent precipitation that will be carried out within the nozzle body. The core, quercetin, has several promising health benefits in humans, a bitter taste that requires masking, and is degraded in the presence of both oxygen and light [63, 64]. Several surface-acting agents are also discussed as encapsulation aids.

2.6.1 Zein

Zein is the collective term for a group of proteins that act as the primary nitrogen storage source in corn seedlings, similar to glutelin and glyadin in wheat endosperm, and is Generally Recognized As Safe (GRAS) for consumption in food by the FDA. Appearing as a dull yellow-orange powder, zein is typically classified into four solubility-differentiated sub-fractions: α, β, γ, and δ zein, though α zein accounts for the majority (~70%) of the makeup of commercially available unrefined zein [65]. Within each sub-

fraction there are also different molecular weight groupings, with the range of molecular weights found in all zein fractions from ~19-27 kda [65, 66].

Notably, zein has a high percentage of hydrophobic amino acid residues (proline, alanine, and leucine) that limit its solubility in polar solvents and contributes to unique secondary and tertiary structures [66, 65]. The non-polar residues result in tightly wound alpha-helices that repeat in multiple units and that are linked together by “bridges” composed of hydrophilic amino acid residues, primarily glutamine [65]. The polar interactions of the side chains between different zein units gives rise to repeated stacking, and consequently the film-forming and self-assembly properties that allow for zein to be an excellent shell matrix for microencapsulation applications [65, 67, 68]. Figure 2.3 illustrates the tertiary conformational structure and stacking of zein protein units. Zein is soluble in aqueous ethanolic solutions between 50-90% v/v ethanol as well as other primarily non-polar solvents.

2.6.1.1 Zein as a Shell Material in Microencapsulation

At its solubility limit, zein will rapidly self-assembly into micellular particles as the secondary and tertiary structure folds to accommodate the shielding of the hydrophobic amino acid residues [67, 69, 70]. This property has made zein a promising compound of study in microencapsulation research; simply by mixing zein with the target core material in aqueous ethanol and then adding water as an anti-solvent to precipitate the zein results in a stable shell/core system as zein folds and encapsulates the core material during self-assembly. Zein has successfully been used to encapsulate anti-microbial agents for use in stabilizing dairy products, flavor compounds, volatile

polyphenolic compounds, and dormant bacterial cells to be used as probiotics [71, 62, 60, 61, 72, 73, 74, 75, 76, 77].

2.6.2 Quercetin

Quercetin (2-(3,4-dihydroxyphenyl)-3,5,7-trihydroxy-4*H*-chromen-4-one) is a water insoluble polyphenolic compound that can be found in a variety of fruits and vegetables, as well as black or green tea and red wine [78]. It is a member of the flavonol class of compounds, which are differentiated from other flavonoid compounds by having a hydroxyl group located at the 3-carbon position on the heterocyclic B-ring. It is one of the most abundant flavonol compounds in a typical human diet [64], and it shares the antioxidant activity of other polyphenolic compounds via free radical scavenging potential stabilized by resonance.

Quercetin specifically has also shown anti-carcinogenic properties through a range of proposed mechanisms that include binding and inactivating oncogenic enzymes as well as pro-apoptic cell cycle disruption in tumor cells [2, 79]. The most common form of quercetin in natural sources exists as a glycoside hybrid of quercetin with a sugar. Unfortunately, this form is less bioavailable due to a range of metabolic activities that occurs on the glycoside hybrid prior to quercetin reaching the intestinal tract [63]. Quercetin is also photodegradable, reducing potential applications in shelf-stable food [80].

2.6.2.1 Health Benefits

Flavonoid compounds are widely regarded as potent antioxidant once ingested and absorbed, and special attention has been given to quercetin as a potential inhibitor of oncogenic activity in the large intestine.

2.6.2.1.1 Antioxidant Activity

Free radical compounds in the human body are highly reactive and exceedingly short-lived molecules with an unpaired electron in the outer valence shell. These compounds naturally occur during human metabolic operation as a result of oxidative stress, and although their role in human aging is not fully understood, these compounds can react with cellular structures with adverse effects to the life-cycle of the cell itself. Polyphenolic compounds, such as quercetin, act as free-radical “sinks” by providing donating an electron to the free radical molecule and stabilizing its loss of a valence pair through chemical resonance.

Studies have born out this structure function claim of quercetin as an antioxidant, as it has been tested both *in vitro* and *in vivo* in rodent and human models and shown to have antioxidant activity [81, 82, 64, 83]. Research has also shown that quercetin is effective at preventing the oxidation of unsaturated oils in food systems or bulk oil products, effectively enhancing the shelf-life of these goods [84, 85].

2.6.2.1.2 Colon Cancer

Colorectal cancer affected approximately 140,000 individuals in 2018 and its diagnostic incidence is on the rise across younger populations [86, 87]. It is currently the second leading cause for cancer death in the United States [88] among individuals 40-79 years of age, and exposure to dietary patterns common in a westernized diet is thought to be one of the major risk factors for colorectal cancer in the general population [89].

Flavonoid compounds, and quercetin especially, have been extensively studied in recent years as preventative measures for and therapeutic treatment of colon cancer. Studies have indicated that quercetin downregulates the expression of several key

oncogenic genes and promotes cell-cycle arrest in nascent tumor cells [90, 91, 92, 86]. *In vivo* trials in rodent models show that regular quercetin consumption has an inti-inflammatory effect in carcinogenically induced tumors [93, 94, 95, 96]. Furthermore, studies have indicated that quercetin may have a positive synergistic effect with class radiation treatment therapy by essentially “weakening” the tumor cells and/or removing any resistance that may exist to the radiation dosage [97, 98].

2.6.3 Surface Agents

When determining the optimal shell material for an encapsulated system, it can be beneficial to modify the surface properties of the microcapsule through the use of various ionic and non-ionic compounds. By interacting with the exposed functional groups or native charge of the shell material, surface agents can influence release kinetics, mitigate particle aggregation and/or emulsion collapse, and alter the wettability of the exposed particle surfaces [99, 100, 101].

Typically, these surface acting agents are amphiphilic compounds like modified food starches, functionalized lipo-oligomers, or proteins [72, 102, 74]. Possessing both a polar “head” grouping attached to a bulky, non-polar “tail” unit, these surface agents are able to assemble in a layer around a variety of different shell matrices, altering surface charge and/or providing steric hindrance to aid in stability. Table 2.3 shows the structure of the various surface acting agents described below.

2.6.3.1 Modified Food Starches

Starch in its native form consists of long carbon chains of either linear (amylose) or branched (amylopectin) chains. Though there are an array of different modifications to native starch that are commonly used in the food industry as additives, the most relevant within the context of microencapsulation are those modified with a bulky polar

side chain. A commonly used functional group for this purpose is octenyl succinic anhydride (OSA; 2,5-furandione, dihydro-3-(octenyl)-), which adds a polar “head” grouping to the generally non-polar structure of native starch [103, 104]. Long used as an emulsifying agent in food systems, OSA-modified starch as more recently been studied in numerous encapsulation studies as a beneficial additive for the emulsion based encapsulated systems, as well as dried microcapsule applications [38, 105, 29, 106, 107, 108].

2.6.3.2 Carrageenan

Derived from sea-weeds and consisting of a number of different sub-classifications, carrageenan has a history of use in foods as a thickener and gelation agent [109]. An oligosaccharide with sulfonated side chains, carrageenan is capable of crosslinking with itself and other charged molecules in a food matrix, lending itself to these applications. This crosslinking capability also make it an attractive option as a surface agent in microencapsulation, and studies have indicated that it can bring added stability to microcapsule systems via increased shell stability [110, 111, 112, 113].

2.6.3.3 Sorbitan Esters

Fatty acids modified with a sorbitan ester attached to the alkyl group form the basis for an important group of non-ionic emulsifying agents that are more commonly used in aerosols and other non-food applications. These compounds are formulated with differing fatty-acid chain lengths depending on the application and are either solely the sorbitan ester attached to a fatty acid (“Spans”) or have an added poly-ethoxylated side-chain (“Tweens”) [114, 115]. Research on their use as emulsifiers and stabilizers in food-related microencapsulation research has shown these compounds have potential as a “designer” option for microcapsule stability [116, 117, 118, 119, 120]. The

customizable length of the non-polar tail grouping allows for more control over the amphiphilic interaction at the shell/solvent interface, which in turn allows for fine-tuning over the final particle size and stability than other options.

2.6.3.4 Sodium Caseinate

Most proteins are naturally amphiphilic, containing amino acid residues with both polar and non-polar side-chains. Casein, a protein ubiquitous in dairy products, occurs natively as a colloidal suspension of micelles [2]. Sodium caseinate is a more commonly available powdered form of this protein that has long been used in instantized food powders; that is, powdered products that must rapidly assimilated into an aqueous environment to provide their intended use. Encapsulated systems have been generated not only with sodium caseinate as the lone shell material, but also as an amphiphilic stabilizer of other shell matrices [121, 122, 123, 71]; in one study, kafirin (the analogue to zein found in sorghum) was complexed with sodium caseinate to produce microcapsules with increased wettability and dispersion in aqueous food systems [124].

2.7 Conclusion

Microencapsulation provides a means for bioactive compounds of interest to food manufacturers to be effectively stabilized for increase shelf life, made more bioavailable post-consumption, and provided a means to be released in a controlled manner or at a targeted site in the GI tract. Multiple technologies for encapsulation exist that can produce microcapsules in a liquid emulsion or dried powder format. Spray-drying provides a highly scalable means of producing dried microcapsules for ease of storage, shipment, and formulation, but requires an additional processing step to accommodate the homogenization of the encapsulated system; spray-drying also tends to suffer from large, widely dispersed dried powder sizes, which can be detrimental for controlled

release applications. Microfluidics offers immense control and customization over a final, uniform particle size, but has major issues with scalability to industrial processes. It is therefore useful to identify a means of offering the same advantages that microfluidics offers with regards to process control while also offering more advantageous scalability parameters.

Quercetin is a promising health compound that could be useful as a therapeutic ingredient in food systems to help combat colon cancer incidence. It has limited bioavailability and is easily degraded by both heat and light, limiting its shelf life; quercetin also has a bitter flavor that would require masking to improve consumer tolerance. Zein is a well-established shell material used in the field of microencapsulation; further research to establish whether zein/quercetin complexes could enhance not only the bioavailability of quercetin but also provide a means for targeted release in the colon. This encapsulated system could benefit from the addition of a surface acting compound; sodium caseinate is a cheap, effective, and safe option that could help improve the physicochemical properties of the final microcapsule.

Overall, future research should focus on maximizing quercetin's potential benefit to human health by engineering not only a stable microcapsule system, but also a microencapsulation technology that provides control over the final particle size and is also scalable to meet the demand of economies of scale. This technology could then be extrapolated to other microencapsulated systems of interest.

2.8 Tables and Figures

Table 2.1 – Encapsulation Benefits

Benefit	Example Core Compounds	References
Enhanced Shelf Life	• Polyunsaturated Fatty Acids • Flavonoids • Carotenoids • Stilbenes • Probiotics (bacterial cells)	[2-12]
Mitigation of Negative Sensory Properties	• Tannins (proanthocyanidins) • Polyphenols • Protein hydrolysates • Citrus flavor/aroma • Mint flavors/aroma	[13-21]
Increased Bioavailability	• Polyphenols (lutein, quercetin) • Calcium chelates • Curcumin	[22-27]
Controlled Release Kinetics	• Retinol • Cholecalciferol • Insulin • Inulin	[28-33]

Table 2.2 – Encapsulation Technologies

Technology	Benefits	Drawbacks
Liquid Emulsion	• Straightforward preparation • Can create oil-in-water or water-in-oil encapsulated systems • Limited exposure to heat for thermolabile core materials	• Particle size variable depending on method used • Liquid phase is bulky for shipment/storage • High capital costs for high-pressure homogenization
Freeze-Drying	• Excellent for thermolabile materials • Powder products are shelf-stable and easy to transport	• Expensive at scale • Potential for wide particle size distributions
Spray-Drying	• Well-understood technology • Industrially scalable • Powder products are shelf-stable and easy to transport	• Non-negligible heat load • Potential for wide particle size distributions
Microfluidic Assembly	• Unparalleled level of process control • Extremely uniform particle size distribution	• Difficult to scale to industrial levels

Table 2.3 – Surface Acting Compounds and Structures

Compound Name	Structure
Octenyl Succinic Anhydride (OSA)	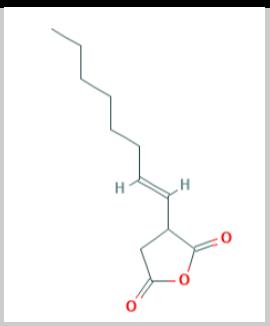 [125]
Carrageenan	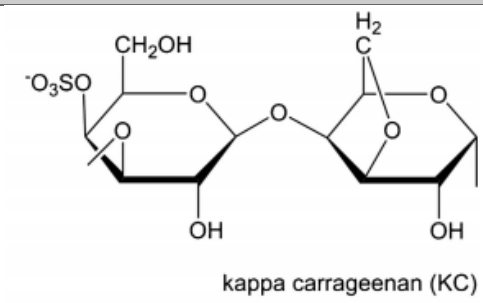 kappa carrageenan (KC) [126]
Span **(Sorbitan ester)**	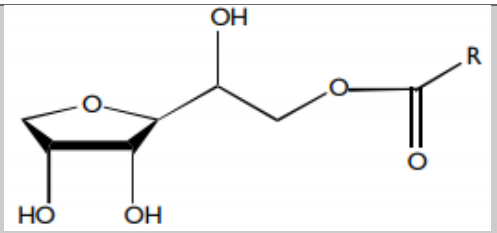 [114]
Tween **(Polyethoxylated Span)**	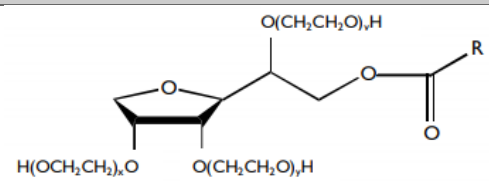 [114]
Sodium Caseinate	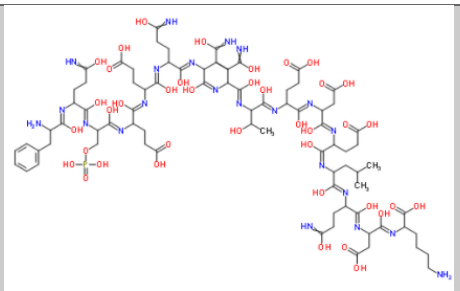 [127]

Figure 2.1 – An Example of Microfluidic Chip (a) with T-Junction (b) and Flow-Focusing (c) Channel Arrangements

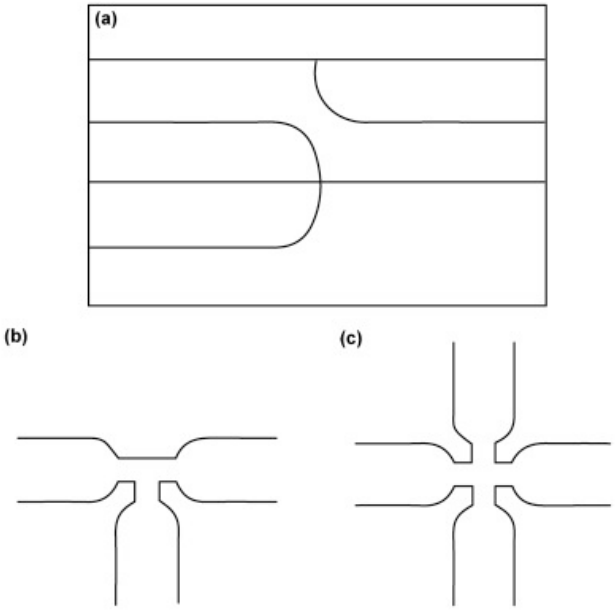

[59]

Figure 2.2 – Two-Fluid and Three-Fluid Spray Drying Nozzle Examples

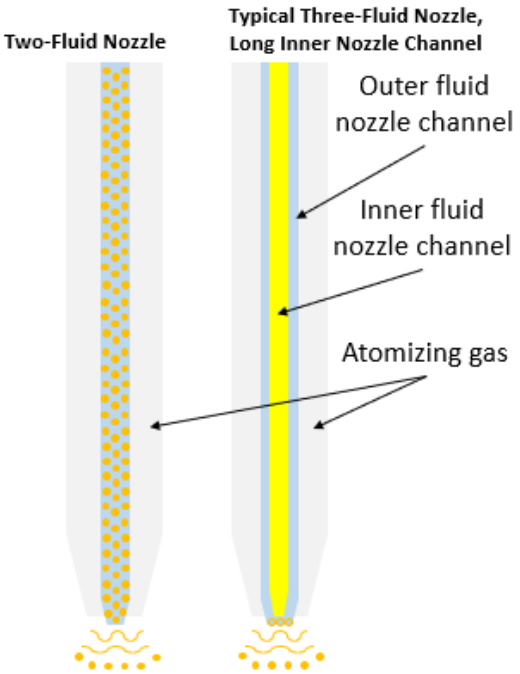

Figure 2.3 – Tertiary Structure of Zein

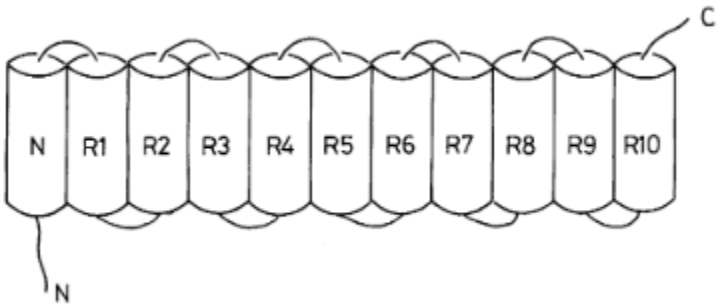

[65]

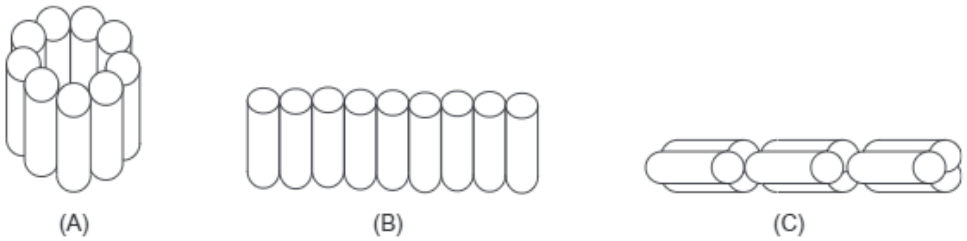

[67]

Top image: Unfolded example of zein tertiary structure; R-groups are repeating α-helical cylinders linked by glutamine turns

A, B, C: Different stacking and/or self-assembly quaternary structures of zein molecules

2.9 References

[1] Q. Ye, N. Georges and C. Selomulya, "Microencapsulation of active ingredients in functional foods: From research stage to commercial food products," *Trends in Food Science and Technology,* vol. 78, pp. 167-179, 2018.

[2] Y. Chen, H. Ge, Y. Zheng, H. Zhang, Y. Li, X. Su, W. Panpipat, O. M. Lai, O. M. Lai, C. P. Tan and L. Z. Cheong, "Phospholipid-Protein Structured Membrane for Microencapsulation of DHA Oil and Evaluation of Its in Vitro Digestibility: Inspired by Milk Fat Globule Membrane," *Journal of Agricultural and Food Chemistry,* vol. 68, no. 22, pp. 6190-6201, 3 6 2020.

[3] L. B. Pham, B. Wang, B. Zisu, T. Truong and B. Adhikari, "Microencapsulation of flaxseed oil using polyphenol-adducted flaxseed protein isolate-flaxseed gum complex coacervates," *Food Hydrocolloids,* vol. 107, p. 105944, 2020.

[4] W. Shao, X. Pan, X. Liu, F. Teng and S. Yuan, "Microencapsulation of Algal Oil Using Spray Drying Technology," vol. 56, no. 1.

[5] Y. Zhang, X. Pang, S. Zhang, L. Liu, C. Ma, J. Lu and J. Lyu, "Buttermilk as a wall material for microencapsulation of omega-3 oils by spray drying," 2020.

[6] N. Lin, C. Wang, J. Ding, L. Su, L. Xu, B. Zhang, Y. Zhang and J. Fan, "Efficacy of nanoparticle encapsulation on suppressing oxidation and enhancing antifungal activity of cyclic lipopeptides produced by Bacillus subtilis," 2020.

[7] J. Azzi, A. Jraij, L. Auezova, S. Fourmentin and H. El Ene Greige-Gerges, "Novel findings for quercetin encapsulation and preservation with cyclodextrins, liposomes, and drug-in-cyclodextrin-in-liposomes," *Food Hydrocolloids,* no. 81, pp. 328-340, 2018.

[8] T. Cardoso, A. Gonçalves, B. N. Estevinho and F. Rocha, "Potential food application of resveratrol microparticles: Characterization and controlled release studies," 2019.

[9] S. Y. Liew, M. Zin, M. Maidin, H. Mamat and M. K. Zainol, "Effect of the different encapsulation methods on the physicochemical and biological properties of Clitoria ternatea flowers microencapsulated in gelatine," *Journal homepage,* vol. 4, no. 4, pp. 1098-1108, 2020.

[10] F. Zanoni, M. Primiterra, N. Angeli and G. Zoccatelli, "Microencapsulation by spray-drying of polyphenols extracted from red chicory and red cabbage: Effects on stability and color properties," 2019.

[11] A. Gadioli Tarone, C. Baú Betim Cazarin and M. Roberto Marostica Junior, "Anthocyanins: New techniques and challenges in microencapsulation," 2020.

[12] Y. Yusnaidar, W. Syahri, M. Latief and A. Y. Chaerunisaa, "Microencapsulation of Macaranga gigantea Leaf Extracts: Production and Characterization," *Phcogj.com Pharmacognosy Journal,* vol. 12, no. 4, pp. 716-740, 2020.

[13] V. Brito de Souza, M. Thomazini, I. Elias Chaves, R. Ferro-Furtado and C. S. Favaro-Trindade, "Microencapsulation by complex coacervation as a tool to protect bioactive compounds and to reduce astringency and strong flavor of vegetable extracts," *Food Hydrocolloids,* vol. 98, 2020.

[14] J. N. Coupland and J. E. Hayes, *Physical approaches to masking bitter taste: Lessons from food and pharmaceuticals,* vol. 31, Springer New York LLC, 2014, pp. 2921-2939.

[15] J. D. Donovan, L. Bauer, G. C. Fahey and Y. Lee, "In Vitro Digestion and Fermentation of Microencapsulated Tributyrin for the Delivery of Butyrate," *Journal of Food Science,* vol. 82, no. 6, pp. 1491-1499, 1 6 2017.

[16] X. Zhao, Y. Ai, Y. Hu, Y. Wang, L. Zhao, D. Yang, F. Chen, X. Wu, Y. Li and X. Liao, "Masking the Perceived Astringency of Proanthocyanidins in Beverages Using Oxidized Starch Hydrogel Microencapsulation," *Foods,* vol. 9, no. 6, p. 756, 8 6 2020.

[17] I. Mennella, V. Fogliano, R. Ferracane, M. Arlorio, F. Pattarino and P. Vitaglione, "Microencapsulated bitter compounds (from Gentiana lutea) reduce daily energy intakes in humans," *British Journal of Nutrition,* vol. 116, no. 10, pp. 1841-1850, 28 11 2016.

[18] H. Alaşalvar and M. Çam, "Ready to drink iced teas from microencapsulated spearmint (Mentha spicata L.) and peppermint (Mentha piperita L.) extracts: physicochemical, bioactive and sensory characterization," *Journal of Food Measurement and Characterization,* vol. 14, no. 3, pp. 1366-1375, 1 6 2020.

[19] C. Zhang, X. Chen, J. Zhang, P. A. Kilmartin and S. Young Quek, "Exploring the effects of microencapsulation on odour retention of fermented noni juice," *Journal of Food Engineering,* vol. 273, p. 109892, 2020.

[20] Z. Nale, I. Tontul, A. S. ße As ßc ß I Arslan, H. S. Nadeem, A. H. Me, T. Ku C U Kc and E. Ti N, "ORIG IN AL RESE ARCH Microbial viability, physicochemical and sensory properties of kefir microcapsules prepared using maltodextrin/Arabic gum mixes," 2017.

[21] N. Ruscheinsky Breternitz, H. M. Andr E Bolini and M. Dupas Hubinger, "Sensory acceptance evaluation of a new food flavoring produced by microencapsulation of a mussel (Perna perna) protein hydrolysate," 2017.

[22] Y. Fu, J. Yang, L. Jiang, L. Ren and J. Zhou, "Encapsulation of Lutein into Starch Nanoparticles to Improve Its Dispersity in Water and Enhance Stability of Chemical Oxidation," 2018.

[23] L.-H. Zhang, X.-D. Xu, B. Shao, Q. Shen, H. Zhou, Y.-M. Hong and L.-M. Yu, "Physicochemical Properties and Bioavailability of Lutein Microencapsulation(LM)," *Food Science and Technology Research,* vol. 21, no. 4, pp. 503-507, 2015.

[24] M. N. Uddin, N. J. Patel, T. Bhowmik, B. D. Souza, A. Akalkotkar, F. Etzlar, C. W. Oettinger and M. D. '. Souza, "Enhanced bioavailability of orally administered antisense oligonucleotide to nuclear

factor kappa B mRNA after microencapsulation with albumin," *J Drug Target,* vol. 21, no. 5, pp. 450-457, 2013.

[25] Y. Mi, Z. Liu, J. Deng, H. Lei, C. Zhu, D. Fan and X. Lv, "Microencapsulation of Phosphorylated Human-Like Collagen-Calcium Chelates for Controlled Delivery and Improved Bioavailability," 2018.

[26] G. Annunziata, M. Jiménez-García, X. Capó, D. Moranta, A. Arnone, G. C. Tenore, A. Sureda and S. Tejada, "Microencapsulation as a tool to counteract the typical low bioavailability of polyphenols in the management of diabetes," 2020.

[27] U. Kannamangalam, V. Nirali, N. Shah, B. Muley and R. S. Singhal, "Complexation of curcumin using proteins to enhance aqueous solubility and bioaccessibility: Pea protein vis-` a-vis whey protein," *Journal of Food Engineering,* vol. 292, pp. 260-8774, 2021.

[28] G. V. L. Gomes, M. R. Sola, A. L. Rochetti, H. Fukumasu, A. A. Vicente and S. Pinho, "b-carotene and a-tocopherol coencapsulated in nanostructured lipid carriers of murumuru (Astrocaryum murumuru) butter produced by phase inversion temperature method: characterisation, dynamic in vitro digestion and cell viability study," *Journal of Microencapsulation,* vol. 36, no. 1, pp. 43-52, 2019.

[29] Z. M. Barzoki, Z. Emam-Djomeh, E. Mortazavian, A. A. Moosavi-Movahedi and M. Rafiee Tehrani, "Formulation, in vitro evaluation and kinetic analysis of chitosan-gelatin bilayer muco-adhesive buccal patches of insulin nanoparticles".

[30] E. Dadkhodazade, A. Mohammadi, S. Shojaee-Aliabadi, A. M. Mortazavian, L. Mirmoghtadaie and S. M. Hosseini, "Yeast Cell Microcapsules as a Novel Carrier for Cholecalciferol Encapsulation: Development, Characterization and Release Properties," *Food Biophysics,* vol. 13, no. 4, pp. 404-411, 1 12 2018.

[31] P. García, C. Vergara and P. Robert, "Release Kinetic in Yogurt from Gallic Acid Microparticles with Chemically Modified Inulin," *Journal of Food Science,* vol. 80, no. 10, pp. C2147-C2152, 1 10 2015.

[32] F. Paulo and L. Santos, "Microencapsulation of caffeic acid and its release using a w/o/w double emulsion method: Assessment of formulation parameters," *Drying Technology,* vol. 37, no. 8, pp. 950-961, 11 6 2019.

[33] F. Goudon, Y. Clément and L. Ripoll, "Controlled release of retinol in cationic co-polymeric nanoparticles for topical application," *Cosmetics,* vol. 7, no. 2, p. 29, 1 6 2020.

[34] L. Ma, Y. Shang, Y. Zhu, X. Zhang, |. Jingjing, L. Zhao and J. Wang, "Study on microencapsulation of Lactobacillus plantarum LIP-1 by emulsification method," 2020.

[35] D. Noviendri, I. Jaswir, M. Taher, F. Mohamed, H. M. Salleh, I. A. Noorbatcha, F. Octavianti, W. Lestari, R. Hendri, H. Ahmad, K. Miyashita and A. Abdullah, "Fabrication of Fucoxanthin-Loaded Microsphere(F-LM) By Two Steps Double-Emulsion Solvent Evaporation Method and

Characterization of Fucoxanthin before and after Microencapsulation," *Journal of Oleo Science,* vol. 65, no. 8, pp. 641-653, 2016.

[36] A. Jamshidi, T. Antequera, J. C. Solomando and T. Perez-Palacios, "Microencapsulation of oil and protein hydrolysate from fish within a high-pressure homogenized double emulsion," *Journal of Food Science and Technology,* vol. 57, no. 1, pp. 60-69, 1 1 2020.

[37] "Freeze-dried, oven-dried, and microencapsulation of essential oil from Allium sativum as potential preservative agents of minced meat," 2020.

[38] H. Arshad, T. M. Ali and A. Hasnain, "Comparative study on efficiency of nutmeg microencapsulation (freeze-drying method) using native and OSA sorghum starch as wall materials in combination with gum arabic," *Cereal Chemistry,* vol. 97, no. 3, pp. 589-600, 26 5 2020.

[39] V. O. Dueik and L. L. Diosady, "Microencapsulation of iron in a reversed enteric coating using spray drying technology for double fortification of salt with iodine and iron," *Journal of Food Process Engineering,* vol. 40, 2017.

[40] C. Femat-Castañeda, A. Chávez-Rodríguez, A. Moises Chávez-Rodríguez, H. Flores-Martínez, V. Sbeyde Farías-Cervantes and I. Andrade-González, "Effect of Agave Fructans and Maltodextrin on Zn 2+ Chlorophyll Microencapsulation by Spray Drying," 2019.

[41] A. García-Gurrola, S. Rincón, A. A. Escobar-Puentes, A. Zepeda and F. Martínez-Bustos, "Microencapsulation of Red Sorghum Phenolic Compounds with Esterified Sorghum Starch as Encapsulant Materials by Spray Drying," vol. 57, no. 3.

[42] L. Mihalcea, V. Barbu, E. Enachi, D. Georgeta Andronoiu, G. Râpeanu, M. Stoica, L. Dumitrașcu and N. Stănciuc, "Microencapsulation of Red Grape Juice by Freeze Drying and Application in Jelly Formulation," vol. 58, no. 1.

[43] B. Wang, S. R. Duke, Y. Wang and C. Yifen Wang, "Microencapsulation of lipid materials by spray drying and properties of products".

[44] W. Gao, •. Meimei Sun, W. Yang and C. Zhang, "Visualization study on solid-core encapsulation behaviors of double emulsion in a flow-focusing microchannel".

[45] C. Katsakouli, X. Jiang, W. K. Lau, J. L. Rohn and M. Edirisinghe, "Generating Antibacterial Microporous Structures Using Microfluidic Processing," *ACS Omega,* vol. 4, no. 1, pp. 2225-2233, 29 1 2019.

[46] M. Agostini, G. Greco and M. Cecchini, "Full-SAW Microfluidics-Based Lab-on-a-Chip for Biosensing," *IEEE Access,* vol. 7, pp. 70901-70909, 2019.

[47] R. Chen, J. E. Wulff and M. G. Moffitt, "Microfluidic Processing Approach to Controlling Drug Delivery Properties of Curcumin-Loaded Block Copolymer Nanoparticles," *Molecular Pharmaceutics,* vol. 15, no. 10, pp. 4517-4528, 1 10 2018.

[48] L. Gasperini, A. P. Marques and R. L. Reis, "Microfluidics for Processing of Biomaterials," in *Advances in Experimental Medicine and Biology*, vol. 1230, Springer, 2020, pp. 15-25.

[49] D. J. Kinahan, L. A. Julius, C. Schoen, T. Dreo and J. Ducree, "Automated DNA purification and multiplexed lamp assay preparation on a centrifugal microfluidic 'Lab-on-a-Disc' platform," in *Proceedings of the IEEE International Conference on Micro Electro Mechanical Systems (MEMS)*, 2018.

[50] T. Klymkovych, N. Bokla and O. Matviykiv, "Microfluidic lab-chip device dedicated for colorimetric detection of hazardous impurities in water samples," in *2019 IEEE 15th International Conference on the Perspective Technologies and Methods in MEMS Design, MEMSTECH 2019 - Proceedings*, 2019.

[51] L. Li, H. Yin and A. J. Mason, "Epoxy Chip-in-Carrier Integration and Screen-Printed Metalization for Multichannel Microfluidic Lab-on-CMOS Microsystems," *IEEE Transactions on Biomedical Circuits and Systems,* vol. 12, no. 2, pp. 416-425, 1 4 2018.

[52] G. Zhang, L. Zhang, X. Wang, A. Chen and Q. Zhang, "Microfluidic processing of HZSM-5 films in a capillary microreactor for the continuous acetalisation reaction of glycerol with acetone," *Reaction Chemistry and Engineering,* vol. 5, no. 3, pp. 539-546, 1 3 2020.

[53] "The Significance of Spray-Drying - IFT.org," [Online]. Available: https://www.ift.org/news-and-publications/food-technology-magazine/issues/2018/april/columns/processing-spray-drying-in-the-food-industry.

[54] Handbook of industrial drying, 2007.

[55] "Preparation and properties of chitosan-based microspheres by spray drying," 2020.

[56] Handbook on spray drying applications for food industries, 2019.

[57] "Air Atomizing Spray Pattern | Spraying Systems Co.," [Online]. Available: https://www.spray.com/resources/spraying-basics/spray-patterns/air-atomizing.

[58] C. S. Kumar, Microfluidic Devices in Nanotechnology, C. S. Kumar, Ed., Hoboken, NJ, USA: John Wiley & Sons, Inc., 2010.

[59] A. G. Olenskyj, Y. Feng and Y. Lee, "Continuous microfluidic production of zein nanoparticles and correlation of particle size with physical parameters determined using CFD simulation," *Journal of Food Engineering,* vol. 211, pp. 50-59, 1 10 2017.

[60] Y. Feng and Y. Lee, "Microfluidic fabrication of hollow protein microcapsules for rate-controlled release," *RSC Adv.,* vol. 7, no. 78, pp. 49455-49462, 24 10 2017.

[61] Y. Feng, L. Alberto Ibarra-Sánchez, L. Luu, M. J. Miller and Y. Lee, "Co-assembly of nisin and zein in microfluidics for enhanced antilisterial activity in Queso Fresco," *LWT - Food Science and Technology,* vol. 111, pp. 355-362, 2019.

[62] Y. F. Dissertation, "MICROFLUIDIC ASSEMBLY OF ZEIN MICROCAPSULES".

[63] Y. Guo and R. S. Bruno, "Endogenous and exogenous mediators of quercetin bioavailability," *Journal of Nutritional Biochemistry,* no. 26, pp. 201-210, 2015.

[64] M. Lesjak, I. Beara, N. Simin, D. Pintać, T. Majkić, K. Bekvalac, D. Orčić and N. Mimica-Dukić, "Antioxidant and anti-inflammatory activities of quercetin and its derivatives," *Journal of Functional Foods,* vol. 40, pp. 68-75, 2018.

[65] N. Matsushima, G.-I. Danno, H. Takezawa and Y. Izumi, "Three-dimensional structure of maize a-zein proteins studied by small-angle X-ray scattering," 1997.

[66] H. Krishnan and E. Coe, "Seed Storage Proteins," in *Encyclopedia of Genetics*, Elsevier, 2001, pp. 1782-1787.

[67] G. W. Padua and L. V. Guardiola, "Microcapsules Produced from Zein," 2015.

[68] Y. Wang and G. W. Padua, "Nanoscale Characterization of Zein Self-Assembly," 2012.

[69] "ZEIN ENCAPSULATION OF AMPHIPHILIC COMPOUNDS".

[70] I. V. Ferreira, W. W. Focke and E. L. du Toit, "Spontaneous microencapsulation of geraniol by zein," *Express Polymer Letters,* vol. 12, no. 11, pp. 986-995, 1 11 2018.

[71] Y. Feng and Y. Lee, "Surface modification of zein colloidal particles with sodium caseinate to stabilize oil-in-water pickering emulsion," *Food Hydrocolloids,* vol. 56, pp. 292-302, 1 5 2016.

[72] H. Li, D. Wang, C. Liu, J. Zhu, M. Fan, X. Sun, T. Wang, Y. Xu and Y. Cao, "Fabrication of stable zein nanoparticles coated with soluble soybean polysaccharide for encapsulation of quercetin," *Food Hydrocolloids,* vol. 87, pp. 342-351, 1 2 2019.

[73] C. J. Cheng, M. Ferruzzi and O. G. Jones, "Fate of lutein-containing zein nanoparticles following simulated gastric and intestinal digestion," 2018.

[74] M. Veneranda, Q. Hu, T. Wang, Y. Luo, K. Castro and J. M. Madariaga, "Formation and characterization of zein-caseinate-pectin complex nanoparticles for encapsulation of eugenol," *LWT - Food Science and Technology,* vol. 89, pp. 596-603, 2017.

[75] Q. Zhong and M. Jin, "Nanoscalar Structures of Spray-Dried Zein Microcapsules and in Vitro Release Kinetics of the Encapsulated Lysozyme As Affected by Formulations," 2009.

[76] Q. Zhong, M. Jin, P. M. Davidson and S. Zivanovic, "Sustained release of lysozyme from zein microcapsules produced by a supercritical anti-solvent process," *Food Chemistry,* vol. 115, pp. 697-700.

[77] F. Zhang, M. Aslam Khan, H. Cheng and L. Liang, "Co-encapsulation of α-tocopherol and resveratrol within zein nanoparticles: Impact on antioxidant activity and stability," *Journal of Food Engineering,* vol. 247, pp. 9-18, 2019.

[78] S. Tanaka, A. Trakooncharoenvit, M. Nishikawa, S. Ikushiro and H. Hara, "Comprehensive Analyses of Quercetin Conjugates by LC/MS/MS Revealed That Isorhamnetin-7-O-glucuronide-4′-O-sulfate Is a Major Metabolite in Plasma of Rats Fed with Quercetin Glucosides," 2019.

[79] S. G. Darband, M. Kaviani, B. Yousefi, S. Sadighparvar, F. G. Pakdel, J. A. Attari, I. Mohebbi, S. Naderi and M. Majidinia, *Quercetin: A functional dietary flavonoid with potential chemo-preventive properties in colorectal cancer,* vol. 233, Wiley-Liss Inc., 2018, pp. 6544-6560.

[80] S. Dall'acqua, G. Miolo, G. Innocenti and S. Caffieri, "The Photodegradation of Quercetin: Relation to Oxidation," *Molecules,* vol. 17, pp. 8898-8907, 2012.

[81] W. M. B. da Silva, S. de Oliveira Pinheiro, D. R. Alves, J. E. S. A. de Menezes, F. E. A. Magalhães, F. C. O. Silva, J. Silva, E. S. Marinho and S. M. de Morais, "Synthesis of Quercetin-Metal Complexes, In Vitro and In Silico Anticholinesterase and Antioxidant Evaluation, and In Vivo Toxicological and Anxiolitic Activities," *Neurotoxicity Research,* vol. 37, no. 4, pp. 893-903, 1 4 2020.

[82] S. Oyedemi, G. Nwaogu, C. Chukwuma and e. al., "Quercetin modulates hyperglycemia by improving the pancreatic antioxidant status and enzymes activities linked with glucose metabolism in type 2 diabetes model of rats: In silico studies of molecular interaction of quercetin with hexokinase and catalase," *Journal of Food Biochemistry,* vol. 44, no. 2, p. 13127, 2020.

[83] M. Ersoz, A. Erdemir, S. Derman, T. Arasoglu and B. Mansuroglu, "Quercetin-loaded nanoparticles enhance cytotoxicity and antioxidant activity on C6 glioma cells," *Pharmaceutical Development and Technology,* vol. 25, no. 6, pp. 757-766, 2 7 2020.

[84] C. Li, X.-L. Qiu, L.-X. Lu, Y.-L. Tang, Q. Long and J.-G. Dang, "Preparation of low-density polyethylene film (LDPE) with quercetin and α-tocopherol loaded with mesoporous silica for synergetic-release antioxidant active packaging," *J Food Process Eng,* vol. 42, 2019.

[85] M. Palma, P. Robert, F. Holgado, J. Velasco and G. Márquez-Ruiz, "Antioxidant Activity and Kinetics Studies of Quercetin, Epicatechin and Naringenin in Bulk Methyl Linoleate," *JAOCS, Journal of the American Oil Chemists' Society,* vol. 94, no. 9, pp. 1189-1196, 1 9 2017.

[86] R. M. Lee, K. Cardona and M. C. Russell, *Historical perspective: Two decades of progress in treating metastatic colorectal cancer,* vol. 119, John Wiley and Sons Inc., 2019, pp. 549-563.

[87] R. L. Siegel, K. D. Miller and A. Jemal, "Cancer statistics, 2019.," *CA: a cancer journal for clinicians,* vol. 69, no. 1, pp. 7-34, 1 2019.

[88] J. Sandhu, V. Lavingia and M. Fakih, *Systemic treatment for metastatic colorectal cancer in the era of precision medicine,* vol. 119, John Wiley and Sons Inc., 2019, pp. 564-582.

[89] J. C. Brown, S. Zhang, D. Niedzwiecki, L. B. Saltz, R. J. Mayer, R. B. Mowat, R. Whittom, A. Hantel, A. Benson, D. Atienza, M. Messino, H. Kindler, A. Venook, S. Ogino, Y. Li, X. Zhang, K. Ng, W. C. Willett, E. L. Giovannucci, C. S. Fuchs and J. A. Meyerhardt, "Grain Intake and Clinical Outcome in Stage III Colon Cancer: Results From CALGB 89803 (Alliance)".

[90] S. Roy, R. Das, B. Ghosh and T. Chakraborty, "Deciphering the biochemical and molecular mechanism underlying the in vitro and in vivo chemotherapeutic efficacy of ruthenium quercetin complex in colon cancer," *Molecular Carcinogenesis,* vol. 57, no. 6, pp. 700-721, 1 6 2018.

[91] B. Pang, X. Xu, Y. Lu, H. Jin, R. Yang, C. Jiang, D. Shao, Y. Liu and J. Shi, "Prediction of new targets and mechanisms for quercetin in the treatment of pancreatic cancer, colon cancer, and rectal cancer," *Food and Function,* vol. 10, no. 9, pp. 5339-5349, 1 9 2019.

[92] S. Özsoy, E. Becer, H. Kabadayı, H. S. Vatansever and S. Yücecan, "Quercetin - Mediated Apoptosis and Cellular Senescence in Human Colon Cancer," *Anti-Cancer Agents in Medicinal Chemistry,* vol. 20, 8 4 2020.

[93] J. Rashedi, A. Ghorbani Haghjo, M. Mesgari Abbasi, A. Dastranj Tabrizi, S. Yaqoubi, D. Sanajou, Z. Ashrafi Jigheh, A. Namvaran, A. Mohammadi, J. Mohammadi Khoshraj and B. Baradaran, "Anti-tumor Effect of Quercetin Loaded Chitosan Nanoparticles on Induced Colon Cancer in Wistar Rats," *Adv Pharm Bull,* vol. 2019, no. 3, pp. 409-415, 2019.

[94] J. Qi, Y. Li, J. Luo, C. Zhang, S. Ou, G. Zhang, X. Yang and X. Peng, "Alternating consumption of β-glucan and quercetin reduces mortality in mice with colorectal cancer," *Food Science and Nutrition,* 2019.

[95] S. G. Darband, S. Sadighparvar, B. Yousefi, M. Kaviani, F. Ghaderi-Pakdel, A. Mihanfar, Y. Rahimi, K. Mobaraki and M. Majidinia, "Quercetin attenuated oxidative DNA damage through NRF2 signaling pathway in rats with DMH induced colon carcinogenesis," *Life Sciences,* vol. 253, p. 117584, 15 7 2020.

[96] D. Kaushik, K. O'Fallon, P. M. Clarkson, C. Patrick Dunne, K. R. Conca and B. Michniak-Kohn, "Comparison of Quercetin Pharmacokinetics Following Oral Supplementation in Humans," *Journal of Food Science,* vol. 77, no. 11, pp. H231-H238, 1 11 2012.

[97] Y. Zhou, J. Zhang, K. Wang, W. Han, X. Wang, M. Gao, Z. Wang, Y. Sun, H. Yan, H. Zhang, X. Xu and D. H. Yang, "Quercetin overcomes colon cancer cells resistance to chemotherapy by inhibiting solute carrier family 1, member 5 transporter," *European Journal of Pharmacology,* vol. 881, p. 173185, 15 8 2020.

[98] Y. Li, Z. Wang, J. Jin, S. X. Zhu, G. Q. He, S. H. Li, J. Wang and Y. Cai, "Quercetin pretreatment enhances the radiosensitivity of colon cancer cells by targeting Notch-1 pathway," *Biochemical and Biophysical Research Communications,* vol. 523, no. 4, pp. 947-953, 19 3 2020.

[99] C. A. Di Battista, D. Constenla, M. Verónica Ramírez-Rigo and J. Piña, "The use of arabic gum, maltodextrin and surfactants in the microencapsulation of phytosterols by spray drying," 2015.

[100] A. A. Sharipova, S. B. Aidarova, D. Grigoriev, B. Mutalieva, G. Madibekova, A. Tleuova and R. Miller, "Polymer-surfactant complexes for microencapsulation of vitamin E and its release," *Colloids and Surfaces B: Biointerfaces,* vol. 137, pp. 152-157, 2016.

[101] C. Butstraen, F. Salaün and E. Devaux, "Sol-gel microencapsulation of oil phase with Pickering and nonionic surfactant based emulsions," 2015.

[102] S. Haghighat-Kharazi, J. M. Milani, M. R. Kasaai and K. Khajeh, "Microencapsulation of α-amylase in beeswax and its application in gluten-free bread as an anti-staling agent," 2018.

[103] M. Matos, A. Marefati, G. Gutiérrez, M. Wahlgren and M. Rayner, "Comparative Emulsifying Properties of Octenyl Succinic Anhydride (OSA)-Modified Starch: Granular Form vs Dissolved State," 2016.

[104] N. R. Breternitz, C. H. de Vasconcelos Fidelis, V. M. Silva, M. N. Eberlin and M. D. Hubinger, "Volatile composition and physicochemical characteristics of mussel (Perna perna) protein hydrolysate microencapsulated with maltodextrin and n-OSA modified starch," *Food and Bioproducts Processing,* vol. 1, no. 5, pp. 12-25, 2017.

[105] E. Agama-Acevedo and L. A. Bello-Perez, "Starch as an emulsions stability: the case of octenyl succinic anhydride (OSA) starch," *Current Opinion in Food Science,* no. 13, pp. 78-83, 2017.

[106] R. Leyva-Lopez, H. Palma-Rodriguez, A. Lopez-Torrez, J. Capataz-Tafur, L. Bello-Perez and A. Vargas-Torres, "Use of enzymatically modified starch in the microencapsulation of ascorbic acid: Microcapsule characterization, release behavior and in vitro digestion Microcapsules were prepared using enzyme-treated corn starch with 16 and 20 h of hydrolysis time (ETCS," *Food Hydrocolloids,* vol. 96, pp. 259-266, 2019.

[107] A. A. Mahdi, J. K. Mohammed, W. Al-Ansi, A. D. S. Ghaleb, A. Al-Maqtari, M. Ma, M. I. Ahmed and H. Wang, "Microencapsulation of fingered citron extract with gum arabic, modified starch, whey protein, and maltodextrin using spray drying," 2019.

[108] P. D. Maia, D. dos Santos Baião, V. P. F. da Silva, V. M. de Araújo Calado, C. Queiroz, C. Pedrosa, V. L. Valente-Mesquita and A. P. T. Pierucci, "Highly Stable Microparticles of Cashew Apple (Anacardium occidentale L.) Juice with Maltodextrin and Chemically Modified Starch," *Food and Bioprocess Technology,* vol. 12, no. 12, pp. 2107-2119, 1 12 2019.

[109] S. Chakraborty, "Carrageenan for encapsulation and immobilization of flavor, fragrance, probiotics, and enzymes: A review," 2017.

[110] N. Devi and T. K. Maji, "Microencapsulation of isoniazid in genipin-crosslinked gelatin-A-k-carrageenan polyelectrolyte complex Isoniazid-encapsulated polyelectrolyte complex," *Drug Development and Industrial Pharmacy,* vol. 36, no. 1, pp. 56-63, 2010.

[111] E. N. Dewi, R. A. Kurniasih, L. Purnamayanti and P. Journal, "Physical Properties of Spirulina Phycocyanin Microencapsulated with Maltodextrin and Carrageenan".

[112] G. Kavoosi, M. Derakhshan, M. Salehi and L. Rahmati, "Microencapsulation of zataria essential oil in agar, alginate and carrageenan," 2017.

[113] L. Mao, Q. Pan, Z. Hou, F. Yuan and Y. Gao, "Development of soy protein isolate-carrageenan conjugates through Maillard reaction for the microencapsulation of Bifidobacterium longum," 2018.

[114] Croda, "Span and Tween," East Yorkshire, 2010.

[115] S. Zhan, Z. Zhou, W. Wang, Q. Zhao and W. Hou, "Effect of nonionic compound emulsifiers Tween80 and Span80 on the properties of microencapsulated phase change materials," *J Microencapsul,* vol. 31, no. 4, pp. 317-322, 2014.

[116] J. Baranauskaite, D. M. Kopustinskiene and J. Bernatoniene, "Impact of Gelatin Supplemented with Gum Arabic, Tween 20, and β-Cyclodextrin on the Microencapsulation of Turkish Oregano Extract".

[117] G. Yildiz, J. Ding, S. Gaur, J. Andrade, N. E. Engeseth and H. Feng, "Microencapsulation of docosahexaenoic acid (DHA) with four wall materials including pea protein-modified starch complex," 2018.

[118] D. Ma, Q. Huang, Y. Wu, J. Chen, X. Lu, D. J. McClements and Y. Wang, "Encapsulation of emulsions by a novel delivery system of fluid core-hard shell biopolymer particles to retard lipid oxidation," *Food & function,* vol. 11, no. 7, pp. 5788-5798, 1 7 2020.

[119] C. Dima and S. Dima, "Water-in-oil-in-water double emulsions loaded with chlorogenic acid: release mechanisms and oxidative stability," 2018.

[120] D. Vanichtanunkul, P. Vayumhasuwan and U. Nimmannit, "The effect of core-to-wall ratio and Span 80 concentration on the properties of ascorbic acid microcapsules," in *Journal of Microencapsulation*, 1998.

[121] L. Pudziuvelyte, M. Marksa, V. Jakstas, L. Ivanauskas, D. M. Kopustinskiene and J. Bernatoniene, "Microencapsulation of Elsholtzia ciliata Herb Ethanolic Extract by Spray-Drying: Impact of Resistant-Maltodextrin Complemented with Sodium Caseinate, Skim Milk, and Beta-Cyclodextrin on the Quality of Spray-Dried Powders".

[122] S. C. Chew, C. P. Tan and K. Lin Nyam, "Microencapsulation of refined kenaf (Hibiscus cannabinus L.) seed oil by spray drying using β-cyclodextrin/gum arabic/sodium caseinate," 2018.

[123] R. Zhang, L. Huang, X. Xiong, M. C. Qian and H. Ji, "Preparation and release mechanism of lavender oil microcapsules with different combinations of coating materials," *Flavour and Fragrance Journal,* vol. 35, no. 2, pp. 157-166, 24 3 2020.

[124] X. Bai, C. Li, L. Yu, Y. Jiang, M. Wang, S. Lang and D. Liu, "Development and characterization of soybean oil microcapsules employing kafirin and sodium caseinate as wall materials," 2019.

[125] "1-Octenylsuccinic anhydride | C12H18O3 - PubChem," [Online]. Available: https://pubchem.ncbi.nlm.nih.gov/compound/1-Octenylsuccinic-anhydride.

[126] M. Dul, K. J. Paluch, H. Kelly, A. M. Healy, A. Sasse and L. Tajber, "Self-assembled carrageenan/protamine polyelectrolyte nanoplexes-Investigation of critical parameters governing their formation and characteristics," *Carbohydrate Polymers,* vol. 123, pp. 339-349, 2015.

[127] "Sodium caseinate - ZellBio GmbH," [Online]. Available: https://www.zellbio.eu/product/sodium-caseinate/.

[128] H. Wang, X. Tong, Y. Yuan, X. Peng, Q. Zhang, S. Zhang, C. Xie, X. Zhang, S. Yan, J. Xu, L. Jiang, B. Qi and Y. Li, "Effect of Spray-Drying and Freeze-Drying on the Properties of Soybean Hydrolysates," 2020.

[129] C. Anandharamakrishnan, Spray drying technique for food ingredient encapsulation, 2015.

CHAPTER 3: Effect of Zein Concentration and Flow Rate on Particle Size and Polydispersity Index of Aqueous Zein Nanoparticles Generated by Novel 3-Fluid Nozzle Design

3.1 Abstract

Zein nano particle suspensions were successfully prepared via a fabricated chip to evaluate the proposed 3-fluid nozzle design. Initial zein concentration (*2%/4%/6%/8%*) and total flow rate (*2/4/8 mL/min)* were both varied to elucidate the respective effects on particle size and Polydispersity Index (PDI). Particle sizes ranged from 172.5 nm – 202.2 nm and PDI ranged from 0.0657 – 0.171, however no particles were generated at 8% initial zein concentration due to plugging of the apparatus. Both initial zein concentration and total flow rate were shown to have a significant effect on both particle size and PDI. As zein concentration increased, both particle size and PDI increased; as the total flow rate increased, particle size decreased while PDI increased.

These results indicate that the proposed nozzle technology not only generates nano-scale (<205 nm) zein particles but also generates relatively narrow particle size distributions per the reported PDI. The proposed technology also allowed for the tuning of both particle size and distribution. Mass flow rate may be a key driver for both particle properties given the significant effects for concentration and flow rate that were observed. Overall, the zein particle generation method proposed with the novel 3-fluid nozzle design shows a promise for scale-up into actual spray-drying applications.

3.2 Introduction

Due to its characteristic self-assembling interaction, zein has been widely studied as a molecule of interest in encapsulation studies and, more broadly, in polymer science [1, 2]. Due to its tertiary structure, zein readily assembles into both micelles and films via a simple anti-solvent precipitation process; as the solvent concentration approaches the solubility limit for zein (in most cases ethanol/water at 50% v/v), the hydrophobic amino acid residues of zein will fold inward into α-helical structures with the more polar glutamine “bridges” between these helices interacting at the zein/fluid interface as well as with other zein molecules [3, 4]. Encapsulation is achieved when the zein micellular structures interact with the targeted core material to effectively shield it from the surrounding environment.

Recently, microfluidics has been increasingly studied as a means for achieving extremely homogenous zein nanoparticles and/or capsules [5, 6, 7, 8, 9]. Due to the laminar flow regime seen in the micron sized channels, as well as unmatched process control response, particles can essentially be tailor-made to a certain mean diameter and/or polydispersity index (PDI). Critically, for controlled release applications, PDI is one of key factors for the release profile of the encapsulated core material [10, 11, 12, 13]. If the PDI is too high (>0.7) the resultant particles are typically not usable for delivery of the core compound, as the variance in surface area to volume leads to unstable release kinetics. Typically, PDI below 0.2 – 0.3 are considered ideal for these types of controlled release applications [13].

Microfluidics provides the means to achieve low particle sizes and distributions; however, it lacks the ability to scale to a meaningful level of throughput. While the

pharmaceutical industry often only needs miniscule amounts of active ingredient to load into a medication, food manufacturers often operate at economies of scale to offset the low margins often seen in food production. Microfluidic preparation of encapsulated compounds for use in foods is therefore not ideal for most commercial applications, as many micro-channels operating in parallel would be required.

Spray-drying, on the other hand, has a wide history of use in the food industry dating back to World War 2, where it was co-opted by the dairy industry for dried milk powder production [14, 15, 16]. It offers superior throughput to microfluidic production and is also highly customizable with regards to operating parameters. However, while it is possible to tune the size of spray-dried particles, it is less achievable to control the particle size distribution, which is often quite broad, rendering it less amenable to the production of microcapsules with stable release kinetics [17].

One of the means of controlling the particle characteristics in spray-drying is the nozzle assembly used to atomize the liquid feedstock into small droplets upon entry into the spray-drying chamber. The atomization process is critical to allow for rapid, even drying of the feed by promoting a larger surface area over which convective heat and mass transfer can occur. Many different atomizing nozzle designs exist, from hydraulic nozzles that atomize only via a large pressure drop across the nozzle orifice, to air-assisted nozzles that use a pressurized gas (usually air or nitrogen) to blast the liquid feedstock into small particles as it leaves the nozzle tip [18]. The pressurized gas assisted “2-fluid nozzles” are often used for applications with highly viscous or high total solids materials as they are less prone to plugging, which most food applications fall into.

More recent studies have also focused on “3-fluid nozzles”, which still use pressurized gas for atomization, but have two separate liquid channels that mix at the nozzle tip interface. Some research has suggested these may provide favorable encapsulation characteristics by allowing a shell material in the outer liquid channel to coat a core material in the inner liquid channel as the atomized feedstock is dried. Emerging research supporting their use in the pharmaceutical industry as well as the food industry indicates the technology holds promise specifically for encapsulation applications [19, 20, 21, 22, 23].

The nozzle design proposed in this study involves the mixing of both microfluidic and spray-drying nozzle technologies; the inner-most liquid nozzle in a 3-fluid nozzle will be shortened, effectively producing an internal contact time between the continuous and dispersed phases used in encapsulation. This setup mimics a flow-focusing microfluidics chip, and though the channels are several thousand times larger (mm instead of μm), the same laminar fluid dynamics apply. The internal contact time will theoretically allow for complete zein self-assembly *prior* to being spray-dried, which in turn will allow for microcapsules to be generated *in situ* with the same benefits to particle size and PDI that are seen in microfluidic chips.

The objective of this study was to evaluate the proposed 3-fluid nozzle design with a scaled-down chip that was fabricated to mimic the contact time and flow rates that would be used in the actual spray-drying nozzle. The hypothesis of this study is that the proposed 3-fluid nozzle will allow for the formation of nano-scale zein particles with a low PDI (<0.2) and will also allow for tunable particle size and PDI based on the process parameters used during assembly.

3.3 Materials and Methods

3.3.1 Materials

Zein was procured from MilliporeSigma (Merck KGaA, Burlington, MA). It is a dark yellow solid that consists of all four known fractions of zein (α, β, γ, δ). 200 proof ethanol was supplied by Decon Laboratories (DLI, Chester, PA) and was diluted to the appropriate concentration with de-ionized water from an in-house filtering system. Two Harvard PHD 2000 syringe pumps (HA, Holliston, MA) were used to deliver the continuous and dispersed phase to the nozzle simulation chip.

The nozzle simulation chip was fabricated using two optically clear polycarbonate sheets supplied by Grainger (GWW, Lake Forest, IL). Channel radii were milled into each sheet such that when they were pressed together, a full circular channel was created; the inner channel diameter is 0.5 mm, the outer channel diameter is 1 mm, and the joined channel diameter is 2 mm. These dimensions were chosen to mimic the geometry of the stock 3-fluid nozzle supplied from Buchi (Buchi, Switzerland). Stock 316 stainless steel was used to make two cut-outs such that the channels would still be visible during experimental operation. A bolt arrangement was milled into both the polycarbonate sheets and steel cut-outs, with one steel cut-out being threaded to facilitate assembly. Generic polytetrafluoroethylene (PTFE) thread tape was used to seal each of the edges of the chip, and a USP grade lubricant supplied by McGlaughlin Oil Company (MOC, Livingston, OH) was applied to the flat planes of the polycarbonate sheets prior to being bolted together; these precautions were taken to prevent air infiltration into the channels during operation. Images of the fully assembled chip can be found in Figure 3.1.

3.3.2 Methods

3.3.2.1 Nanoparticle Production

Zein stock solutions were prepared by first diluting 200 proof ethanol to ~70% v/v with de-ionized water. The ethanol solution was placed on a magnetic stir plate and set to stir at ~300 rpm and allowed to briefly mix. While being continuously stirred, powdered zein was slowly added to the ethanol solution at the appropriate mass concentration corresponding to the formulas found in Table 3.1. The solution was covered with parafilm and allowed to stir overnight (or at a minimum 8 hours) to allow the zein to fully hydrate and dissolve.

For the continuous phase, 500 mL of de-ionized water was measured into a clean beaker. 30 mL of the zein stock solution (the dispersed phase) was then loaded into a 50 mL BD luer lock syringe, placed into one of the syringe pumps, and plumbed to the middle channel of the nozzle simulation chip. 50 mL of de-ionized water was then loaded into two separate 50 mL BD luer lock syringes; both syringes were placed into the second syringe pump and plumbed to the two outer channels of the nozzle simulation chip. The syringe pumps were programmed with the diameter of the BD syringes (26.7 mm) and set to pump at the appropriate flow rate as shown in the experimental design in Table 3.1. The flow ratio was held constant at 3:1 continuous to dispersed phase for all treatments. A diagram of the set-up of the pumps and nozzle simulation chip can be found in Figure 3.2

The experiments began by first starting the continuous phase syringe pumps until flow was established through the outer channels and joined channel of the simulation chip. The dispersed phase syringe pump was then started; collection of the resultant particle suspension began 10 seconds after the first visibly turbid droplet was

discharged from the joined channel of the simulation chip. 20 mL of suspended zein particles were collected per experiment. The nozzle simulation chip was then thoroughly cleaned with de-ionized water and 70% ethanol solution. In between treatment groups, the chip was completely disassembled, cleaned with 70% ethanol, and re-sealed with PTFE tape and food-grade mineral oil.

3.3.2.2 Dynamic Light Scattering

Particle size and polydispersity index (PDI) of the resultant zein particle suspensions were measured using a ZetaPALS Dynamic Light Scattering (DLS) detector from Brookhaven (BIC, Holtsville, NY). PDI is defined as the ratio of weight average (M_w) to number average (M_n) of molecular weight, shown in Equation 1 below [13].

$$PDI = \frac{M_w}{M_n} \quad [1]$$

Samples were diluted 40:1 with de-ionized water that had been adjusted to approximately pH 3.4 using 1 M HCl; this pH is consistent with the pH of the particle suspensions collected from the nozzle simulation chip. The isoelectric point of zein, where it will have the highest tendency to aggregate, is about pH 6.8; therefore, using an acid-adjusted diluent will mitigate any possible agglomeration of particles prior to the measurement. Diluted samples were then added to disposable 1 cm plastic cuvets supplied by Fisher (TFS, Waltham, MA) before being loaded into the measuring cell of the DLS. A refractive index (RI) of 1.49 and a viscosity of 1 cP were used for the DLS algorithm programming; these are equivalent to the RI of zein and viscosity of water,

respectively. Mean particle size and PDI were recorded for each sample after convergence of 5.0 x 10^{-3} was reached.

3.3.2.3 Statistics

Statistical analyses were conducted with the R programming language in an RStudio environment. ANOVA was used to evaluate mean differences between treatment groups; the Shapiro-Wilkes test was used to confirm normality of residuals and the Levene-Forsythe test was used to confirm homogeneity of variance prior to ANOVA being conducted. For the particle size data, it was found that the residuals were not normally distributed; a Box-Cox procedure was run and the data was exponentially transformed to the -2 power. Residuals were re-tested and found to be normal. All *post-hoc* mean separation tests were conducted using Tukey's HSD within R. All statistical plots were generated in R via the "ggplot" package of data visualization functions. Raw statistical outputs have been included in section 3.7 of this chapter.

3.4 Results and Discussion

Zein particles at nano-scale were successfully produced at each of the flow and concentration levels tested with the exception of the 8% w/w zein concentration. At all flow conditions with 8% w/w zein concentration, the nozzle simulation chip clogged with agglomerated zein that required complete shutdown and disassembly of the nozzle simulation chip. As such, no data is reported for 8% w/w zein concentration.

3.4.1 Mean Particle Size

Mean particle sizes are listed in Table 3.2. Mean particle size ranged from 172.5 nm – 202.2 nm, and a significant effect of both initial zein concentration and total flow rate was observed with no significant interaction at $p < 0.05$. Treatment groups were also detected as having statistically different mean particle sizes at $p < 0.05$.

Importantly, all particles generated were on the scale of nanometers (less than 205 nm) in diameter, providing evidence that the “macro-fluidic” assembly approach may be viable to scale to actual spray-drying nozzle technology. These particle sizes are in line with reported particle diameters from studies that generated them via microfluidics [5, 6, 7, 9, 24].

Figures 3.3 and 3.4 illustrate the effect of both total flow rate and initial zein concentration on resultant mean particle size. Mean particle size was statistically lower at the 8 mL/min total flow condition than at 2 mL/min, and in general particle size appears to be negatively correlated with increasing flow rate. With regards to initial zein concentration, particles produced from the 6% w/w zein stock solutions were statistically larger than the 2% w/w treatment group. Mean particle size appears to be positively correlated with increasing initial zein concentration. The smallest zein nanoparticles were produced at the C2F8 treatment level with a mean particle diameter of 137.3 nm with the largest particles produced at the C6F2 treatment level with a mean particle diameter of 261.3 nm. Figures 3.5 and 3.6 are plots of mean particle size with standard error and the 95% confidence interval, respectively.

These results agree with a microfluidic assembly study done with zein and anti-solvent precipitation [25]. That study proposes that the system pressure is most heavily correlated with resultant nano-particle size; however, it is unknown if the same magnitude of pressure change is seen in the macro-scale channels of the simulation chip compared to the microfluidic apparatus. Increasing total flow rate will also cause the mass transfer boundary layer to be thinner, increasing the diffusive rate of ethanol into antisolvent and facilitating more rapid self-assembly. This increase in kinetics may

lead to smaller particles. It should be noted that the laminar flow regime was observed in all trials, ruling out transitional flow as being responsible for the observed differences.

With regards to the effect of the initial concentration of zein on the resultant particle size, the rate of mass transfer may be also responsible for the observed increase in particle size at higher zein concentrations. The viscosity of the zein solution increases with increasing concentrations of zein, lowering the diffusion constant of ethanol into the anti-solvent and increasing the time it takes to reach the solubility limit at which time self-assembly would occur. It is also possible that an increase in number density of particles per unit area within the channel may lead to more aggregation of nanoparticles prior to hardening completely in the anti-solvent media.

3.4.2 Polydispersity Index (PDI)

Table 3.3 summarizes the PDI at each treatment level. Mean PDI was statistically different across at least one treatment level in both concentration and flow condition treatment levels at $p < 0.05$. No significant interaction between flow and concentration was observed. Individual treatment levels were also detected as having significantly different PDI's at $p < 0.05$. Importantly, mean PDI at all treatment levels was < 0.2, indicating that the "macro-scale" assembly approach is capable of producing mono-disperse solutions of nanoparticles, which could be an important factor for its use in spray-drying nozzle technology to facilitate more uniformly dispersed dried powders. Again these PDI tend to match up with ranges found in other studies carried out with microfluidic chips [5, 6, 7, 9, 24].

Figures 3.7 and 3.8 illustrate the effect of total flow rate and initial zein concentration on PDI, respectively. The PDI of the nanoparticle dispersions was

statistically higher at the 8 mL/min flow treatment than at the 2 mL/min treatment level. The total flow rate appears to be positively correlated with PDI. Observed PDI's were statistically lower at the 2% w/w zein treatment group than at 8% w/w zein, and the initial zein concentration appears to be positively correlated with PDI. The lowest PDI occurred at the C2F2 treatment level with a value of 0.0657 ± 0.0254; the highest PDI occurred at the C6F8 treatment level with a value of 0.171 ± 0.0480. Figures 3.9 and 3.10 plots of PDI with standard error and the 95% confidence interval, respectively.

These results also agree with the microfluidic study [25], which saw increasing PDI with increasing flow rate within the microfluidics chip and again proposed total system pressure change as the key driver for PDI during microfluidic particle assembly. As discussed for particle size, mass transfer may have impacted PDI as well. The increased kinetic drive for convective mass transfer at higher flow rates responsible for generating smaller particles could also be responsible for more rapid hardening of the particle surfaces. This rapid hardening would in turn limit the extent of particle aggregation, which may play a part in creating more uniform distributions. Small particles (< 50-100 nm) may be more prone to agglomerate into particles that are more similar in size to the overall mean particle size, reducing variability in the resulting distribution.

Interestingly, though there would also be an increased drive for mass transfer at the lower initial zein concentrations due to a higher rate of diffusion, the lower initial zein concentrations resulted in lower PDI than at higher initial zein concentrations. This trend could suggest that, instead of the rate of convective mass transfer, the mass flow rate could be a more effective parameter to control PDI. Due to higher total solids,

treatments with a higher initial zein concentration will result in a higher rate of mass transfer at the same flow rate than treatments with lower zein concentrations. It therefore appears that the higher the mass flux through the system, the higher the resultant PDI of the nanoparticle suspension is, which could be an important parameter when designing process parameters for the proposed nozzle technology.

3.5 Conclusions

The nozzle simulation chip was successfully able to generate mono-disperse (PDI < 0.200) zein nanoparticles by varying total flow rates and initial zein concentrations. By adjusting these two process parameters, significantly different particle sizes and PDI can be achieved. Higher flow rates and lower initial zein concentrations led to smaller mean particle sizes for the zein nanoparticles; whereas, both lower flow rates and lower initial zein concentrations led to smaller PDI's of the zein nanoparticle distributions. These results are encouraging proof-of-concept for the proposed nozzle technology, as it offers the ability to not only create uniformly small particles of zein, but also the ability to tune the final physical characteristics of the particles to best fit the potential encapsulation application. It is therefore possible that the hallmark large particle size and wide distribution seen in spray-drying may be able to be counteracted by the proposed nozzle technology.

3.6 Figures and Tables

Table 3.1 – Experimental Design

Treatment Code	Initial Zein Concentration (% w/w)	Total Flow Rate (mL/min)
C2F2	2	2
C2F4	2	4
C2F8	2	8
C4F2	4	2
C4F4	4	4
C4F8	4	8
C6F2	6	2
C6F4	6	4
C6F8	6	8

Table 3.2 – Mean Particle Size by Treatment Level

Treatment Code	Mean Particle Size (nm)
C2F2	172.5 ± 9.2^{bc}
C2F4	155.0 ± 3.0^{ab}
C2F8	137.3 ± 6.9^{a}
C4F2	217.7 ± 35.1^{cd}
C4F4	195.6 ± 40.2^{bcd}
C4F8	171.9 ± 27.4^{cd}
C6F2	261.3 ± 34.9^{d}
C6F4	243.0 ± 41.9^{cd}
C6F8	202.2 ± 19.2^{bcd}

Table 3.3 – Mean PDI by Treatment Level

Treatment Code	PDI
C2F2	0.0657 ± 0.025^{a}
C2F2	0.101 ± 0.028^{ab}
C2F2	0.144 ± 0.022^{ab}
C4F4	0.118 ± 0.032^{ab}
C4F4	0.129 ± 0.050^{ab}
C4F4	0.166 ± 0.022^{b}
C6F8	0.149 ± 0.024^{ab}
C6F8	0.136 ± 0.028^{ab}
C6F8	0.171 ± 0.048^{b}

Figure 3.1 – Fully Assembled Nozzle Simulation Chip

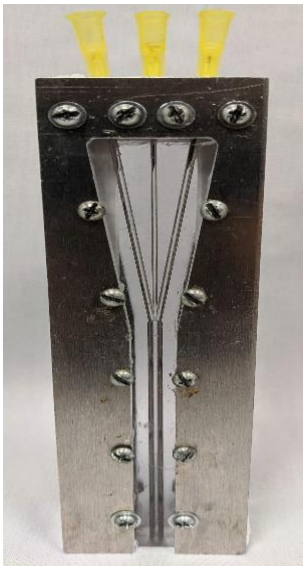

Figure 3.2 – Process Flow of Nozzle Simulation Chip Trials

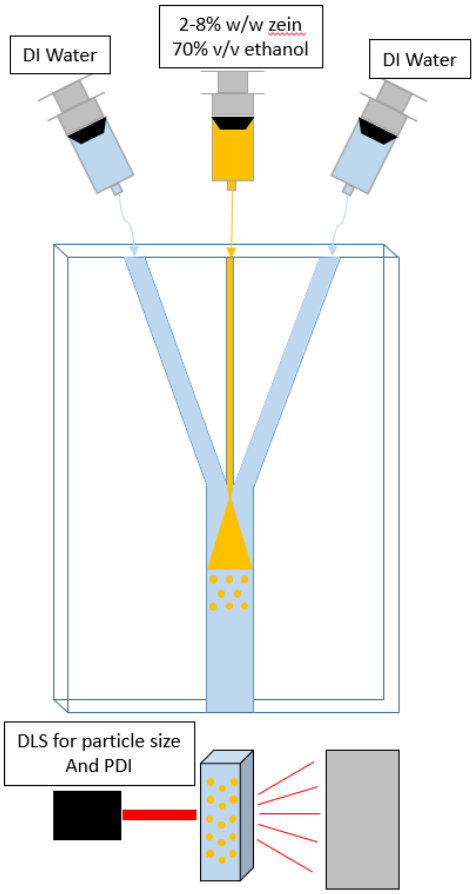

Figure 3.3 – Flow Rate Effect on Mean Particle Size

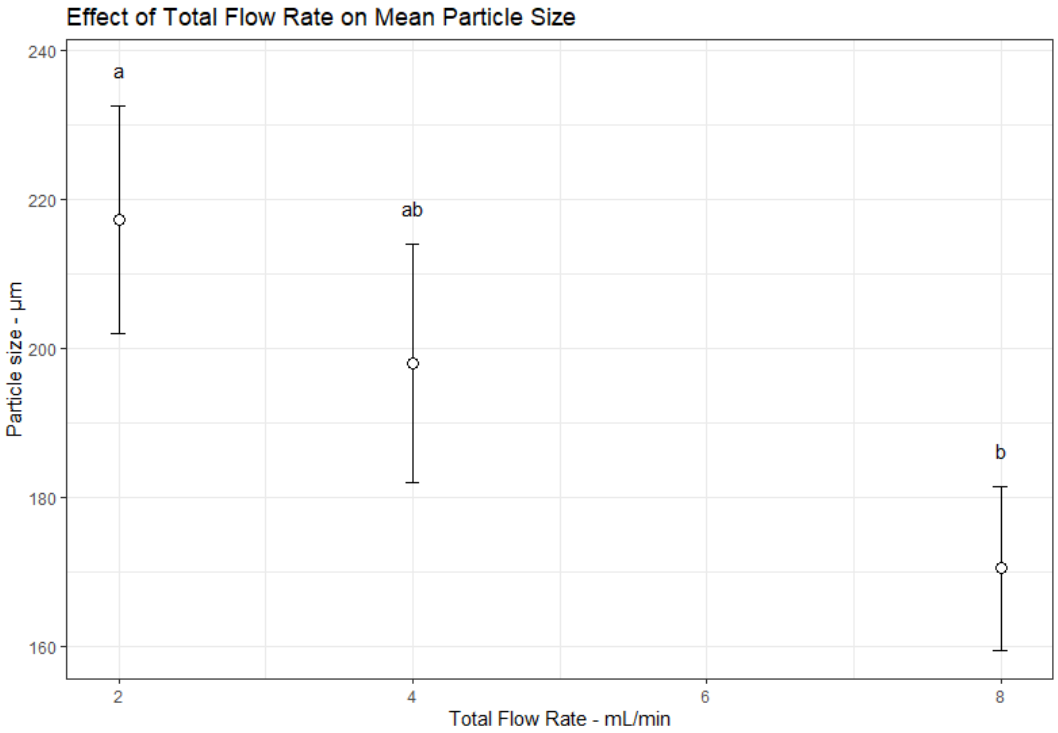

Figure 3.4 – Zein Concentration Effect on Mean Particle Size

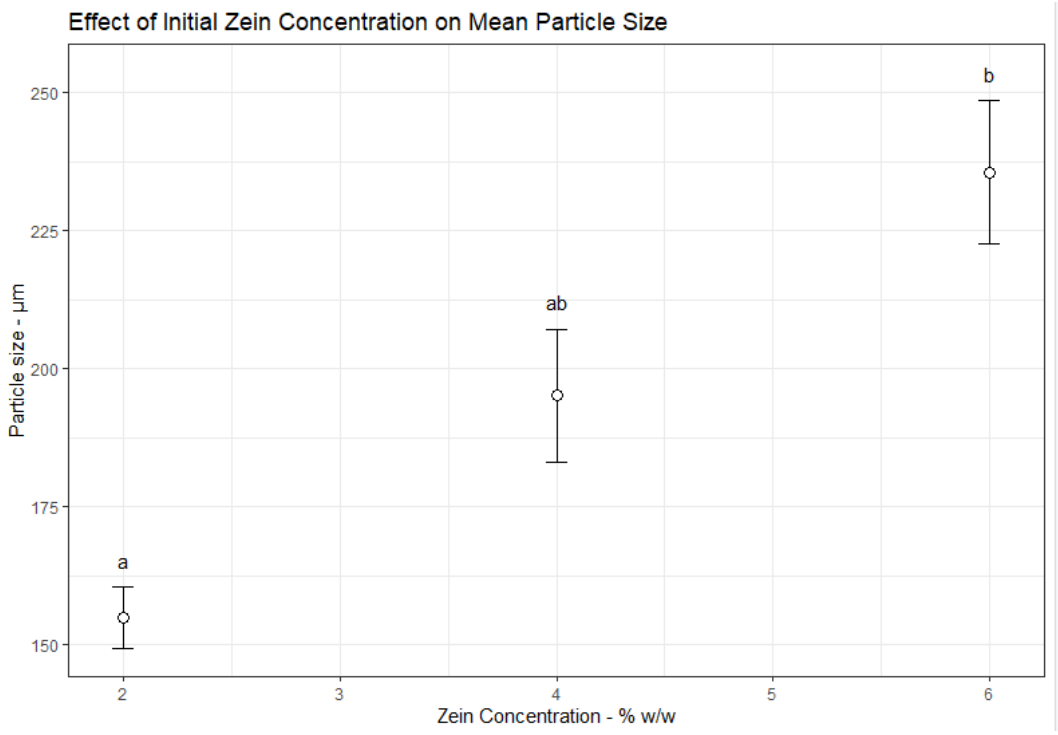

Figure 3.5 – Mean Particle Size by Treatment Group

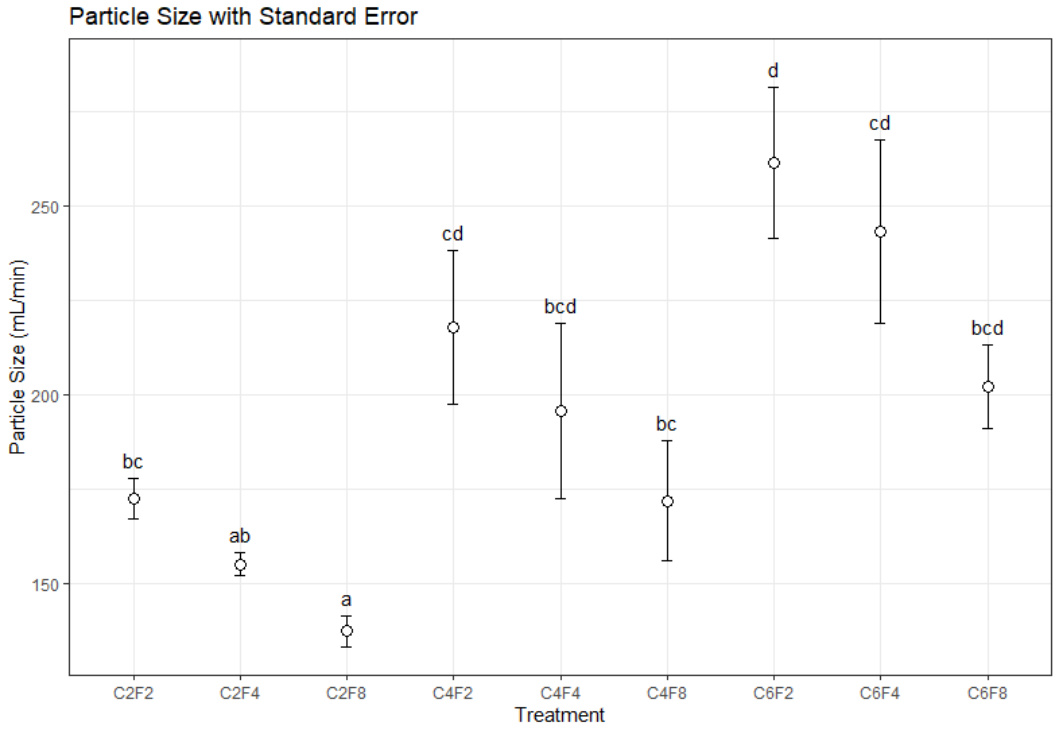

Figure 3.6 – 95% Confidence Interval for Mean Particle Size

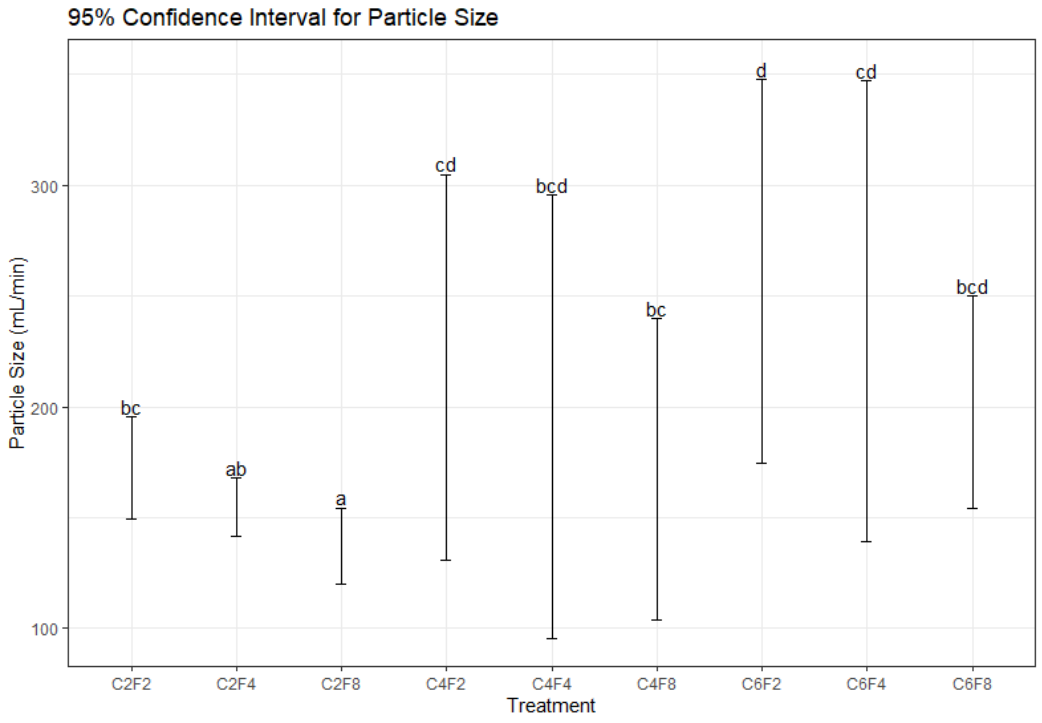

Figure 3.7 – Total Flow Rate Effect on Polydispersity Index

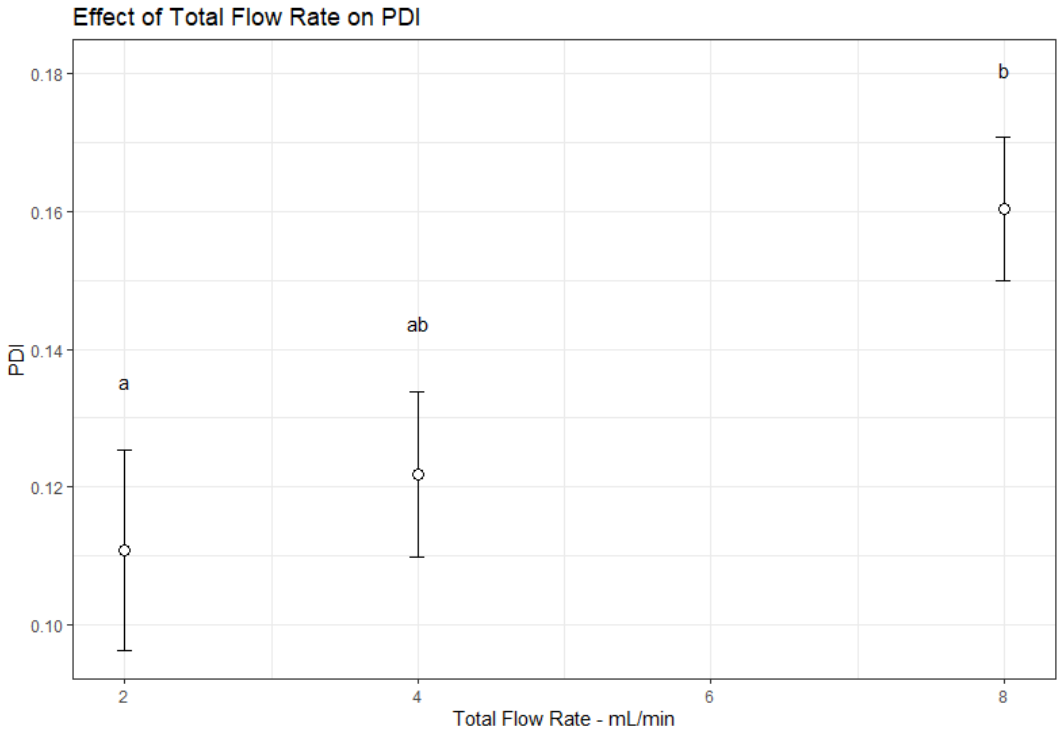

Figure 3.8 – Zein Concentration Effect on Polydispersity Index

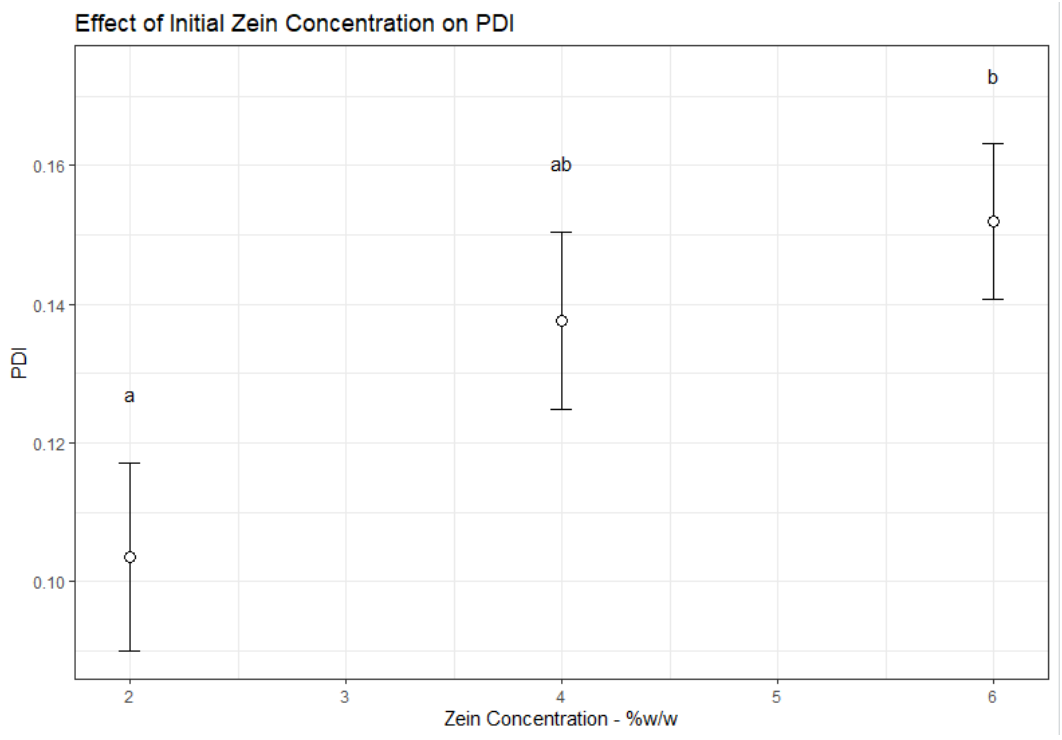

Figure 3.9 – Polydispersity Index by Treatment Group

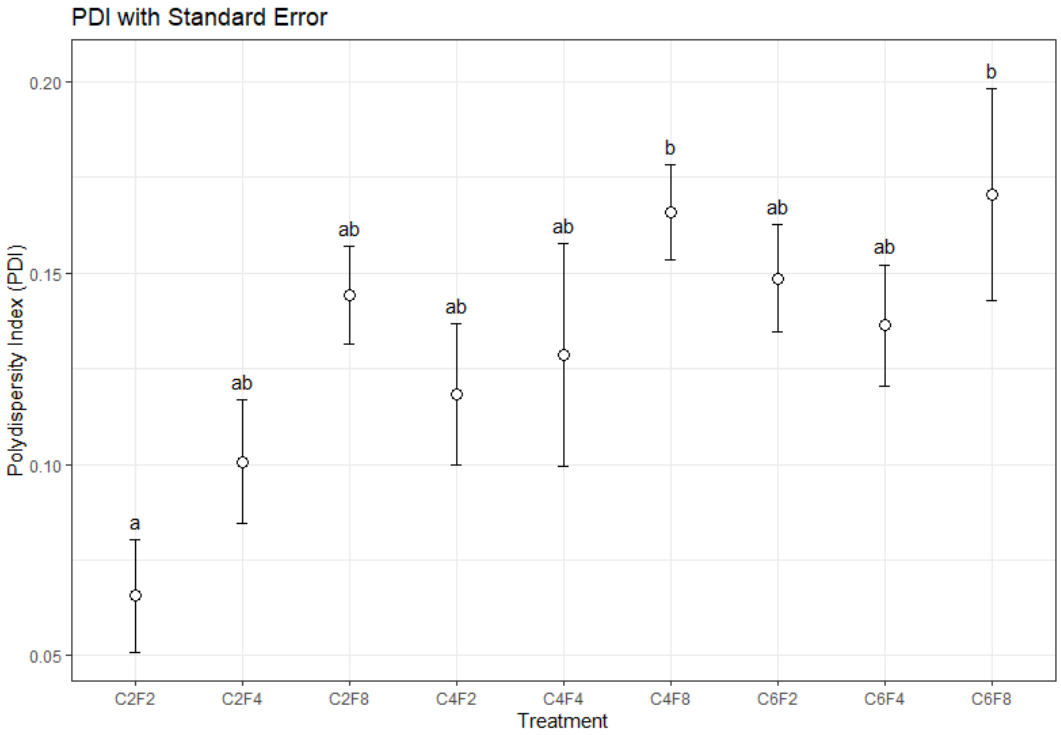

Figure 3.10 – 95% Confidence Interval for Polydispersity Index

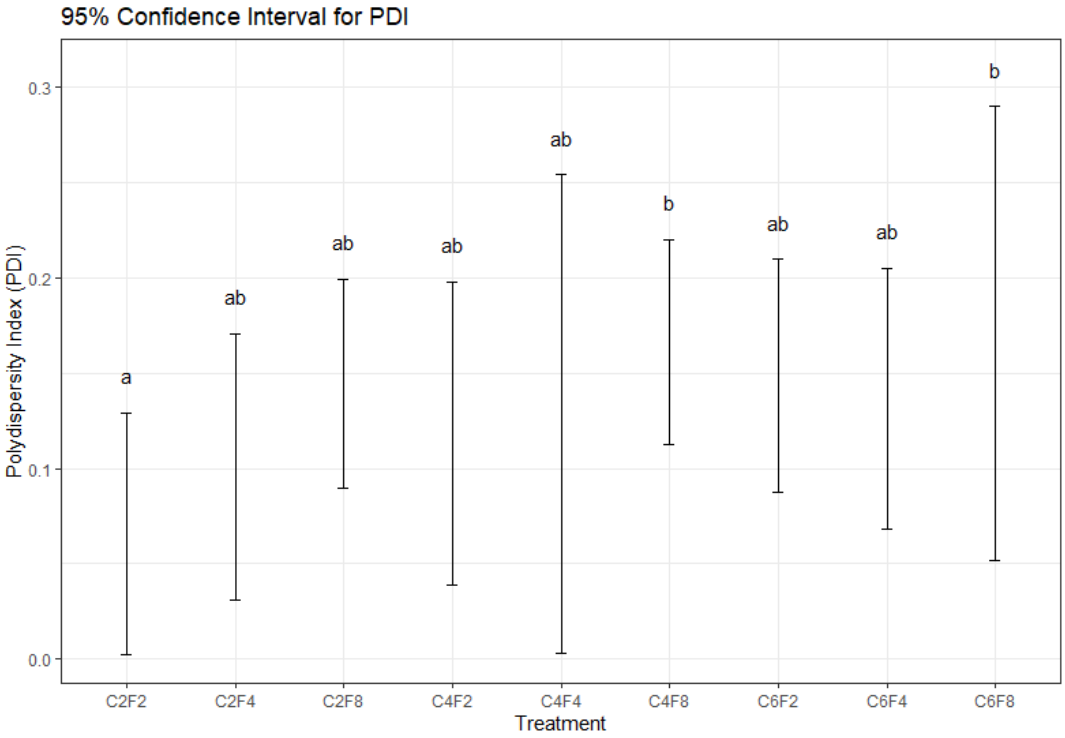

3.7 Raw Statistical Output

3.7.1 – Box-Cox Procedure for Particle Size

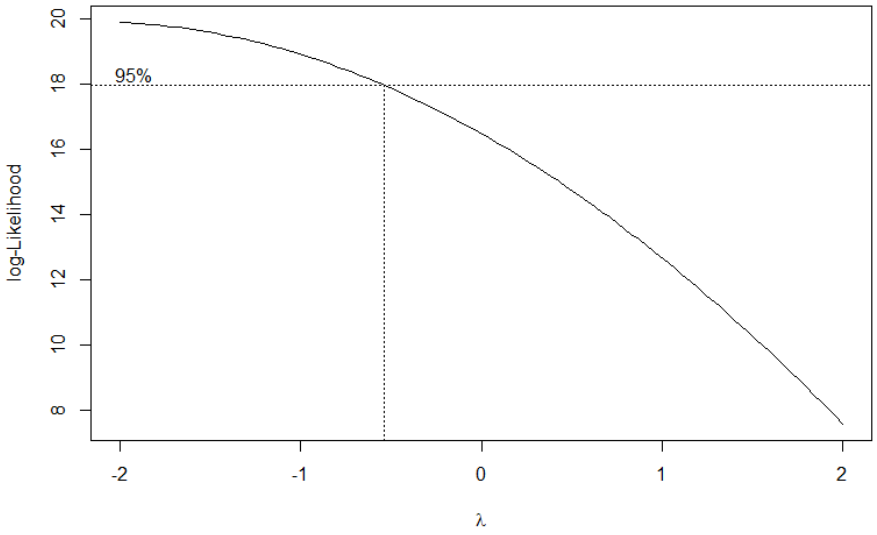

3.7.2 – 2-Way ANOVA for Particle Size

```
Analysis of Variance Table

Response: pstrans
                    Df     Sum Sq    Mean Sq F value    Pr(>F)
Flow                 2 9.2183e-10 4.6091e-10 11.8844 0.0005126 ***
Concentration        2 2.5523e-09 1.2761e-09 32.9041 9.725e-07 ***
Flow:Concentration   4 7.5770e-11 1.8940e-11  0.4884 0.7442027
Residuals           18 6.9810e-10 3.8780e-11
---
Signif. codes:  0 '***' 0.001 '**' 0.01 '*' 0.05 '.' 0.1 ' ' 1
```

3.7.3 – 2-Way ANOVA for PDI

```
Analysis of Variance Table

Response: PDI
                    Df    Sum Sq   Mean Sq F value  Pr(>F)
Flow                 2 0.0121312 0.0060656  5.6796 0.01224 *
Concentration        2 0.0111059 0.0055529  5.1995 0.01651 *
Flow:Concentration   4 0.0027766 0.0006941  0.6500 0.63423
Residuals           18 0.0192233 0.0010680
---
Signif. codes:  0 '***' 0.001 '**' 0.01 '*' 0.05 '.' 0.1 ' ' 1
```

3.7.4 – Mean Separation for Particle Size ~ Concentration

```
 Concentration   lsmean       SE df lower.CL upper.CL
 Four          2.86e-05 2.08e-06 18 2.31e-05 3.40e-05
 Six           1.93e-05 2.08e-06 18 1.38e-05 2.48e-05
 Two           4.29e-05 2.08e-06 18 3.75e-05 4.84e-05

Results are averaged over the levels of: Flow
Confidence level used: 0.95
Conf-level adjustment: sidak method for 3 estimates

$contrasts
 contrast    estimate       SE df t.ratio p.value
 Four - Six  9.27e-06 2.94e-06 18  3.157  0.0143
 Four - Two -1.44e-05 2.94e-06 18 -4.893  0.0003
 Six - Two  -2.36e-05 2.94e-06 18 -8.050  <.0001

Results are averaged over the levels of: Flow
P value adjustment: tukey method for comparing a family of 3 estimates
```

3.7.5 – Mean Separation for Particle Size ~ Flow

```
 Flow    lsmean       SE df lower.CL upper.CL
 Eight 3.79e-05 2.08e-06 18 3.24e-05 4.33e-05
 Four  2.93e-05 2.08e-06 18 2.38e-05 3.47e-05
 Two   2.37e-05 2.08e-06 18 1.82e-05 2.91e-05

Results are averaged over the levels of: Concentration
Confidence level used: 0.95
Conf-level adjustment: sidak method for 3 estimates

$contrasts
 contrast     estimate       SE df t.ratio p.value
 Eight - Four 8.60e-06 2.94e-06 18 2.930   0.0231
 Eight - Two  1.42e-05 2.94e-06 18 4.840   0.0004
 Four - Two   5.60e-06 2.94e-06 18 1.909   0.1648

Results are averaged over the levels of: Concentration
P value adjustment: tukey method for comparing a family of 3 estimates
```

3.7.6 – Mean Separation for PDI ~ Concentration

```
 Concentration lsmean     SE df lower.CL upper.CL
 Four           0.138 0.0109 18   0.1090    0.166
 Six            0.152 0.0109 18   0.1232    0.181
 Two            0.104 0.0109 18   0.0749    0.132

Results are averaged over the levels of: Flow
Confidence level used: 0.95
Conf-level adjustment: sidak method for 3 estimates

$contrasts
 contrast   estimate     SE df t.ratio p.value
 Four - Six  -0.0142 0.0154 18 -0.923  0.6331
 Four - Two   0.0341 0.0154 18  2.214  0.0957
 Six - Two    0.0483 0.0154 18  3.137  0.0150

Results are averaged over the levels of: Flow
P value adjustment: tukey method for comparing a family of 3 estimates
```

3.7.7 – Mean Separation for PDI ~ Flow

```
 Flow  lsmean     SE df lower.CL upper.CL
 Eight  0.160 0.0109 18   0.1317    0.189
 Four   0.122 0.0109 18   0.0932    0.151
 Two    0.111 0.0109 18   0.0822    0.140

Results are averaged over the levels of: Concentration
Confidence level used: 0.95
Conf-level adjustment: sidak method for 3 estimates

$contrasts
 contrast     estimate     SE df t.ratio p.value
 Eight - Four   0.0384 0.0154 18 2.496   0.0559
 Eight - Two    0.0494 0.0154 18 3.210   0.0128
 Four - Two     0.0110 0.0154 18 0.714   0.7584

Results are averaged over the levels of: Concentration
P value adjustment: tukey method for comparing a family of 3 estimates
```

3.7.8 – One-Way ANOVA for Particle Size

```
Analysis of Variance Table

Response: pstrans2
          Df     Sum Sq    Mean Sq F value    Pr(>F)
Treatment  8 3.5498e-09 4.4373e-10  11.441 1.191e-05 ***
Residuals 18 6.9810e-10 3.8780e-11
---
Signif. codes:  0 ‘***’ 0.001 ‘**’ 0.01 ‘*’ 0.05 ‘.’ 0.1 ‘ ’ 1
```

3.7.9 – One-Way ANOVA for PDI

```
Analysis of Variance Table

Response: PDI
          Df   Sum Sq   Mean Sq F value  Pr(>F)
Treatment  8 0.026014 0.0032517  3.0448 0.02369 *
Residuals 18 0.019223 0.0010680
---
Signif. codes:  0 ‘***’ 0.001 ‘**’ 0.01 ‘*’ 0.05 ‘.’ 0.1 ‘ ’ 1
```

3.7.10 – Mean Separation for Particle Size

contrast	estimate	SE	df	t.ratio	p.value
C1F1 - C1F2	-7.96e-06	5.08e-06	18	-1.565	0.8107
C1F1 - C1F3	-1.95e-05	5.08e-06	18	-3.839	0.0256
C1F1 - C2F1	1.17e-05	5.08e-06	18	2.297	0.3923
C1F1 - C2F2	5.59e-06	5.08e-06	18	1.099	0.9670
C1F1 - C2F3	-1.66e-06	5.08e-06	18	-0.326	1.0000
C1F1 - C3F1	1.86e-05	5.08e-06	18	3.668	0.0362
C1F1 - C3F2	1.59e-05	5.08e-06	18	3.124	0.1029
C1F1 - C3F3	8.88e-06	5.08e-06	18	1.747	0.7127
C1F2 - C1F3	-1.16e-05	5.08e-06	18	-2.274	0.4043
C1F2 - C2F1	1.96e-05	5.08e-06	18	3.862	0.0245
C1F2 - C2F2	1.35e-05	5.08e-06	18	2.664	0.2277
C1F2 - C2F3	6.30e-06	5.08e-06	18	1.240	0.9363
C1F2 - C3F1	2.66e-05	5.08e-06	18	5.233	0.0015
C1F2 - C3F2	2.38e-05	5.08e-06	18	4.689	0.0045
C1F2 - C3F3	1.68e-05	5.08e-06	18	3.312	0.0723
C1F3 - C2F1	3.12e-05	5.08e-06	18	6.136	0.0002
C1F3 - C2F2	2.51e-05	5.08e-06	18	4.938	0.0027
C1F3 - C2F3	1.79e-05	5.08e-06	18	3.514	0.0490
C1F3 - C3F1	3.82e-05	5.08e-06	18	7.507	<.0001
C1F3 - C3F2	3.54e-05	5.08e-06	18	6.963	<.0001
C1F3 - C3F3	2.84e-05	5.08e-06	18	5.587	0.0007
C2F1 - C2F2	-6.09e-06	5.08e-06	18	-1.198	0.9469
C2F1 - C2F3	-1.33e-05	5.08e-06	18	-2.622	0.2434
C2F1 - C3F1	6.97e-06	5.08e-06	18	1.371	0.8947
C2F1 - C3F2	4.21e-06	5.08e-06	18	0.827	0.9943
C2F1 - C3F3	-2.79e-06	5.08e-06	18	-0.550	0.9997
C2F2 - C2F3	-7.24e-06	5.08e-06	18	-1.425	0.8740
C2F2 - C3F1	1.31e-05	5.08e-06	18	2.569	0.2647
C2F2 - C3F2	1.03e-05	5.08e-06	18	2.025	0.5469
C2F2 - C3F3	3.30e-06	5.08e-06	18	0.648	0.9989
C2F3 - C3F1	2.03e-05	5.08e-06	18	3.993	0.0188
C2F3 - C3F2	1.75e-05	5.08e-06	18	3.450	0.0556
C2F3 - C3F3	1.05e-05	5.08e-06	18	2.073	0.5182
C3F1 - C3F2	-2.77e-06	5.08e-06	18	-0.544	0.9997
C3F1 - C3F3	-9.77e-06	5.08e-06	18	-1.921	0.6097
C3F2 - C3F3	-7.00e-06	5.08e-06	18	-1.377	0.8926

P value adjustment: tukey method for comparing a family of 9 estimates

3.7.11 – Mean Separation for PDI

contrast	estimate	SE	df	t.ratio	p.value
C1F1 - C1F2	-0.03500	0.0267	18	-1.312	0.9151
C1F1 - C1F3	-0.07867	0.0267	18	-2.948	0.1411
C1F1 - C2F1	-0.05267	0.0267	18	-1.974	0.5775
C1F1 - C2F2	-0.06300	0.0267	18	-2.361	0.3592
C1F1 - C2F3	-0.10033	0.0267	18	-3.760	0.0301
C1F1 - C3F1	-0.08300	0.0267	18	-3.111	0.1054
C1F1 - C3F2	-0.07067	0.0267	18	-2.648	0.2335
C1F1 - C3F3	-0.10500	0.0267	18	-3.935	0.0211
C1F2 - C1F3	-0.04367	0.0267	18	-1.637	0.7741
C1F2 - C2F1	-0.01767	0.0267	18	-0.662	0.9987
C1F2 - C2F2	-0.02800	0.0267	18	-1.049	0.9747
C1F2 - C2F3	-0.06533	0.0267	18	-2.449	0.3171
C1F2 - C3F1	-0.04800	0.0267	18	-1.799	0.6825
C1F2 - C3F2	-0.03567	0.0267	18	-1.337	0.9068
C1F2 - C3F3	-0.07000	0.0267	18	-2.623	0.2430
C1F3 - C2F1	0.02600	0.0267	18	0.974	0.9838
C1F3 - C2F2	0.01567	0.0267	18	0.587	0.9995
C1F3 - C2F3	-0.02167	0.0267	18	-0.812	0.9949
C1F3 - C3F1	-0.00433	0.0267	18	-0.162	1.0000
C1F3 - C3F2	0.00800	0.0267	18	0.300	1.0000
C1F3 - C3F3	-0.02633	0.0267	18	-0.987	0.9825
C2F1 - C2F2	-0.01033	0.0267	18	-0.387	1.0000
C2F1 - C2F3	-0.04767	0.0267	18	-1.786	0.6898
C2F1 - C3F1	-0.03033	0.0267	18	-1.137	0.9600
C2F1 - C3F2	-0.01800	0.0267	18	-0.675	0.9986
C2F1 - C3F3	-0.05233	0.0267	18	-1.961	0.5851
C2F2 - C2F3	-0.03733	0.0267	18	-1.399	0.8842
C2F2 - C3F1	-0.02000	0.0267	18	-0.750	0.9970
C2F2 - C3F2	-0.00767	0.0267	18	-0.287	1.0000
C2F2 - C3F3	-0.04200	0.0267	18	-1.574	0.8063
C2F3 - C3F1	0.01733	0.0267	18	0.650	0.9989
C2F3 - C3F2	0.02967	0.0267	18	1.112	0.9647
C2F3 - C3F3	-0.00467	0.0267	18	-0.175	1.0000
C3F1 - C3F2	0.01233	0.0267	18	0.462	0.9999
C3F1 - C3F3	-0.02200	0.0267	18	-0.824	0.9944
C3F2 - C3F3	-0.03433	0.0267	18	-1.287	0.9228

P value adjustment: tukey method for comparing a family of 9 estimates

3.8 References

[1] M. Stanisz, Ł. Klapiszewski and T. Jesionowski, *Recent advances in the fabrication and application of biopolymer-based micro- and nanostructures: A comprehensive review,* vol. 397, Elsevier B.V., 2020, p. 125409.

[2] G. W. Padua and L. V. Guardiola, "Microcapsules Produced from Zein," 2015.

[3] "ZEIN ENCAPSULATION OF AMPHIPHILIC COMPOUNDS".

[4] Y. Wang and G. W. Padua, "Nanoscale Characterization of Zein Self-Assembly," 2012.

[5] Y. Feng and Y. Lee, "Microfluidic assembly of food-grade delivery systems: Toward functional delivery structure design," *Trends in Food Science & Technology,* vol. 86, pp. 465-478, 2019.

[6] Y. Feng and Y. Lee, "Microfluidic fabrication of hollow protein microcapsules for rate-controlled release," *RSC Adv.,* vol. 7, no. 78, pp. 49455-49462, 24 10 2017.

[7] Y. Feng, L. A. Ibarra-Sánchez, L. Luu, M. J. Miller and Y. Lee, "Co-assembly of nisin and zein in microfluidics for enhanced antilisterial activity in Queso Fresco," *LWT,* vol. 111, pp. 355-362, 1 8 2019.

[8] C. Katsakouli, X. Jiang, W. K. Lau, J. L. Rohn and M. Edirisinghe, "Generating Antibacterial Microporous Structures Using Microfluidic Processing," *ACS Omega,* vol. 4, no. 1, pp. 2225-2233, 29 1 2019.

[9] R. Chen, J. E. Wulff and M. G. Moffitt, "Microfluidic Processing Approach to Controlling Drug Delivery Properties of Curcumin-Loaded Block Copolymer Nanoparticles," *Molecular Pharmaceutics,* vol. 15, no. 10, pp. 4517-4528, 1 10 2018.

[10] M. Badran, "FORMULATION AND IN VITRO EVALUATION OF FLUFENAMIC ACID LOADED DEFORMABLE LIPOSOMES FOR IMPROVED SKIN DELIVERY".

[11] C. van Ballegooie, A. Man, I. Andreu, B. D. Gates and D. Yapp, "Using a Microfluidics System to Reproducibly Synthesize Protein Nanoparticles: Factors Contributing to Size, Homogeneity, and Stability," *Processes,* vol. 7, no. 5, p. 290, 15 5 2019.

[12] F. Paulo and L. Santos, "Microencapsulation of caffeic acid and its release using a w/o/w double emulsion method: Assessment of formulation parameters," *Drying Technology,* vol. 37, no. 8, pp. 950-961, 11 6 2019.

[13] M. Danaei, M. Dehghankhold, S. Ataei, F. Hasanzadeh Davarani, R. Javanmard, A. Dokhani, S. Khorasani and M. R. Mozafari, *Impact of particle size and polydispersity index on the clinical applications of lipidic nanocarrier systems,* vol. 10, MDPI AG, 2018.

[14] E. N. Dewi, R. A. Kurniasih, L. Purnamayanti and P. Journal, "Physical Properties of Spirulina Phycocyanin Microencapsulated with Maltodextrin and Carrageenan".

[15] Y. Zhang, X. Pang, S. Zhang, L. Liu, C. Ma, J. Lu and J. Lyu, "Buttermilk as a wall material for microencapsulation of omega-3 oils by spray drying," 2020.

[16] "The Significance of Spray-Drying - IFT.org," [Online]. Available: https://www.ift.org/news-and-publications/food-technology-magazine/issues/2018/april/columns/processing-spray-drying-in-the-food-industry.

[17] Handbook on spray drying applications for food industries, 2019.

[18] "Air Atomizing Spray Pattern | Spraying Systems Co.," [Online]. Available: https://www.spray.com/resources/spraying-basics/spray-patterns/air-atomizing.

[19] K. Kondo, T. Niwa and K. Danjo, "Preparation of sustained-release coated particles by novel microencapsulation method using three-fluid nozzle spray drying technique," 2014.

[20] D. Leng, K. Thanki, C. Foged and M. Yang, "Formulating Inhalable Dry Powders Using Two-Fluid and Three-Fluid Nozzle Spray Drying," *Pharmaceutical Research,* vol. 35, no. 12, pp. 1-11, 1 12 2018.

[21] M. Maria Leena, M. Gover Antoniraj, J. A. Moses and C. Anandharamakrishnan, "Three fluid nozzle spray drying for co-encapsulation and controlled release of curcumin and resveratrol," *Journal of Drug Delivery Science and Technology,* vol. 57, p. 101678, 1 6 2020.

[22] X. Shi and Y. Lee, "Encapsulation of tributyrin with whey protein isolate (WPI) by spray-drying with a three-fluid nozzle," *Journal of Food Engineering,* vol. 281, p. 109992, 1 9 2020.

[23] T. Sunderland, J. G. Kelly and Z. Ramtoola, "Application of a novel 3-fluid nozzle spray drying process for the microencapsulation of therapeutic agents using incompatible drug-polymer solutions," *Archives of Pharmacal Research,* vol. 38, no. 4, pp. 566-573, 1 4 2015.

[24] S. Ebert, C. K. Koo, J. Weiss and D. J. McClements, "Continuous production of core-shell protein nanoparticles by antisolvent precipitation using dual-channel microfluidization: Caseinate-coated zein nanoparticles," *Food Research International,* vol. 92, pp. 48-55, 1 2 2017.

[25] A. Olenskyj, Y. Feng and Y. Lee, "Continuous microfluidic production of zein nanoparticles and correlation of particle size with physical parameters determined using CFD simulation," *Journal of Food Engineering,* vol. 211, pp. 50-59, 10 2017.

CHAPTER 4: Challenges Related to the Scale-Up of the Nozzle Simulation Chip to a Bench-Scale Spray-Dryer

4.1 Abstract

Experiments were conducted to scale-up the work done in the simulation chip to a bench-top spray-drying setup. It was discovered that zein alone tends to agglomerate into a plug that blocks all flow out of the nozzle tip at volumes as little as 20 mL of disperse phase sprayed. Four different surfactants were tried with zein in an attempt to mitigate the nozzle plugging during spray-drying operations. I-carrageenan failed to generate a stable suspension of nanoparticles when tested in the nozzle simulation chip. OSA-modified starch at a mass ratio of 4:1 starch:zein successfully stabilized zein nanoparticles in the simulation chip, but failed to prevent agglomeration at the nozzle tip during spray-drying.

Span 80 and sodium caseinate were then both tried directly in the spray-dryer. Span 80 at a 1:1 mass ratio completely mitigated the nozzle plugging issue, while sodium caseinate at a 1.25:1 mass ratio of caseinate:zein required a pH adjustment and a split addition of sodium caseinate to both continuous and dispersed phases to accomplish the same results. Span 80 produced slightly larger (6 µm – 9 µm) particles than sodium caseinate (4 µm). Overall, sodium caseinate was selected as the optimal surfactant for further experiments due to its low cost and more conventional use as a food ingredient.

4.2 Introduction

Often in microencapsulation applications it is either favorable or necessary to stabilize the generated microcapsules at the surface/carrier fluid interface. The addition of surfactant can enhance long term stability by preventing particle aggregation or modify physicochemical properties like wettability of the resultant powder [1, 2]. A wide range of compounds can be used and most of them share the similar traits such as a wide range of solubility and amphiphilic characteristics that allow the molecules to interact with non-polar and polar surfaces simultaneously. Due to the tendency of zein to form both films and micelles upon self-assembly, it has the capacity to form large aggregates under the right circumstances. The aggregation can be mitigated via the addition of surfactants and it has been applied in several encapsulation studies to improve encapsulation with zein [3, 4, 5].

I-carrageenan is a sulfonated polysaccharide derived from seaweed that has historically used as an emulsifier in food products. With respect to zein, the less polar carbohydrate backbone can interact with the hydrophobic residues at the surface layer of zein micelles while the polar sulfone groups interact with the aqueous solvent. Several studies have indicated this potential complexation as potentially beneficial for encapsulation with a variety of hydrophobic shell materials, including zein. It is both easily sourced and can be considered a natural ingredient for food label considerations [6, 7, 8, 9].

Modified starches have also been presented as food ingredients with a variety of different functions, from thickeners to emulsifiers. Starch modified with an octenyl succinic anhydride (OSA) moiety becomes a highly amphiphilic molecule, as the OSA

“head” group is much more polar than the carbohydrate backbone “tail”. Studies have also indicated the potential for OSA-modified starches to provide surface stabilization of hydrophobic shell materials in encapsulation [10, 11, 12, 13].

In a similar manner, fatty acids, which have characteristic long, aliphatic carbon chains to interact with non-polar molecules, can be functionalized with a polar head grouping. Sorbitan esters have been used to create a customizable line of emulsifiers known as “Spans” with differing molecular weights depending on the number of carbons on the associated fatty acid. These non-ionic emulsifiers are liquid at room temperature and more easily incorporated directly into the dispersed phase with zein, which may confer different benefits during the anti-solvent precipitation step that forms the microcapsules [14, 15, 16].

Most proteins are also slightly to moderately amphiphilic, depending on their structure. Casein protein from dairy is also known as a micelle-former and has been used as shell compounds in some encapsulation studies. Due to its mildly amphiphilic nature and large molecular weight, it can add increased stability as a surfactant via steric hindrance as it interacts with hydrophobic surfaces like those found on self-assembled zein capsules. It is also an economical and food-label friendly ingredient that already being used in a variety of powdered food applications [17, 18, 19, 5].

The objective of this study was to scale-up the experiments described in Chapter 3 to a bench-scale spray-drying setup. The hypothesis of this study is that the incorporation of surfactant molecules to the zein microcapsules will mitigate the tendency of zein to agglomerate, which will enable the spray-drying of zein-based microcapsules at bench-top scale.

4.3 Materials and Methods

4.3.1 Materials

Zein was procured from MilliporeSigma (Merck KGaA, Burlington, MA). 200 proof ethanol was supplied by Decon Laboratories (DLI, Chester, PA) and was diluted to the appropriate concentration with de-ionized water from an in-house filtering system. An OSA-modified starch was obtained from Ingredion (INGR, Westchester, IL), ι-carrageenan was obtained from Research Products International (RPI, Mt. Prospect, IL), and Span 80 as well as casein sodium salt from bovine milk were obtained from Millipore Sigma (Merck KGaA, Burlington, MA).

Two Harvard PHD 2000 syringe pumps (HA, Holliston, MA) were used to deliver the dispersed and continuous phases to the spray-dryer. The spray-dryer used for all experiments was a Buchi B-290 Mini Spray-Dryer (Buchi AG, Switzerland). Inlet air was treated through a Buchi B-296 Dehumidifier and expelled through an outlet filter, both of which were also procured from Buchi. Nitrogen was used as the atomizing gas via compressed gas cylinders provided by AirGas (Air Liquide S.A., Paris, France). For the trials where nanoparticles were pre-generated, the nozzle simulation chip described in Chapter 3 was used to facilitate the anti-solvent precipitation of zein.

The stock 2-fluid nozzle with a 0.5 mm nozzle tip and 1.5 mm nozzle cap provided by Buchi for the B-290 unit was used for the pre-generated capsules One 7.8 cm long stainless-steel nozzle collar was fabricated by the UIUC ECE Machine Shop and fit to thread into the body of the stock 3-fluid nozzle provided by Buchi in order to vary contact time between the dispersed and continuous phases. Figure 4.1 illustrates these modifications done to the stock 3-fluid nozzle.

4.3.2 Methods

4.3.2.1 Spray-Drying Zein Nanoparticle Suspensions Prepared in Nozzle Simulation Chip

Zein nanoparticles with and without added surface acting agents were first generated in the nozzle simulation chip using a similar method as described in Chapter 3. Briefly, dispersed phase stock solutions of zein at 2% and 4% w/w were prepared in 70% v/v ethanol and allowed to hydrate fully overnight. Continuous phase stock solutions of de-ionized water and (if applicable) a surface acting agent were also prepared in advance and allowed to hydrate overnight. OSA-modified starch was added to the continuous phase at 1:1, 2:1, and 4:1 mass ratios (OSA:zein) based on the zein concentration in the dispersed phase. Iota-carrageenan was added to the dispersed phase at 0.25:1, 0.5:1 and 1:1 mass ratios (carrageenan:zein) based on the zein concentration in the dispersed phase. Both phases were delivered via syringe pumps with the dispersed phase being plumbed to the inner channel of the simulation chip and the continuous phase being plumbed to the two outer channels of the chip.

Microcapsules were generated with a total flow rate of 4 mL/min and a flow ratio of 3:1 continuous to dispersed, which is analogous to one of the treatment groups from the nozzle simulation chip trials. This treatment level was chosen because it offers a middle ground between throughput, particle size, and PDI. The resultant zein particle suspensions were allowed to settle overnight to determine if the resultant suspensions were stable or if aggregation would occur.

4.3.2.2 Spray-Drying Trials with Pre-Generated Zein Microcapsules

All pre-generated zein nanoparticles that were spray-dried were pumped through the stock Buchi 2-fluid nozzle. Atomizing gas pressure and flow rate were held constant at 40 psi and 40% on the rotameter; nitrogen via compressed gas cylinders was used

as the atomizing gas in all trials. When possible, powder was collected and analyzed for yield.

4.3.2.3 Spray-Drying Trials with 3-fluid Nozzle and in situ Assembly of Particles

Span 80 and sodium caseinate were also tested as possible surface acting agents only with spray dryer equipped with 3-fluid nozzle. Stock solutions for Span 80 and sodium caseinate samples were similarly prepared and allowed to hydrate, then directly spray-dried using the Buchi 3-fluid nozzle modified with the 7.8 cm long nozzle collar. Notably, Span 80 was directly incorporated into the dispersed phase at a mass ratio of 1:1 of zein:Span 80 rather than the continuous phase. Sodium caseinate was split between both phases at a total mass ratio of 1.25:1 of sodium caseinate:zein, with mass ratio of 0.25:1 of sodium caseinate:zein in the dispersed phase and a the remainder of sodium caseinate in the continuous phase. It was apparent that even if successful particle generation occurred in the nozzle simulation chip, plugging could still be a limiting factor in subsequent spray-drying trials of the same preparation.

Sodium caseinate solutions were adjusted to a pH of ~ 3.0 via 1.0M HCl. pH of the stock solutions were adjusted and allowed to hydrate overnight. The following day, pH of the stock solution was adjusted to 3 again if necessary prior to spray-drying. Inlet temperature and total flow-rate were varied in these trials to attempt to mitigate nozzle plugging issues. Particles generated via Span 80 and sodium caseinate complexation with zein were tested for particle size using a SALD 2300 Laser Diffraction Particle Sizer (Shimadzu, Japan). . In cases where enough particles were present to merit it, yield was also calculated.

4.4 Results and Discussion

Attempts were fast made to spray-dry zein-only nanoparticles prepared with nozzle simulation chip. However, yield was extremely low and it was noticed that the nozzle tip where the combined phases would be ejected from would completely solidify with a plug of aggregated zein material, limiting the ability to even collect enough powder for any kind of analysis. It was then hypothesized that surface acting agents will reduce the aggregating tendencies of zein at the interface of the nozzle and main spray drying chamber [1, 2, 3, 4].

Initially, two surface acting agents were chosen for preliminary testing. An OSA-modified starch was chosen based on its extensive use as a surfactant in encapsulation research as well as its ease of being incorporated into the water-based continuous phase [10, 11, 12, 13]. I-carrageenan was also selected as a potential candidate for complexation with zein due to similar use as a microencapsulation aid as well as being more food-label friendly for potential application foods, especially in scaled-up applications [6, 7, 8, 9].

4.4.1 Pre-generated Zein/OSA-Starch or Zein/Carrageenan Nanoparticles Spray-Dried with a 2-Fluid Nozzle

Preliminary trials were conducted to determine the optimal concentration range for OSA-starch and carrageenan as surfactants with zein to stabilize aggregation over time. Only at or above 4:1 ratios of OSA-starch to zein stabilized the resultant nanoparticle suspensions; the 1:1 and 2:1 ratio samples had visible precipitation after only a few minutes, and a thick sediment of aggregated particles after 24 hours. At the 4:1 ratio, no visible precipitation was noticed after the settling time, so this ratio was selected for spray-drying trials with the 2-fluid nozzle. All carrageenan trials (0.25:1,

0.5:1 and 1:1 mass ratios) resulted in coagulated masses of zein and carrageenan. Though no plugging of the simulation chip occurred, the trials were deemed incompatible with further spray-drying due to the high viscosity and macro-scale aggregates formed in the liquid. Thus, carrageenan was abandoned as a potential surfactant.

The spray-drying trials of OSA-starch added samples with the two-fluid nozzle were successful at generating higher yields of powder than zein alone. However, complete nozzle occlusion still occurred relatively quickly (~20-30 mL of dispersed phase sprayed) into each spray-drying trial. The high amount of OSA-starch, at least 4:1 OSA-starch:zein mass ratio, was required to at least partially stabilize the zein particles. Therefore, the continued spray-drying of zein/starch complexes was ruled out as feasible for a process that was ostensibly to be easily scalable for industrial production of encapsulated materials.

4.4.2 In-situ Generation and Spray-Drying of Zein/Sodium Caseinate and Zein/Span 80 Complexes with Novel 3-Fluid Nozzle

Span 80 was tested as a potential stabilizer for the zein particles based on other studies claiming beneficial results for encapsulation [14, 15, 16]. It was selected because of its non-polar nature, which allowed for direct incorporation into the dispersed phase. It also does not meaningfully contribute to the overall viscosity of the combined phases, which was thought to be detrimental for continuous spray-drying where nozzle plugging was the main issue.

All preliminary spray-drying with Span 80 as a surfactant were completed with significantly higher powder yields than the spraying drying of either the zein-alone or zein-OSA starch. Resultant particle size was measured at between 6 µm to 9 µm and

the particle size dispersion was noted as being quite narrow compared to typical spray-drying distributions [20, 21, 22]. Span 80 was deemed an excellent candidate for potential zein encapsulation applications that used the novel 3-fluid nozzle design proposed in this study.

Sodium caseinate was also tested as a potential surfactant due its reliable use as both a wall material and surfactant in various encapsulation studies [17, 18, 19, 5], as well as being a cheaper and more food-label friendly option than Span 80. Initially, all of the sodium caseinate was incorporated into the continuous phase at a mass ratio of 1.25:1 caseinate to zein. The 3-fluid nozzle was plugged almost immediately. Although lowering inlet temperature and increasing the total feed flow rate both delayed the onset of the nozzle occlusion, adjusting spray-drying parameters was not able to prevent complete plugging of the nozzle before the production of enough powders.

Sodium caseinate was then incorporated into both continuous and dispersed phases. It was hypothesized that large aggregates of zein and sodium caseinate were forming during the contact time between the dispersed and continuous phases. These aggregates were more likely to partially occlude the nozzle tip and dry, so more aggregates could be attached. By adding sodium-caseinate to the dispersed phase, it was hypothesized that rapid complexation between zein and sodium caseinate would occur, reducing the formation of large aggregates.

The addition of some of the sodium caseinate to the dispersed phase helped mitigate full nozzle occlusion; however, the nozzle was still plugged with zein/sodium caseinate. In these trials, however, it was observed that the plugs would result in a small window of complete flow stoppage followed by a corresponding increase in spray-

drying outlet temperature. Then, due to the pressure building up behind the plug as the syringe pumps were still running, the plug was ejected into the spray-drying chamber and flow in the nozzle resumed as normal.

In an attempt to counteract this partial plugging, both continuous and dispersed phases were adjusted to pH 3 via 1.0 M hydrochloric acid. Studies indicate that sodium caseinate is only minimally soluble in ethanolic aqueous solutions; however, the solubility increases to close to 100% below pH 3.5 [23]. By fully dissolving all of the sodium caseinate into the dispersed phase, it was once again hypothesized that more immediate complexation will take place as the two phases mixed and smaller aggregates will form.

All preliminary trials conducted with sodium caseinate at pH3 were successful. No nozzle pluggage was detected throughout the course of a full spray-drying run. Yields were consistently ~70% and the resultant particle size, measured at ~ 4 µm, was slightly smaller than the particles produced with Span 80 with a similarly narrow size distribution. Table 4.2 summarizes each surfactant used as well as the overall results of the preliminary trials completed to scale up the nozzle simulation chip described in Chapter 3 to bench-top spray-drying.

4.5 Conclusion

Excessive difficulties scaling up the proposed nozzle technology to the actual spray-drying operation were encountered following the nozzle simulation chip trials. Zein solutions had a tendency to form plugs at the nozzle tip, resulting in a complete stoppage of flow to the spray-dryer before a meaningful amount of powder could be collected. Several surfactant molecules were tested to see if it would result in more

stable zein particles that did not aggregate at the spray-drying tip. Carrageenan did not move past the nozzle simulation trial, and OSA-starch was rapidly ruled out due to a large required mass relative to zein and nozzle plugging still being observed.

Both Span 80 and sodium caseinate were able to produce substantial amounts of powder at high yields and sizes/distributions that are favorable for controlled release kinetics when prepared accordingly. While less processing steps are involved in achieving particles with Span 80, sodium caseinate offers numerous benefits in terms of low price and more conventional use in the food industry as an ingredient. Therefore, for all future trials done in this study, sodium caseinate was used as the surfactant; however, Span 80 could still be a promising technology for other encapsulation applications using the same novel 3-fluid nozzle technology.

4.6 Figure and Table

Figure 4.1 – Modification to Stock 3-Fluid Nozzle with Extension Collar

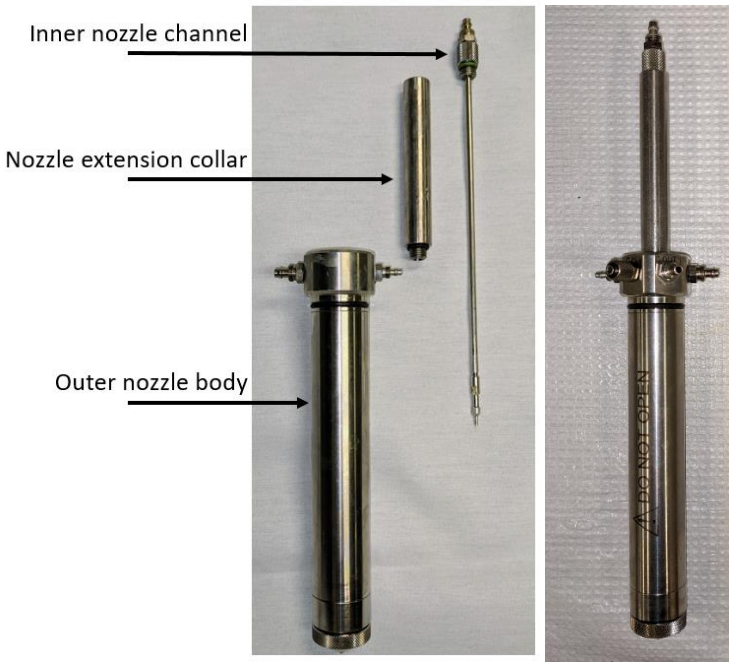

Table 4.1 – Summary of Surfactants Tested and Results

Surfactant	General Structure	Result
OSA-Modified Starch	Polar head group functionalized onto non-polar starch backbone	Required high mass ratios to fully stabilize zein in solution, still resulted in nozzle plugs
Carrageenan	Sulfonated polysaccharide	Viscous sludge of zein aggregates formed, not moved on to spray-drying trials
Span 80	Non-ionic fatty acid sorbitan ester	Eliminates nozzle plugging, potential issues with food labelling due to its synthetic nature
Sodium caseinate	Protein	Eliminates nozzle plugging with correct preparation, most food-label friendly

4.7 References

[1] C. Butstraen, F. Salaün and E. Devaux, "Sol-gel microencapsulation of oil phase with Pickering and nonionic surfactant based emulsions," 2015.

[2] L. Dai, C. Sun, Y. Wei, X. Zhan, L. Mao and Y. Gao, "Formation and characterization of zein-propylene glycol alginate-surfactant ternary complexes: Effect of surfactant type," *Food Chemistry,* vol. 258, pp. 321-330, 8 2018.

[3] C. A. Di Battista, D. Constenla, M. Verónica Ramírez-Rigo and J. Piña, "The use of arabic gum, maltodextrin and surfactants in the microencapsulation of phytosterols by spray drying," 2015.

[4] A. A. Sharipova, S. B. Aidarova, D. Grigoriev, B. Mutalieva, G. Madibekova, A. Tleuova and R. Miller, "Polymer-surfactant complexes for microencapsulation of vitamin E and its release," *Colloids and Surfaces B: Biointerfaces,* vol. 137, pp. 152-157, 2016.

[5] M. Veneranda, Q. Hu, T. Wang, Y. Luo, K. Castro and J. M. Madariaga, "Formation and characterization of zein-caseinate-pectin complex nanoparticles for encapsulation of eugenol," *LWT - Food Science and Technology,* vol. 89, pp. 596-603, 2017.

[6] E. N. Dewi, R. A. Kurniasih, L. Purnamayanti and P. Journal, "Physical Properties of Spirulina Phycocyanin Microencapsulated with Maltodextrin and Carrageenan".

[7] N. Devi and T. K. Maji, "Microencapsulation of isoniazid in genipin-crosslinked gelatin-A-k-carrageenan polyelectrolyte complex Isoniazid-encapsulated polyelectrolyte complex," *Drug Development and Industrial Pharmacy,* vol. 36, no. 1, pp. 56-63, 2010.

[8] S. Chakraborty, "Carrageenan for encapsulation and immobilization of flavor, fragrance, probiotics, and enzymes: A review," 2017.

[9] L. Mao, Q. Pan, Z. Hou, F. Yuan and Y. Gao, "Development of soy protein isolate-carrageenan conjugates through Maillard reaction for the microencapsulation of Bifidobacterium longum," 2018.

[10] E. Agama-Acevedo and L. A. Bello-Perez, "Starch as an emulsions stability: the case of octenyl succinic anhydride (OSA) starch," *Current Opinion in Food Science,* no. 13, pp. 78-83, 2017.

[11] H. Arshad, T. M. Ali and A. Hasnain, "Comparative study on efficiency of nutmeg microencapsulation (freeze-drying method) using native and OSA sorghum starch as wall materials in combination with gum arabic," *Cereal Chemistry,* vol. 97, no. 3, pp. 589-600, 26 5 2020.

[12] N. R. Breternitz, C. H. de Vasconcelos Fidelis, V. M. Silva, M. N. Eberlin and M. D. Hubinger, "Volatile composition and physicochemical characteristics of mussel (Perna perna) protein hydrolysate microencapsulated with maltodextrin and n-OSA modified starch," *Food and Bioproducts Processing,* vol. 1, no. 5, pp. 12-25, 2017.

[13] M. Matos, A. Marefati, G. Gutiérrez, M. Wahlgren and M. Rayner, "Comparative Emulsifying Properties of Octenyl Succinic Anhydride (OSA)-Modified Starch: Granular Form vs Dissolved State," 2016.

[14] C. Dima and S. Dima, "Water-in-oil-in-water double emulsions loaded with chlorogenic acid: release mechanisms and oxidative stability," 2018.

[15] D. Noviendri, I. Jaswir, M. Taher, F. Mohamed, H. M. Salleh, I. A. Noorbatcha, F. Octavianti, W. Lestari, R. Hendri, H. Ahmad, K. Miyashita and A. Abdullah, "Fabrication of Fucoxanthin-Loaded Microsphere(F-LM) By Two Steps Double-Emulsion Solvent Evaporation Method and Characterization of Fucoxanthin before and after Microencapsulation," *Journal of Oleo Science,* vol. 65, no. 8, pp. 641-653, 2016.

[16] D. Vanichtanunkul, P. Vayumhasuwan and U. Nimmannit, "The effect of core-to-wall ratio and Span 80 concentration on the properties of ascorbic acid microcapsules," in *Journal of Microencapsulation*, 1998.

[17] S. C. Chew, C. P. Tan and K. Lin Nyam, "Microencapsulation of refined kenaf (Hibiscus cannabinus L.) seed oil by spray drying using β-cyclodextrin/gum arabic/sodium caseinate," 2018.

[18] X. Bai, C. Li, L. Yu, Y. Jiang, M. Wang, S. Lang and D. Liu, "Development and characterization of soybean oil microcapsules employing kafirin and sodium caseinate as wall materials," 2019.

[19] K.-K. Li, X. Zhang, Q. Huang, S.-W. Yin, X.-Q. Yang, Q.-B. Wen, C.-H. Tang and F.-R. Lai, "Continuous preparation of zein colloidal particles by Flash NanoPrecipitation (FNP)," *Journal of Food Engineering,* vol. 127, pp. 103-110, 2014.

[20] Handbook on spray drying applications for food industries, 2019.

[21] C. Anandharamakrishnan, Spray drying technique for food ingredient encapsulation, 2015.

[22] S. Quispe-Condori, D. A. Saldaña and F. Temelli, "Microencapsulation of flax oil with zein using spray and freeze drying," 2011.

[23] S. Mezdour, G. Brulé and J. Korolczuk, "Physicochemical analysis of casein solubility in water-ethanol solutions," *Lait,* vol. 86, pp. 435-452, 2006.

CHAPTER 5: Spray Drying of Zein/Sodium Caseinate Powder via a Modified 3-Fluid Nozzle

5.1 Abstract

Zein and sodium caseinate particles were successfully spray-dried with a novel 3-fluid nozzle design that provides contact time between dispersed and continuous phases within the nozzle body. Particle sizes were small (< 10 µm) and relatively narrow compared to typical spray-drying ranges. Powder yields were greater than 60% at all treatment levels except for the high (6% w/w) zein concentration and low (4 mL/min) flow rate condition.

Both initial zein concentration and total flow rate had a significant effect on powder yield, while only initial zein concentration had a significant effect on both median particle diameter and particle size interquartile range (IQR). This result may be the result of heavy wall-spray observed in these trials causing both substantial yield loss as well as resulting in smaller overall particle sizes. These smaller sizes are likely a result of the aggregated larger particles hitting and sticking to the spray-dryer walls while smaller particles passing through to the cyclone. Zein concentration of 6% may be above the limit of zein concentration when working at the bench-top scale spray dryer used in this study. Overall, the production of powder is considered successful and could provide a means for producing microcapsules that have beneficial physical properties for controlled release of the core material.

5.2 Introduction

Spray-drying is a well understood and high throughput technology that can be used for microencapsulation applications [1, 2, 3, 4]. The powdered microcapsules are advantageous for food formulations due to their long shelf life and ease of shipment over liquid emulsions of microcapsules. While spray-drying itself is a highly dynamic process that allows for tuning of powder characteristics by changing key operating parameters, it can still be difficult to produce uniformly small powder particle size distributions [5, 6, 7]. Highly polydisperse powders are not ideal for controlled release applications due to larger variance in the diffusion kinetics [8, 9].

Microfluidic processing has seen increased use as an encapsulation technology for food and pharmaceutical ingredients in several recent studies [9, 10, 11, 12, 13]. Due to the extremely small time-scale at which all transport phenomena are carried out in the micron-scale channels, microfluidics offers unparalleled process control over spray-drying and other encapsulation methods. This control allows for fine tuning of microcapsules characteristics, including both particle size and the size distribution [8, 13]. The extremely monodisperse capsules produced with microfluidics are excellent for controlled release applications; however, they can only be produced at very small scales due to the relatively low flow rates used in microfluidics. With the only option for scale-up being multiple microfluidic chips in parallel, the technology rapidly becomes unfeasible for economies of scale.

Previous work done in this study has indicated that it may be possible to scale-up the concepts from microfluidic processing into millimeter-scale channels to increase throughput while mimicking the fine level of control that microfluidics offers. Zein

nanoparticles with highly uniform particle sizes were generated in a test device scaled to match a proposed 3-fluid spray-drying nozzle design. It was also shown that particle size and the polydispersity index (PDI) were both capable of being tuned by altering either initial zein concentration or total flow-rate.

Zein, a predominantly hydrophobic nitrogen storage protein sourced from maize, has seen wide use in encapsulation systems generated via both microfluidic processing as well as spray-drying [12, 14, 15, 16, 17]. Its tendency to self-assemble into micelles during anti-solvent precipitation makes it an excellent candidate for the shell material in an encapsulated model system. Other previous work in this study indicates that zein can be successfully spray-dried using the proposed 3-fluid nozzle technology on a bench-scale spray-dryer; however, the use of a surfactant, specifically sodium caseinate, is required. An amphiphilic molecule, sodium caseinate has also seen use as a shell material in encapsulation, but here it is being specifically utilized to interact at the zein particle surface to help increase stability and decrease the tendency of zein to agglomerate into large masses that had a tendency to clog the nozzle tip in spray-drying trials [18, 19, 20, 21].

The objective of this study was to characterize the effect of initial zein concentration and total flow rate, the two parameters varied in the nozzle simulation chip trials, on spray-dried powder yield, particle size, and size dispersion. The hypothesis of this study was that increasing zein concentration will result in larger spray-dried powders with higher PDI, while increasing total flow rate will result in smaller spray-dried powders with higher PDI. This hypothesis is based on the findings from the previous study using a nozzle simulation chip.

5.3 Materials and Methods

5.3.1 Materials

Zein was procured from MilliporeSigma (Merck KGaA, Burlington, MA). 200 proof ethanol was supplied by Decon Laboratories (DLI, Chester, PA) and was diluted to the appropriate concentration with de-ionized water from an in-house filtering system. Casein sodium salt from bovine milk was also obtained from Millipore Sigma (Merck KGaA, Burlington, MA). Hydrochloric acid with a purity between 36.5 – 38% was obtained from Fisher Scientific (TFS, Waltham, MA). De-ionized water for the continuous phase was obtained from an in-house filtration system.

Two Model 1000X syringe pumps (NEPS Inc., Farmingdale, NJ) were used to deliver the dispersed phase to the spray-dryer. The spray-dryer used for all experiments was a Buchi B-290 Mini Spray-Dryer (Buchi AG, Switzerland). Inlet air was treated through a Buchi B-296 Dehumidifier and expelled through an outlet filter, both of which were also procured from Buchi. Nitrogen was used as the atomizing gas via compressed gas cylinders provided by AirGas (Air Liquide S.A., Paris, France). The continuous phase was fed to the dryer via the peristaltic pump mounted on and controlled by the Buchi B-290 spray-dryer. The pH of both phases was measured with an Orion 8157BNUMD pH/ATC Triode hooked into an Orion VersaStar Advanced Electrochemistry Meter.

A 7.8 cm long stainless-steel nozzle “collar” was fabricated by the University of Illinois at Urbana Champaign Electrical and Computer Engineering Machine Shop and fit to thread into the body of the stock 3-fluid nozzle provided by Buchi in order to provide for increased contact time between the continuous and dispersed phases. Figure 5.1 shows the actual nozzle plus collar setup. This design is to provide

analogous conditions to what was done with the nozzle simulation chip however, the contact times are slightly longer due a larger diameter of outer fluid channel in the spray-drying nozzle body. Table 5.1 lists the contact times used in this experiment based on the total flow rate, Table 5.2 summarizes the experimental design.Powders produced were analyzed via a laser diffraction particle size analyzer (SALD 2300, Shimadzu Co., Kyoto, Japan). Powder samples were imaged with a FEI Quanta FEG 450 Environmental Scanning Electron Microscope (FEI Co., Hillsboro, OR) at the Beckman Institute for Advanced Science and Technology in Urbana, IL.

5.3.2 Methods

5.3.2.1 Stock Solution Preparation

Aqueous solutions of 70% v/v ethanol were prepared at a volume of 200 mL, to which either 4% or 6% w/w zein was added. Sodium caseinate was added at a ratio of 0.25:1 (caseinate:zein) and quercetin at a ratio of 1:20 (quercetin:zein) to the dispersed phase. Three mL of 1.0 M HCl was then added to adjust the pH. The dispersed phase was covered with parafilm as well as a cardboard shield to block any light exposure and allowed to continuously stir overnight (at least 8 hours) to fully hydrate. For continuous phase, 800 mL of de-ionized water was added to a beaker and pH was adjusted with 7 mL of 1.0 M HCl. Sodium caseinate was added to the continuous phase to reach a mass ratio of 1:1 caseinate:zein. The beaker was then covered with parafilm and allowed to stir overnight (at least 8 hours) to fully hydrate. All liquids were also weighed for yield calculation.

5.3.2.2 Spray-Drying

To spray-dry, Buchi B-290 unit and Buchi B-296 dehumidification unit were both cycled on with the aspirator for the B-290 set to 90% output. The inlet temperature was set at either 130°C for the 4 mL/min treatment groups or 145°C for the 8 mL/min treatment groups. The difference of inlet temperatures was to normalize the average outlet temperature for all treatments at 80°C. The peristaltic feed pump was set to either 8% (~ 3mL/min)) or 12% (~6 mL/min). Approximate flow rates were measured by collecting the continuous phase in a graduated cylinder for 1 minute. The syringe pumps were set to a syringe diameter of 26.67 mm (standard 50 mL BD syringe) and a flow rate of either 60 mL/hr (for the 4 mL/min total flow treatments) or 120 mL/hr (for the 8 mL/min total flow treatments). Atomizing air pressure was set at 40 psi and the flow adjusted to 40 on the rotameter for each trial.

The stock 3-fluid nozzle from Buchi was modified with the 7.8 cm long collar extension for the inner nozzle tube on all treatment groups. The contact time between the dispersed and continuous phases at the 4 mL/min total flow treatment was 24.5 seconds and 12.2 seconds at the 8 mL/min total flow treatment. The dispersed phase was connected to the inner liquid nozzle channel and the continuous phase to the outer liquid nozzle channel. 100 mL of zein stock solution was spray-dried (two syringes each with 50 mL of solution) and the double pump setup allowed for uninterrupted flow of zein stock solution to the nozzle. Upon completion of the spray-drying, the B-290 was turned off and allowed to cool down before the powder was collected from the collector attached to the bottom of the cyclone. The equipment was thoroughly cleaned after each run, and a new outlet filter was installed.

5.3.2.3 Yield Calculations

Only powder in the collection vessel was recovered from the spray-dryer. Any attempt to recover powder from the cyclone and/or spray-drying vessel would be inefficient upon scale-up to industrial levels. The collected powder was weighed and stored in opaque 50 mL tubes. The remaining amount of both dispersed and continuous phases were also weighed so that the total amount of each phase sprayed could be calculated. Equations 2-7 give the calculation steps used for percent yield.

$$Total\ Solids, Dispersed\ Phase = \frac{M_{zein} + M_{Caseinate} + M_{Quercetin}}{Total\ Phase\ Mass} = TS, D \quad [2]$$

$$Total\ Solids, Continuous\ Phase = \frac{M_{Caseinate}}{Total\ Phase\ Mass} = TS, C \quad [3]$$

$$Mass\ Dispersed\ Sprayed = Initial - Final\ Mass = MS, D \quad [4]$$

$$Mass\ Continuous\ Sprayed = Initial - Final\ Mass = MS, C \quad [5]$$

$$Maximum\ Theoretical\ Powder\ Weight = (TS, D)(MS, D) + (TS, C)(MS, C) \quad [6]$$

$$\%\ Yield = \frac{Recovered\ Powder\ Weight}{Maximum\ Theoretical\ Powder\ Weight} x100 \quad [7]$$

Note that these calculations assume a moisture content of 0% because moisture content analysis was not conducted on powder samples. At 2% moisture content, actual yields would be between 1.5% - 2% smaller than reported, which does not bring any yield measurements out of an acceptable range.

5.3.2.4 Particle Size

Powder samples were analyzed in triplicate using a laser diffraction (LD) analyzer with an attached cyclone-injection module (SALD 2300 and SALD-DS5,

Shimadzu, Japan). Briefly, powder samples were loaded into sampling container until it was approximately halfway full. The samples were then loaded into the cyclone-injection module. An apparatus would then lift the sampling container into a nozzle that injects pressurized air to atomize the particles apart before being vacuum transferred across the laser detection sensor. Analysis of the laser diffraction scan was carried out with the native WingSALD software provided by Shimadzu. Median particle size (LD,50) is reported for all samples.

5.3.2.5 Particle Size Distribution

Though polydispersity index was used for nanoparticle suspensions described in a previous chapter, there is no standard means of differentiating particle size distributions for dry powders. In order to evaluate particle size distribution in this study, the interquartile range (IQR) of each powder sample was calculated and compared. The interquartile range is calculated by subtracting the particle size below which 25% of all particles fall (LD,25) from the particle size below which 75% of all particles fall (LD,75), which can be shown in equation 8 below. Wider particle size distributions will have larger IQR's.

$$IQR = LD,75 - LD,25 \quad [8]$$

5.3.2.6 Scanning Electron Microscopy

Powder samples were first mounted on double sided carbon tape and coated with a ~ 1 nm thick layer of gold/platinum (Au/Pd) with a Desk II Turbo Sputter Coater (Denton Vacuum, Moorestown, NJ). Samples were imaged with a FEI Quanta FEG 450 Environmental Scanning Electron Microscope (FEI Co., Hillsboro, OR) at the Beckman Institute for Advanced Science and Technology in Urbana, IL.

5.3.2.7 Statistics

Statistical analyses were conducted with the R programming language in an RStudio environment. ANOVA was used to evaluate mean differences between treatment groups; the Shapiro-Wilkes test was used to confirm normality of residuals and the Levene-Forsythe test was used to confirm homogeneity of variance prior to ANOVA being conducted. All *post-hoc* mean separation tests were conducted using Tukey's HSD within R. All statistical plots were generated in R via the "ggplot" package of data visualization functions. Raw statistical outputs have been included in section 5.7 of this chapter.

5.4 Results and Discussion

Spray-dried powder was successfully collected at each of the different treatment levels; no significant nozzle plugging issues were noted during these trials. However, at the 6% zein concentration treatment level, less than 100 mL were spray dried due to the formation of a zein and sodium caseinate sludge in the dispersed phase in the syringes over the course of the experiment. The syringe pumps could not overcome the viscosity of this material and stalled at approximately 2 mL remaining in each syringe; this was consistent over all trials at the 6% zein treatment grouping. This could cause issues during scale-up if there is significant residence time in unagitated holding tanks or lengthy runs of pipe between pumps, as slow precipitation of zein would result in a lower actual total solids content being delivered to the spray-dryer versus theoretical. It should be noted that 6% zein therefore may not be a feasible concentration unless this sedimentation can be avoided via constant agitation of the dispersed phase during spray-drying.

5.4.1 Yield

Yield across both zein concentration and total flow rate was significantly different at $p < 0.05$. No significant interaction was detected between zein and flow at $p < 0.05$, however, a significant interaction was detected at $p < 0.1$. Yield is significantly lower at the 4 mL/min total flow rate treatment level and at the 6% zein concentration treatment level. Figures 5.2 and 5.3 illustrate the effect of zein concentration and total flow rate on percent yield, respectively. An interaction plot, shown in Figure 5.4, shows that at low total flow rate, a lower concentration of zein results in higher yield, however when extended to high flow rate, a higher concentration of zein may result in higher yield.

Table 5.3 shows the calculated average yield across each treatment combination. Interestingly, only the yield for the treatment level at 6% zein concentration and 4 mL/min total flow rate was significantly lower than the yield at all other treatment groups. No difference in yield were noted between the three other treatment subsets with the average yields ranging from 56.5% to 65.1%, which would be considered well within tolerance for the bench-scale spray dryer used in this study. The 6% zein/4 mL/min treatment group had an average yield of 46.8% ± 6.6%. It was observed during these trials that a much thicker “crust” of zein and sodium caseinate formed on the side walls of the main spray drying chamber, which could account for the lost powder mass and lower yield.

Mechanistically, it is most likely that 6% initial zein concentration approaches the maximum zein concentration allowable for spray-drying at the parameters that were tested. Wall-spray can either be caused by a wide spray-angle or by a partial nozzle occlusion that alters the trajectory of the atomized mist leaving the nozzle tip. The

higher liquid viscosity at 6% zein concentrations would actually cause the spray angle to decrease due to a higher energy requirement to break particle surface tension [22], which means viscosity was not a factor in the observed wall spray at 6% zein concentrations. The ratio of atomizing air flow to liquid feed flow is also important for determining spray angle [23], with higher ratios (more air to feed) producing wider angles by providing more energy input into the liquid feedstock. However, there was no observed wall-spray at the 4Z4F treatment level, which would have the same atomizing air to liquid feed flow ratio as the 6Z4F treatment level where the wall spray was observed. Taking all of these into account, it is likely that the wall spray that occurred during these trials was a result of partial nozzle occlusion altering the spray-angle of the nozzle.

Because the viscosity and total solids of the combined phases is higher at 6% initial zein, the lower flow rate treatment group may not provide enough velocity to prevent partial drying of liquid feedstock at the nozzle/dryer interface. Small aggregates of zein and sodium caseinate building up on the side of the nozzle would harden on the nozzle tip case, which is heated to the same temperature as the inlet air, causing a deflection of the feed stream as it enters the dryer.

It is also worth noting that this individual treatment combination may explain the variance between samples conducted in the two-way ANOVA analysis, which could erroneously cause significant mean differences between treatment levels to be observed. More replicates at other treatment levels should be conducted to increase statistical power and verify whether or not the differences are valid. However, a visually compelling case is made in Figure 5.5 and 5.6, which show the average yield with

standard error as well as the 95% confidence interval for yield at each treatment combination.

5.4.2 Particle Size

Median particle size was significantly different across only the initial zein concentration treatment levels at $p < 0.05$. No significant interaction or significant total flow rate effect were found. Median particle size was significantly lower (3.81 µm ± 0.70 µm) at the higher initial zein concentration as compared to the lower initial zein concentration (5.30 µm ± 0.85 µm). Figure 5.7 illustrates the effect of initial zein concentration on median particle size.

At the treatment combination level, the median particle size was found to be significantly different ($p < 0.05$) between the 4Z4F and the 6Z4F trials. The median particle size of the 6Z4F sample was smaller than at 4Z4F. Table 5.4 shows the average median particle size across each treatment combination, and Figures 5.8 and 5.9 illustrates the median particle size for all treatment groups and the 95% confidence interval for particle size, respectively.

SEM images of the samples confirms the particle size distribution reported by the laser diffraction particle sizer. Importantly, it also shows that the size and structure of the zein particles have fundamentally changed from what was provided by the manufacturer. Zein powder prior to being dissolved and spray-dried with sodium caseinate exists as much larger (~ 50 µm) particles with more angular geometric surface patterns. The spray-dried powder samples consist of either round or wrinkled spheroid particles, and much more closely resemble the structure of sodium caseinate as provided by the manufacturer. This observation of surface morphology may be an

indicator that there is successful interaction of sodium caseinate on the zein particle surface. Table 5.5 shows SEM images of relevant samples.

It should be noted that the 6Z4F sample was also the only sample that had a significantly different percent yield, which was also lower than any other treatment group. The smaller particle size at this treatment combination could potentially also be explained by partial nozzle occlusion. As the stream becomes deflected by the hardened plug of zein, more of it will come into contact with the side of the main spray drying chamber. As a result, any particles that are not fully hardened at this point will have a greater tendency to stick there and become unrecoverable yield loss. Larger droplets have much more chances to not have fully hardened surfaces than smaller droplets at the same distance travelled from the nozzle orifice to the wall of drying chamber, which could result in a lower net particle size in the powder collection vessel.

Importantly, this result contradicts the findings in the nozzle simulation trial, where particle size tended to trend up at higher initial zein concentrations given a constant flow rate. Here, we see a constant flow-rate of 4 mL/min generate smaller particles at a higher initial zein concentration. As seen above, the most likely explanation for this is that the spray-drying parameters, not the particle assembly method used, has a dominant effect on the resultant physical parameters of the powder samples, at least within the parameters tested in this study.

5.4.3 Particle Size Distribution

The IQR for powder samples was significantly different across zein concentration treatment levels, similar to median particle size. No significant interaction between zein concentration and total flow rate was detected, nor was there a significant flow rate

effect on the IQR. The IQR was significantly lower at the 6% zein concentration treatment level than at the 4% zein treatment level. Table 5.6 summarizes the IQR results for each treatment group, and Figure 5.10 illustrates the effect that zein concentration had on resultant particle size IQR. No significant difference between individual treatment groups was detected; Figures 5.11 and 5.12 show the IQR with standard error for each sample and the 95% confidence interval over IQR, respectively.

These results also contradict the findings in the nozzle simulation chip study. The data from the simulation ship suggested that PDI increased with increasing zein concentration; whereas, the IQR data from the dry powder collected during these experiments shows that the particle size IQR was lower for both 6% zein treatments. It is again possible that the impaction of large particles against the side-walls of the main drying chamber at the higher zein concentrations could result in more uniformly small dried powder particles; however, the yield in the 6Z8F trial did not suffer the same drop-off as seen in the 6Z4F, suggesting there was not the same level of wall-spray related yield loss in both treatments.

Most importantly, all powder samples had IQR ranges much lower than what is typically seen in spray-drying applications. Other studies have indicated that it is not unusual to have particle size ranges from single digit micrometers all the up through 100 microns and larger. The much lower IQR from this study indicates that either the means of assembling the zein particles with the novel 3-fluid nozzle technology used in this study and/or the spray drying parameters set for this experiment are optimal for creating small, narrowly dispersed powder sizes. The small IQR is an important distinction for

applications where targeted, controlled release is of special importance. Such is the case in a study conducted in a following chapter.

5.5 Conclusion

Spray-dried zein and sodium caseinate complexed powders were successfully generated with the novel 3-fluid nozzle design proposed in this study. Yield was within a reasonable range for all treatments. Particle size and distributions were both small and relatively mono-disperse across all treatment levels compared to typical spray-dried powders, with the high zein concentration treatment groups having smaller size and IQR. The observed differences could be a result of the partial nozzle occlusion seen at the 6% zein and 4 mL/min treatment level causing large aggregates to collide and stick with the main drying chamber wall.

This study suggests that the novel 3-fluid nozzle is capable of generating powders with narrow particle size distribution and is therefore ready to be tested with the a model system described in previous chapters. This study does, however, suggest that it may be challenging to tune the resultant powder size and distribution with the use of the 3-fluid nozzle because the dominant force governing these characteristics may be the act of spray-drying and not the act of assembling the particles. Additional work should be done to assess whether or not contact time between the two phases is an important factor in determining particle size and distribution.

5.6 Tables and Figures

Table 5.1 – Flow Rates and Corresponding Contact Times

Flow Rate	Contact Time
4 mL/min	24.47 seconds
8 mL/min	12.23 seconds

Table 5.2 – Experimental Design

Treatment Coding	Zein Concentration	Total Flow Rate
4Z4F	4% w/w	4 mL/min
4Z8F	4% w/w	8 mL/min
6Z4F	6% w/w	4 mL/min
6Z8F	6% w/w	8 mL/min

Table 5.3 – Percent Yield by Treatment Group

Treatment Group	Percent Yield (%)
4Z4F	62.8 ± 2.4
4Z8F	64.0 ± 4.7
6Z4F	46.8 ± 6.6
6Z8F	59.2 ± 2.5

Table 5.4 – Median Particle Size by Treatment Group

Treatment Group	Median Particle Size (μm)
4Z4F	5.60 ± 0.65
4Z8F	5.01 ± 1.05
6Z4F	3.46 ± 0.85
6Z8F	4.21 ± 0.28

Table 5.5 – Scanning Electron Microscope Images

Zein – **Manufacturer –** **50 μm view**	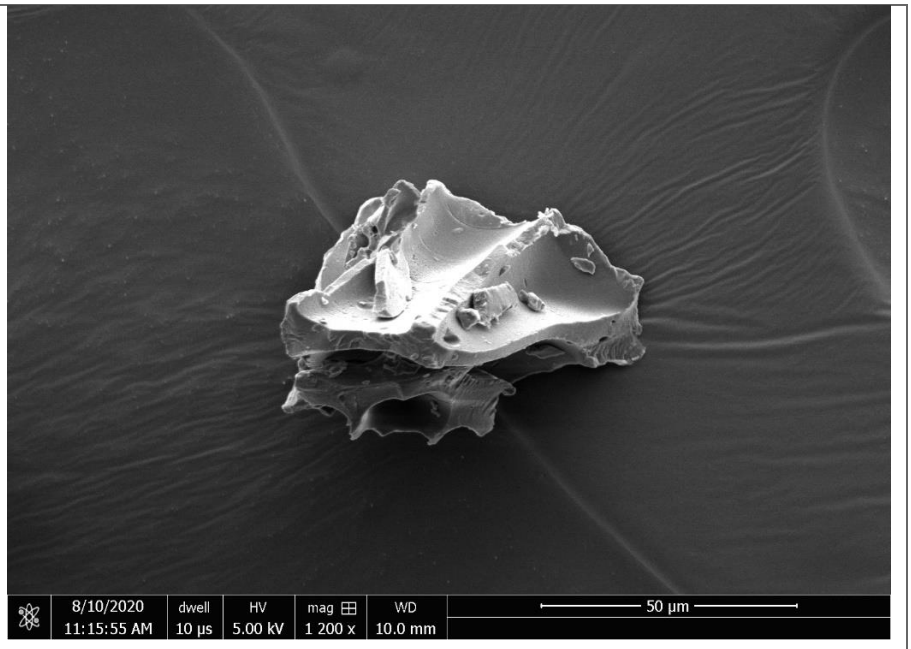

Table 5.5 (cont)

Sodium Caseinate – **Manufacturer –** **50 µm view**	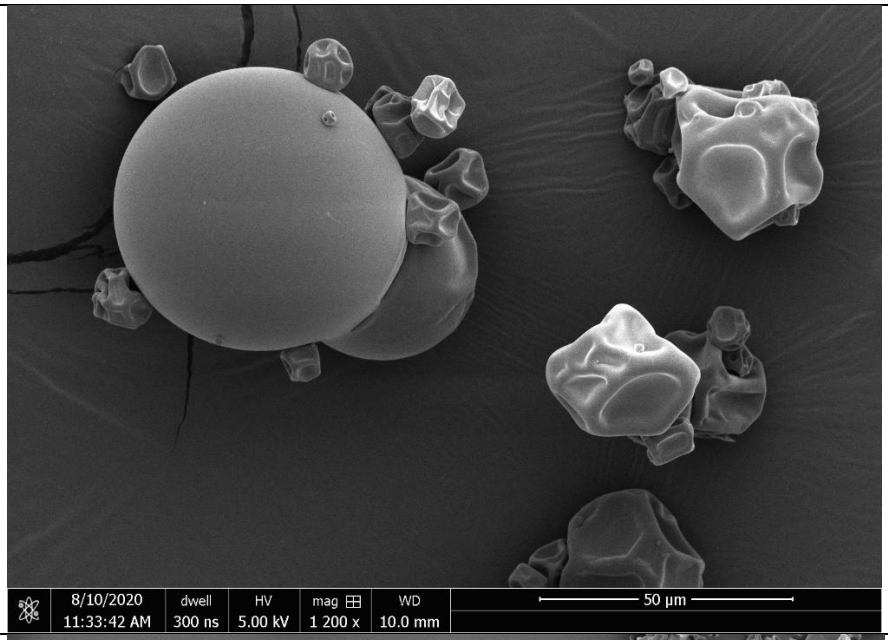
4Z4F – **50 µm view**	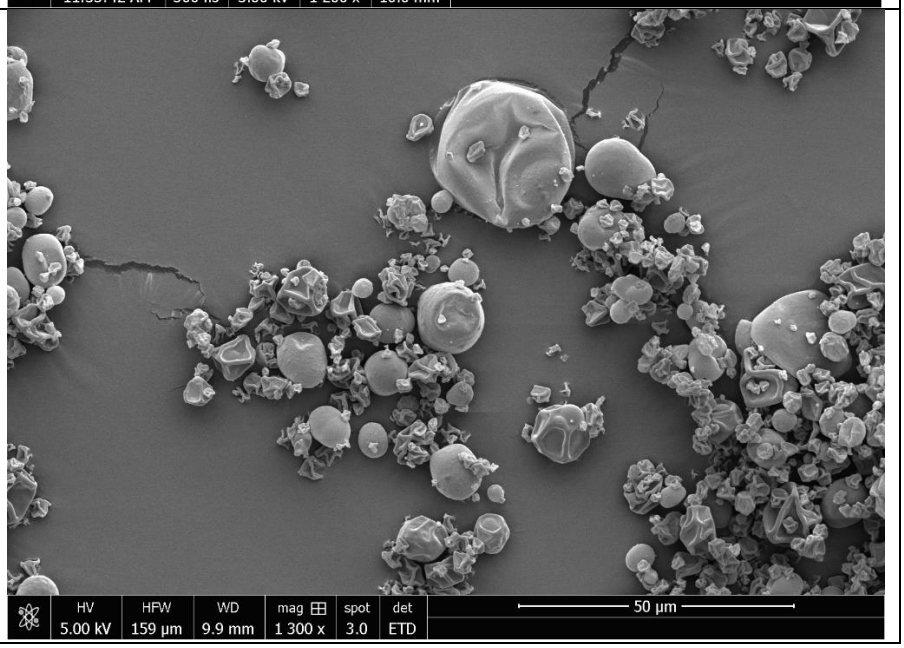

Table 5.5 (cont)

4Z8F – **50 µm view**	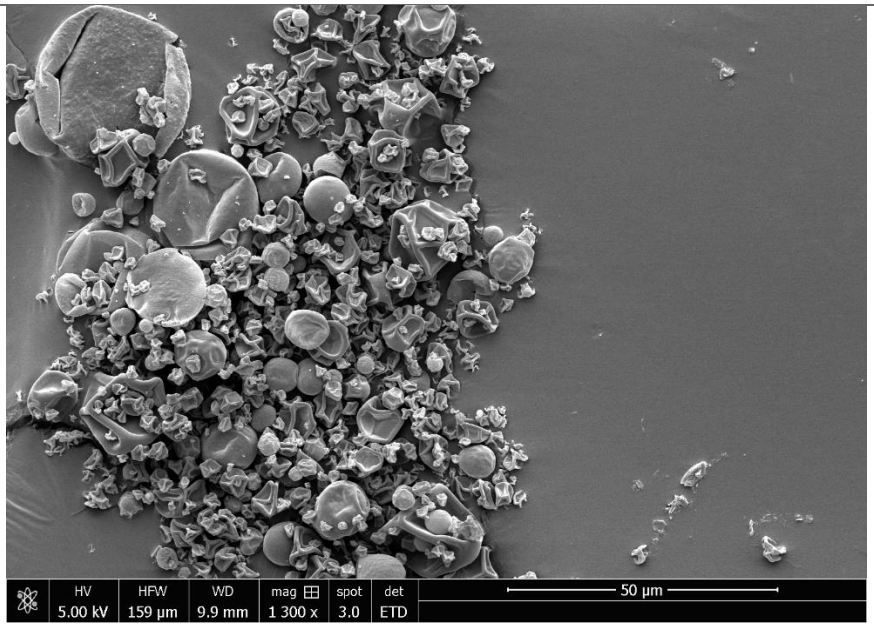
6Z4F – **50 µm view**	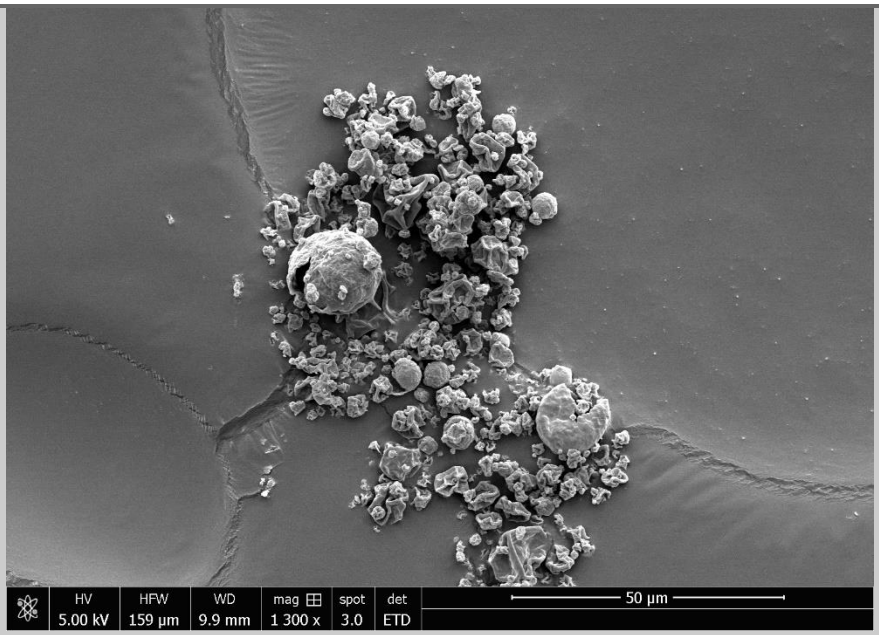

Table 5.5 (cont)

6Z8F – **50 µm view**	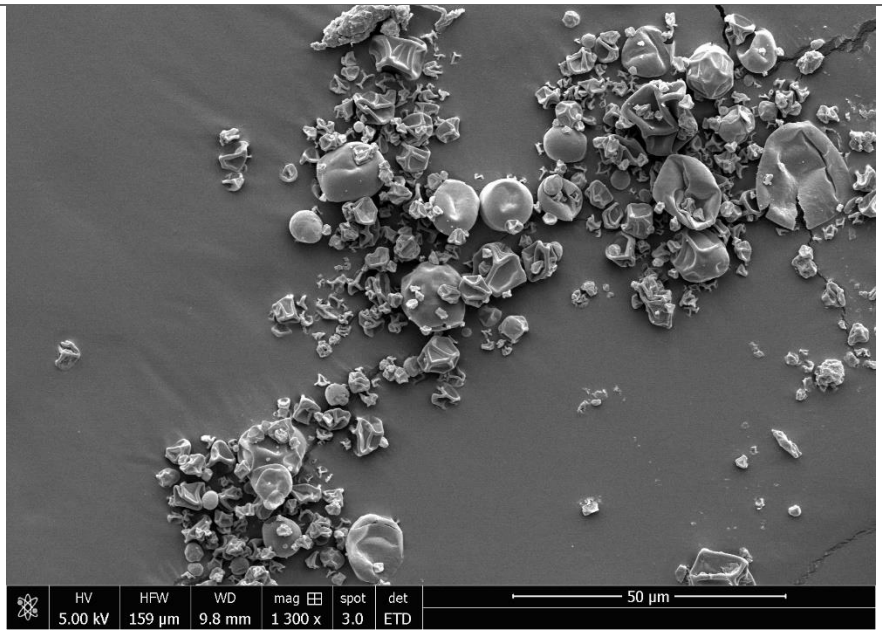

Table 5.6 – Particle Size Interquartile Range (IQR) by Treatment Group

Treatment Group	IQR (µm)
4Z4F	5.28 ± 0.86
4Z8F	5.02 ± 1.47
6Z4F	3.57 ± 0.89
6Z8F	3.69 ± 0.41

Figure 5.1 – 3-Fluid Nozzle with Collar Extension

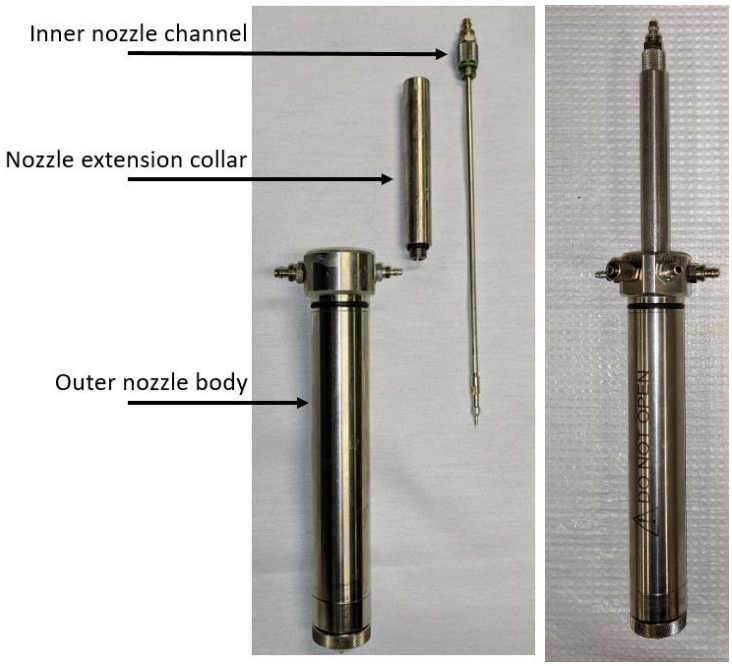

Figure 5.2 – Effect of Zein Concentration on Yield

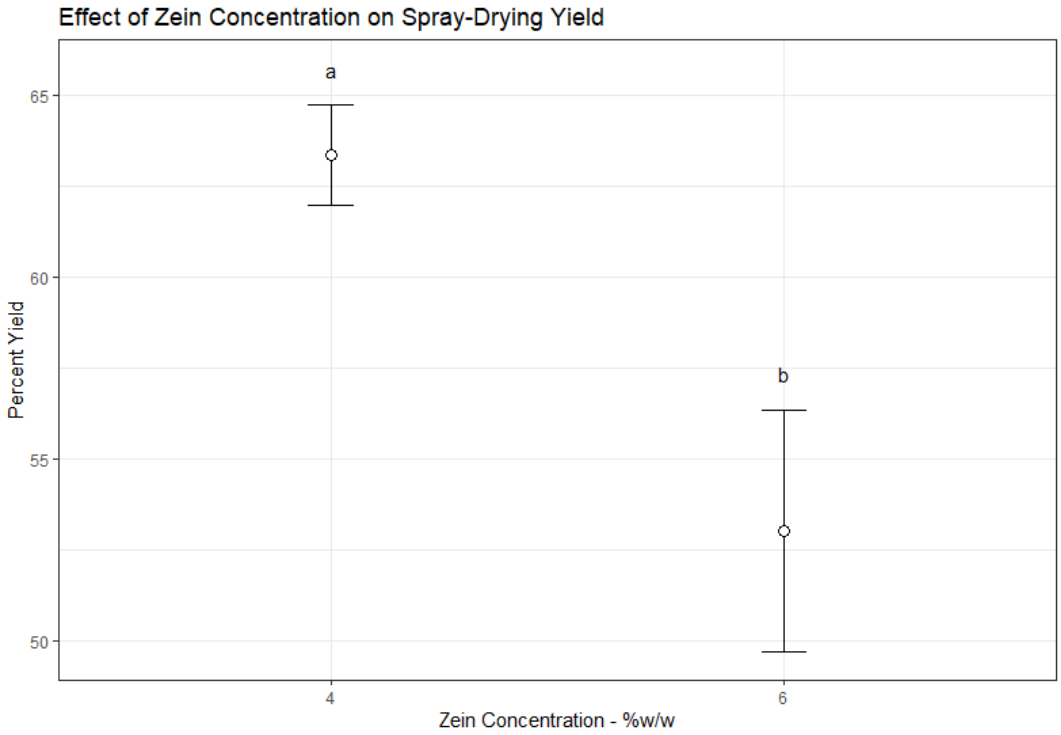

Figure 5.3 – Effect of Total Flow Rate on Yield

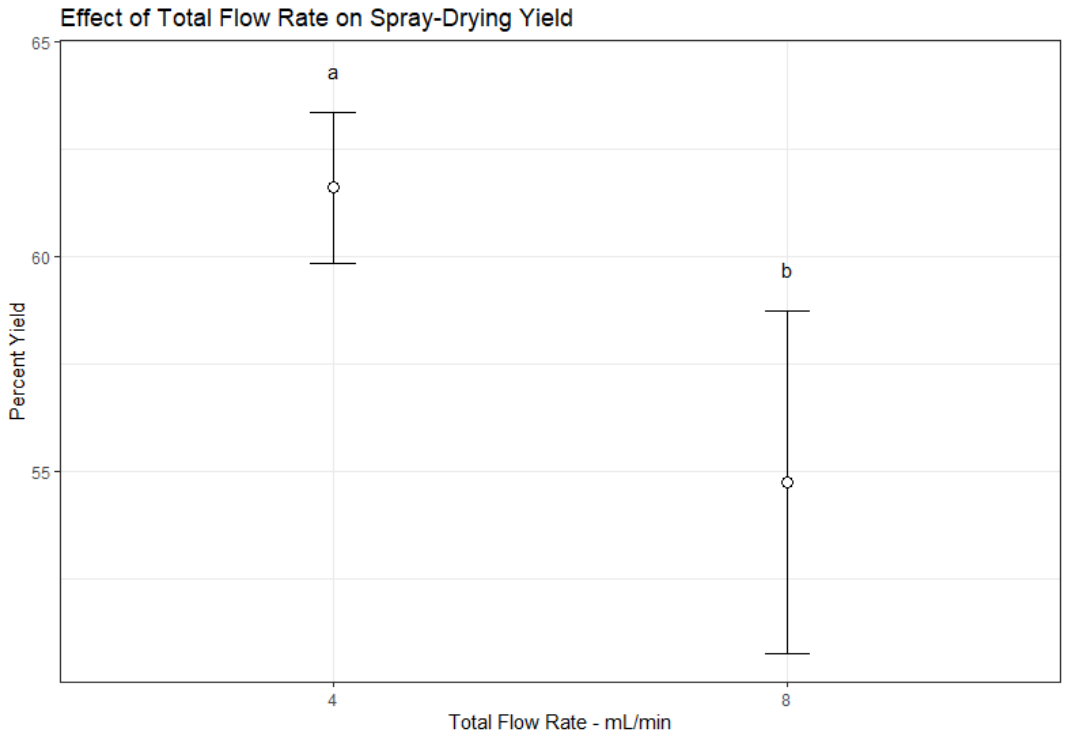

Figure 5.4 – Interaction Plot for Percent Yield

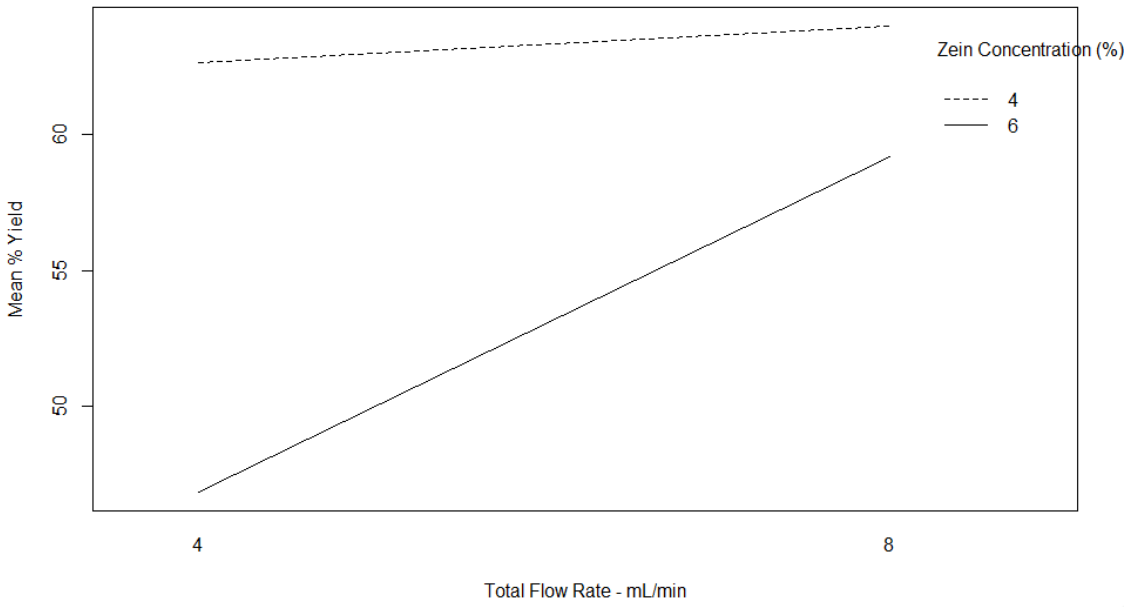

Figure 5.5 – Percent Yield by Treatment Group with Standard Error

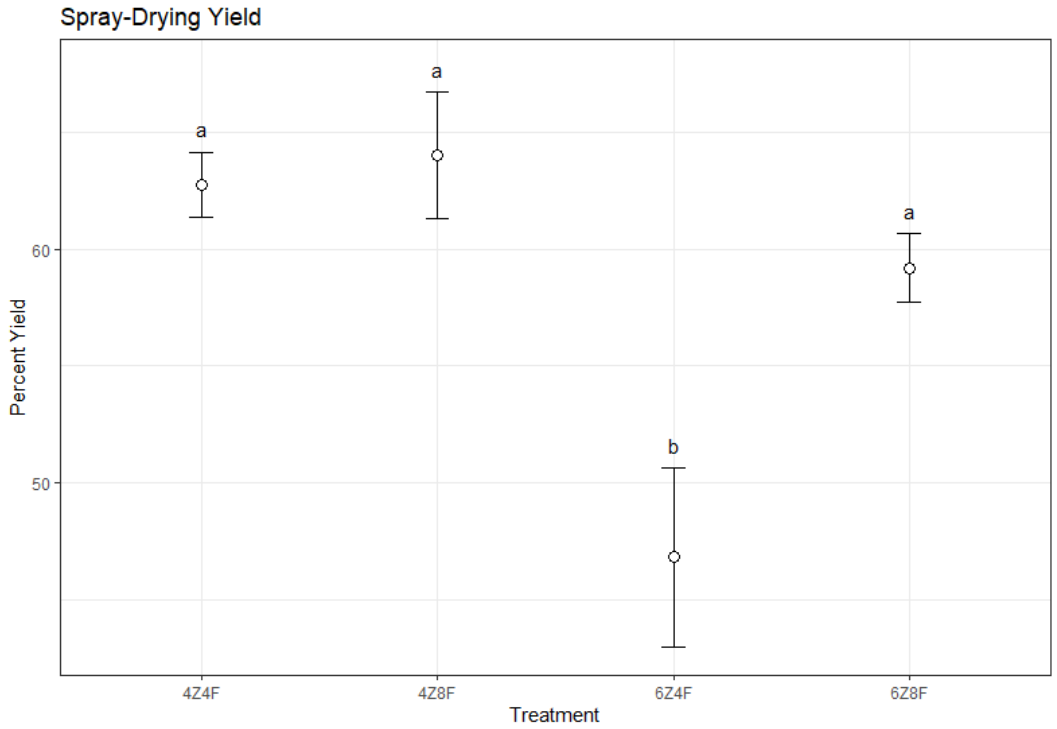

Figure 5.6 – 95% Confidence Interval for Yield by Treatment Group

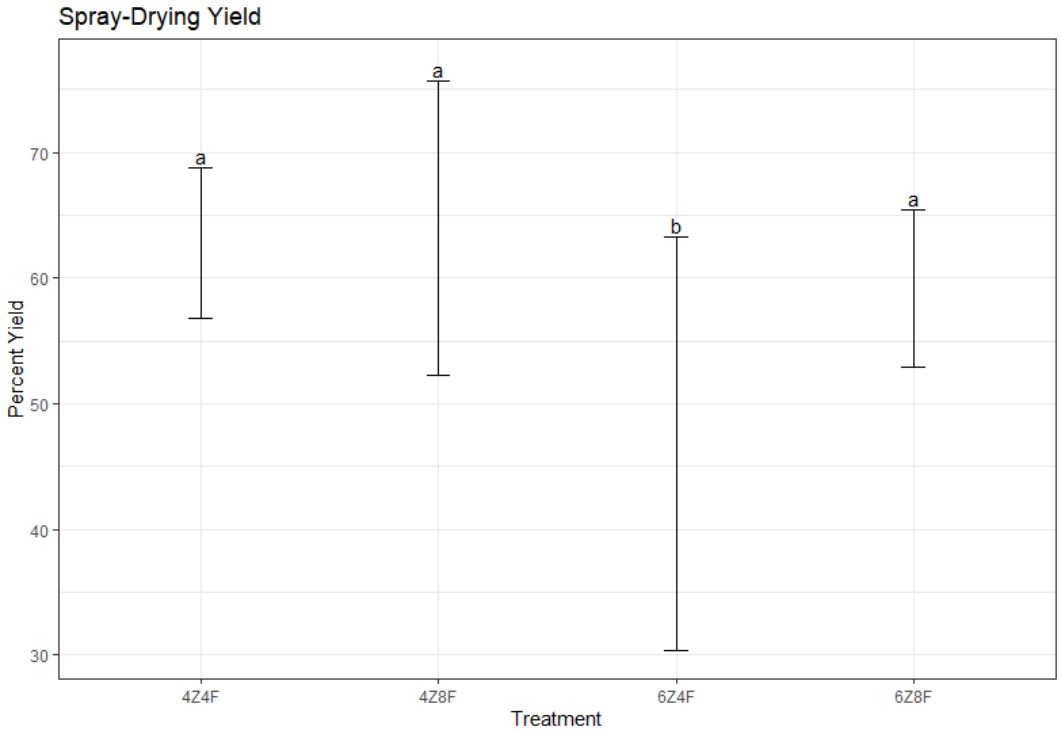

Figure 5.7 – Effect of Zein Concentration on Particle Size

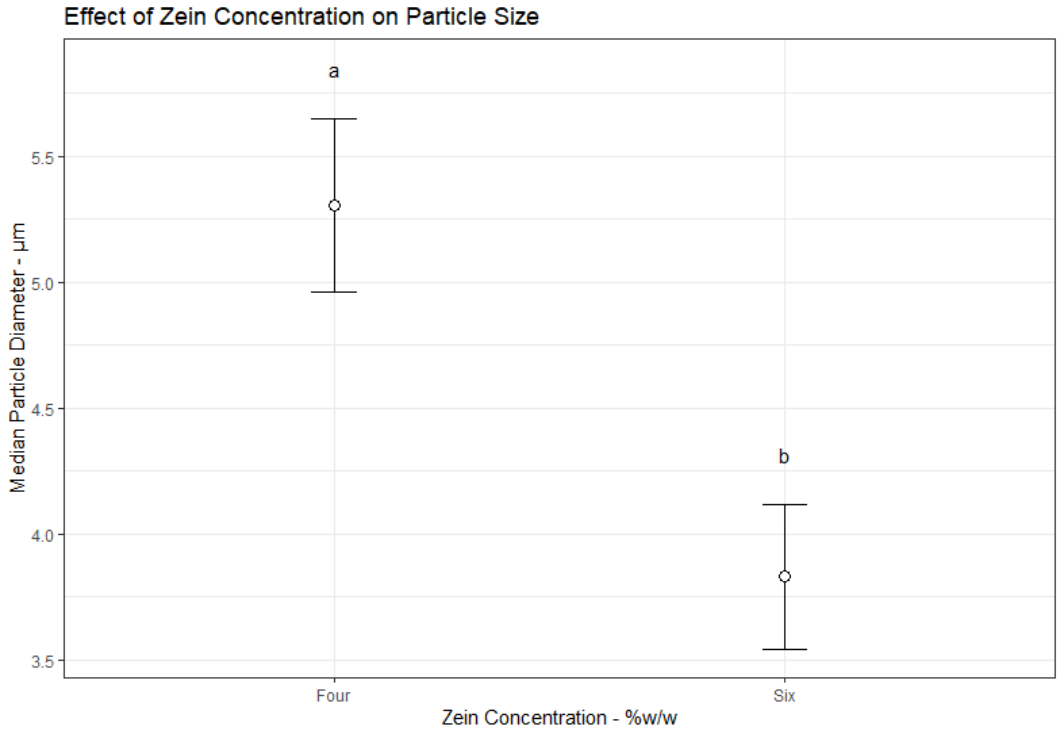

Figure 5.8 – Median Particle Diameter by Treatment Group with Standard Error

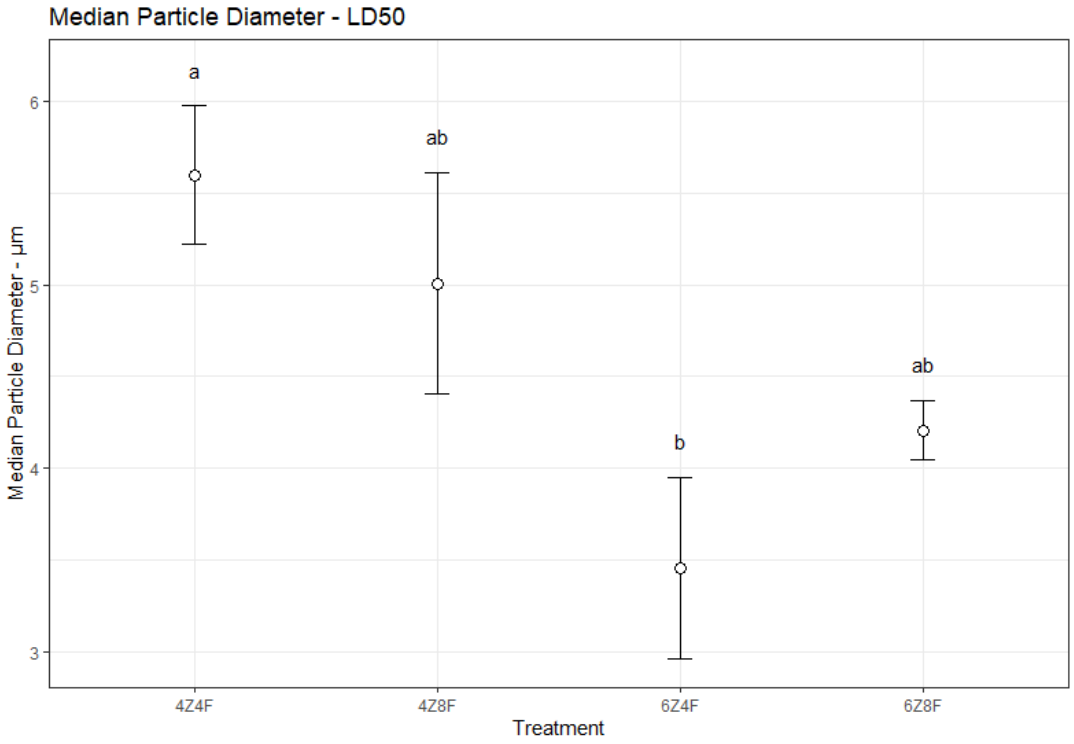

Figure 5.9 – 95% Confidence Interval for Median Particle Size

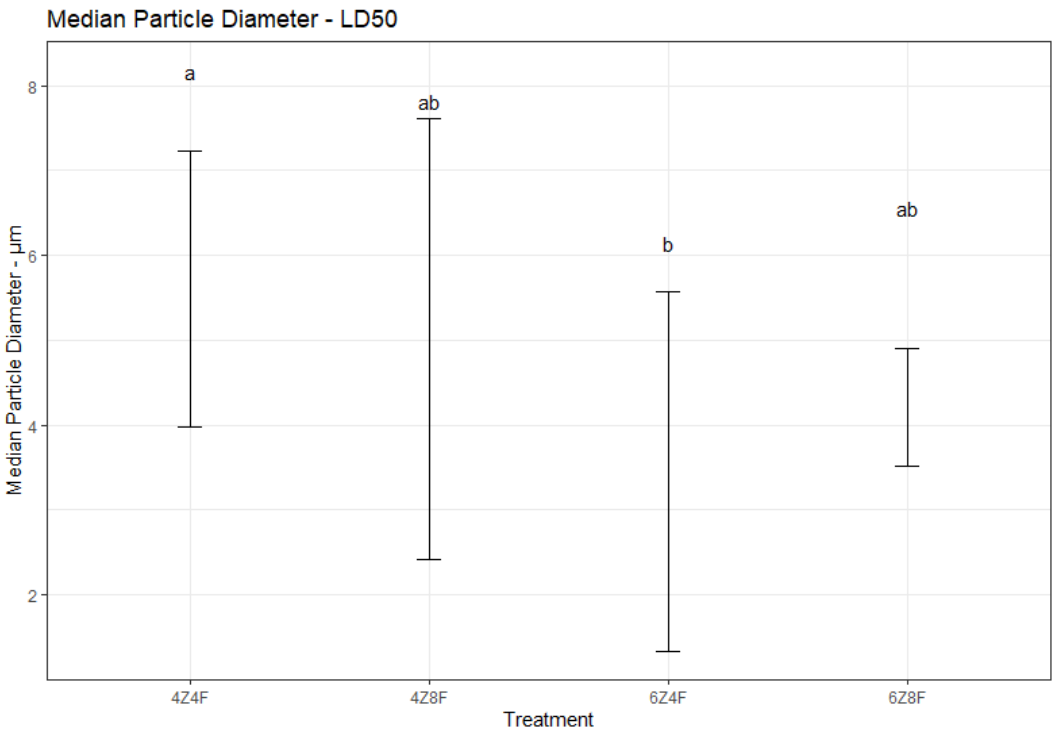

Figure 5.10 – Effect of Zein Concentration on Particle Size IQR

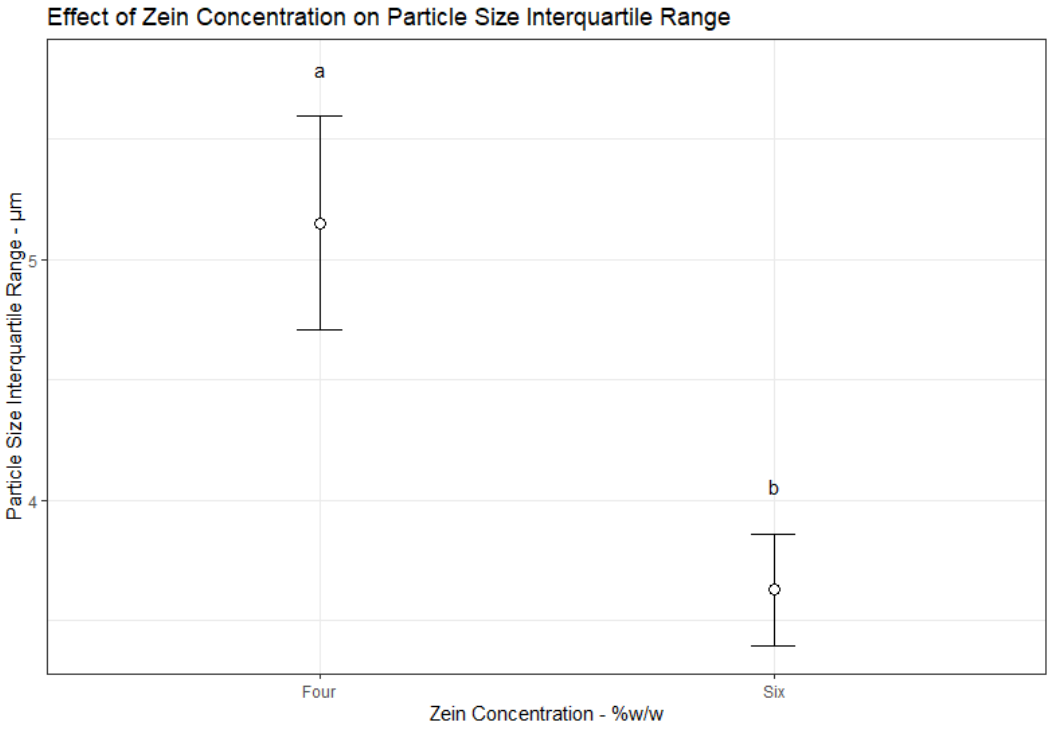

Figure 5.11 – Particle Size IQR by Treatment Group with Standard Error

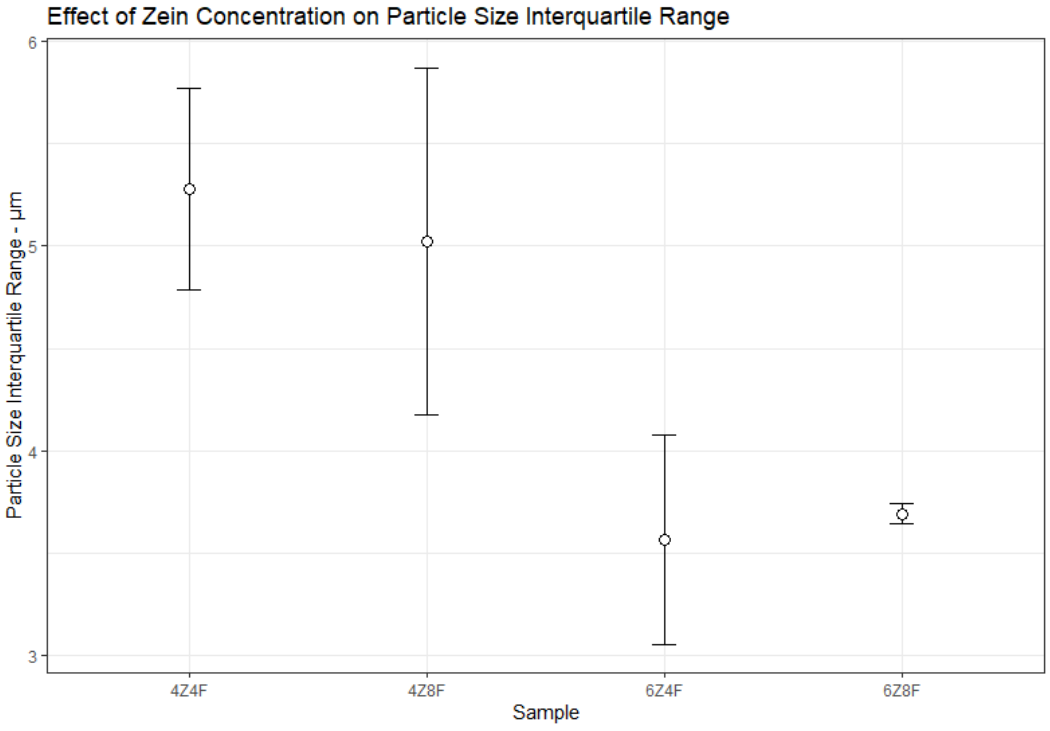

Figure 5.12 – 95% Confidence Interval for Particle Size IQR

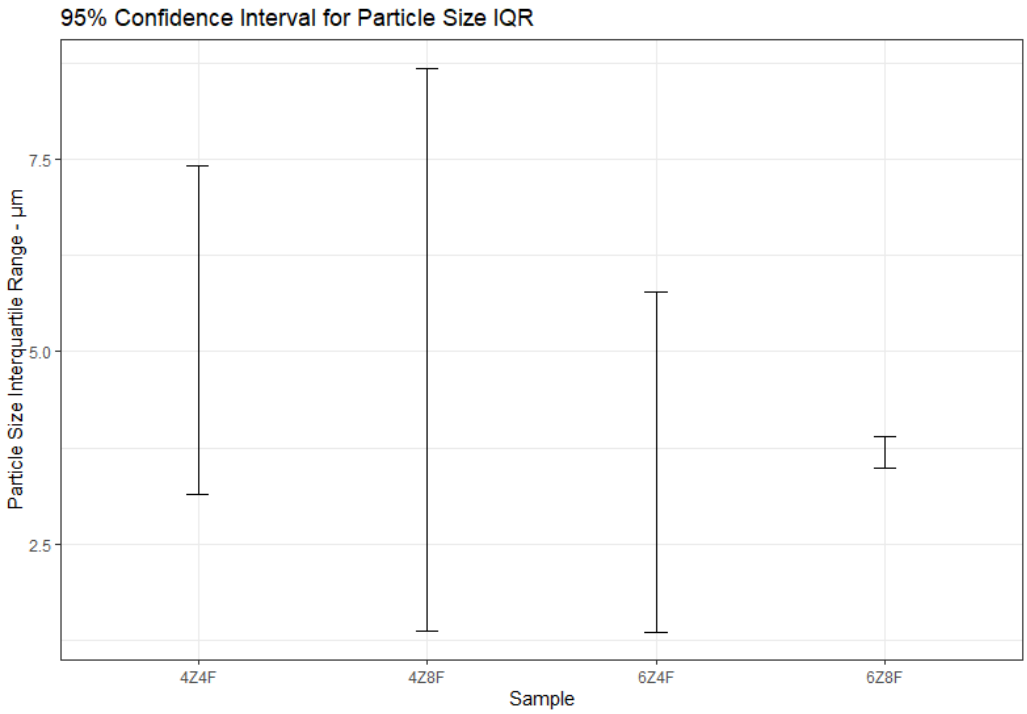

5.7 Raw Statistical Output

5.6.1 – Two-Way ANOVA for Yield

```
Analysis of Variance Table

Response: Yield
          Df Sum Sq Mean Sq F value   Pr(>F)
Zein       1 319.30  319.30 16.5427 0.003597 **
Flow       1 140.77  140.77  7.2930 0.027051 *
Zein:Flow  1  91.30   91.30  4.7302 0.061348 .
Residuals  8 154.41   19.30
---
Signif. codes:  0 ‘***’ 0.001 ‘**’ 0.01 ‘*’ 0.05 ‘.’ 0.1 ‘ ’ 1
```

5.6.2 – One-Way ANOVA for Yield

```
Analysis of Variance Table

Response: Yield
          Df Sum Sq Mean Sq F value   Pr(>F)
Trial      3 554.09 184.696  9.4756 0.005197 **
Residuals  8 155.93  19.492
---
Signif. codes:  0 ‘***’ 0.001 ‘**’ 0.01 ‘*’ 0.05 ‘.’ 0.1 ‘ ’ 1
```

5.6.3 – Two-Way ANOVA for Median Particle Diameter

```
Analysis of Variance Table

Response: Dfifty
          Df Sum Sq Mean Sq F value Pr(>F)
Zein       1 6.5033  6.5033 11.1681 0.0102 *
Flow       1 0.0189  0.0189  0.0325 0.8614
Zein:Flow  1 1.3530  1.3530  2.3234 0.1659
Residuals  8 4.6585  0.5823
---
Signif. codes:  0 ‘***’ 0.001 ‘**’ 0.01 ‘*’ 0.05 ‘.’ 0.1 ‘ ’ 1
```

5.6.4 – One-Way ANOVA for Median Particle Diameter

```
Analysis of Variance Table

Response: Dfifty
          Df Sum Sq Mean Sq F value  Pr(>F)
Sample     3 7.8752 2.62506   4.508 0.03933 *
Residuals  8 4.6585 0.58231
---
Signif. codes:  0 ‘***’ 0.001 ‘**’ 0.01 ‘*’ 0.05 ‘.’ 0.1 ‘ ’ 1
```

5.6.5 – Mean Separation for Median Particle Diameter

```
Confidence level used: 0.95
Conf-level adjustment: sidak method for 4 estimates

$contrasts
 contrast    estimate    SE df t.ratio p.value
 4Z4F - 4Z8F    0.592 0.623  8  0.950  0.7799
 4Z4F - 6Z4F    2.144 0.623  8  3.441  0.0358
 4Z4F - 6Z8F    1.393 0.623  8  2.236  0.1933
 4Z8F - 6Z4F    1.552 0.623  8  2.491  0.1362
 4Z8F - 6Z8F    0.801 0.623  8  1.285  0.5959
 6Z4F - 6Z8F   -0.751 0.623  8 -1.205  0.6406

P value adjustment: tukey method for comparing a family of 4 estimates
```

5.6.6 – Two-Way ANOVA for Particle Size Interquartile Range

```
Analysis of Variance Table

Response: IQR
          Df Sum Sq Mean Sq F value  Pr(>F)
Zein       1 6.9525  6.9525  7.5294 0.02529 *
Flow       1 0.0128  0.0128  0.0139 0.90916
Zein:Flow  1 0.1087  0.1087  0.1177 0.74039
Residuals  8 7.3870  0.9234
---
Signif. codes:  0 ‘***’ 0.001 ‘**’ 0.01 ‘*’ 0.05 ‘.’ 0.1 ‘ ’ 1
```

5.6.7 – One-Way ANOVA for Particle Size Interquartile Range

```
Analysis of Variance Table

Response: IQR
          Df Sum Sq Mean Sq F value Pr(>F)
Sample     3  7.074 2.35799  2.5537 0.1286
Residuals  8  7.387 0.92338
```

5.8 References

[1] S. Quispe-Condori, D. A. Saldaña and F. Temelli, "Microencapsulation of flax oil with zein using spray and freeze drying," 2011.

[2] X. Shi and Y. Lee, "Encapsulation of tributyrin with whey protein isolate (WPI) by spray-drying with a three-fluid nozzle," *Journal of Food Engineering,* vol. 281, p. 109992, 1 9 2020.

[3] B. Wang, S. R. Duke, Y. Wang and C. Yifen Wang, "Microencapsulation of lipid materials by spray drying and properties of products".

[4] F. Zanoni, M. Primiterra, N. Angeli and G. Zoccatelli, "Microencapsulation by spray-drying of polyphenols extracted from red chicory and red cabbage: Effects on stability and color properties," 2019.

[5] E. N. Dewi, R. A. Kurniasih, L. Purnamayanti and P. Journal, "Physical Properties of Spirulina Phycocyanin Microencapsulated with Maltodextrin and Carrageenan".

[6] Handbook on spray drying applications for food industries, 2019.

[7] "The Significance of Spray-Drying - IFT.org," [Online]. Available: https://www.ift.org/news-and-publications/food-technology-magazine/issues/2018/april/columns/processing-spray-drying-in-the-food-industry.

[8] M. Danaei, M. Dehghankhold, S. Ataei, F. Hasanzadeh Davarani, R. Javanmard, A. Dokhani, S. Khorasani and M. R. Mozafari, *Impact of particle size and polydispersity index on the clinical applications of lipidic nanocarrier systems,* vol. 10, MDPI AG, 2018.

[9] C. van Ballegooie, A. Man, I. Andreu, B. D. Gates and D. Yapp, "Using a Microfluidics System to Reproducibly Synthesize Protein Nanoparticles: Factors Contributing to Size, Homogeneity, and Stability," *Processes,* vol. 7, no. 5, p. 290, 15 5 2019.

[10] R. Chen, J. E. Wulff and M. G. Moffitt, "Microfluidic Processing Approach to Controlling Drug Delivery Properties of Curcumin-Loaded Block Copolymer Nanoparticles," *Molecular Pharmaceutics,* vol. 15, no. 10, pp. 4517-4528, 1 10 2018.

[11] Y. Feng and Y. Lee, "Microfluidic assembly of food-grade delivery systems: Toward functional delivery structure design," *Trends in Food Science & Technology,* vol. 86, pp. 465-478, 2019.

[12] Y. Feng, L. Alberto Ibarra-Sánchez, L. Luu, M. J. Miller and Y. Lee, "Co-assembly of nisin and zein in microfluidics for enhanced antilisterial activity in Queso Fresco," *LWT - Food Science and Technology,* vol. 111, pp. 355-362, 2019.

[13] C. S. Kumar, Microfluidic Devices in Nanotechnology, C. S. Kumar, Ed., Hoboken, NJ, USA: John Wiley & Sons, Inc., 2010.

[14] H. Li, D. Wang, C. Liu, J. Zhu, M. Fan, X. Sun, T. Wang, Y. Xu and Y. Cao, "Fabrication of stable zein nanoparticles coated with soluble soybean polysaccharide for encapsulation of quercetin," *Food Hydrocolloids,* vol. 87, pp. 342-351, 1 2 2019.

[15] A. G. Olenskyj, Y. Feng and Y. Lee, "Continuous microfluidic production of zein nanoparticles and correlation of particle size with physical parameters determined using CFD simulation," *Journal of Food Engineering,* vol. 211, pp. 50-59, 1 10 2017.

[16] F. Zhang, M. Aslam Khan, H. Cheng and L. Liang, "Co-encapsulation of α-tocopherol and resveratrol within zein nanoparticles: Impact on antioxidant activity and stability," *Journal of Food Engineering,* vol. 247, pp. 9-18, 2019.

[17] Q. Zhong and M. Jin, "Nanoscalar Structures of Spray-Dried Zein Microcapsules and in Vitro Release Kinetics of the Encapsulated Lysozyme As Affected by Formulations," 2009.

[18] X. Bai, C. Li, L. Yu, Y. Jiang, M. Wang, S. Lang and D. Liu, "Development and characterization of soybean oil microcapsules employing kafirin and sodium caseinate as wall materials," 2019.

[19] Y. Chen, H. Ge, Y. Zheng, H. Zhang, Y. Li, X. Su, W. Panpipat, O. M. Lai, O. M. Lai, C. P. Tan and L. Z. Cheong, "Phospholipid-Protein Structured Membrane for Microencapsulation of DHA Oil and Evaluation of Its in Vitro Digestibility: Inspired by Milk Fat Globule Membrane," *Journal of Agricultural and Food Chemistry,* vol. 68, no. 22, pp. 6190-6201, 3 6 2020.

[20] M. Veneranda, Q. Hu, T. Wang, Y. Luo, K. Castro and J. M. Madariaga, "Formation and characterization of zein-caseinate-pectin complex nanoparticles for encapsulation of eugenol," *LWT - Food Science and Technology,* vol. 89, pp. 596-603, 2017.

[21] R. Zhang, L. Huang, X. Xiong, M. C. Qian and H. Ji, "Preparation and release mechanism of lavender oil microcapsules with different combinations of coating materials," *Flavour and Fragrance Journal,* vol. 35, no. 2, pp. 157-166, 24 3 2020.

[22] "Viscosity | Lechler USA," [Online]. Available: https://www.lechlerusa.com/en/news/spray-facts/viscosity/.

[23] A. S. Mujumdar, "Industrial Spray Drying Systems," pp. 241-282, 8 11 2006.

CHAPTER 6: Encapsulation of Quercetin in Zein/Sodium Caseinate Microcapsules Spray-Dried with Varying Contact Times in a 3-Fluid Nozzle

6.1 Abstract

Microcapsules of spray-dried quercetin in a zein and sodium caseinate shell were successfully produced using a novel 3-fluid nozzle technology. Powder yields were consistently 60% or greater with median particle diameters between 3 µm – 6 µm. Quercetin encapsulation efficiency in the resultant powder exceeded 67% in all samples. All spray-dried powder samples exhibited the ability to scavenge between 8.2% - 17.7% of free DPPH (2,2-diphenyl-1-picrylhydrazyl) radical, with the least effective sample having ~80% of the scavenging capacity as a quercetin control sample.

Nozzle collar length, total flow rate, and contact time were not found to significantly affect the resultant powder yield, median particle diameter, particle size interquartile range (IQR), or antioxidant capacity. There was a significant effect of the nozzle collar length on encapsulation efficiency, with the 7.8 cm (long) collar producing higher encapsulation efficiency than the 5.2 cm or 3.9 cm collars. It could be due to the lack of fully developed flow in the shorter two nozzle collars. Overall, it was demonstrated that the novel 3-fluid nozzle technology is effective at producing encapsulated quercetin that maintained its intended function and may provide a new option for other encapsulation applications within the food industry.

6.2 Introduction

There is a large body of research suggesting that quercetin, a member of the polyphenolic flavonol group of compounds, provides both antioxidant benefits and anti-inflammatory characteristics in humans that may mitigate the risk for colorectal cancer, which is the second leading cause of cancer death in the U.S. [1, 2]. Further studies have shown that quercetin can induce cell cycle arrest and apoptosis in established cancer cells, stemming tumor growth [3, 4]. However, there are issues with quercetin as a food ingredient due to its low bioavailability as a result of minimal solubility in water [5], rapid degradation in the presence of both heat and light [6], and the bitter and astringent perception to food it imparts which further limits its application in food matrices [7].

Several studies have indicated potential benefits for the encapsulation of quercetin as a means to enhance its long-term shelf life and bioavailability in humans; however, most research in quercetin encapsulation has not included a focus on a continuous and scalable process that could be applied to commercial use [8, 9].

Microfluidic devices can be used to create particles with narrow size distribution but the throughput is extremely low, in the order of ml/hour for a typical laboratory system. Common nanoparticle production techniques using high-shear homogenizers create a large variation of particle size (large polydispersity index (PDI)) due to the spatial gradient of shear stress outward from the mixing element. Spray-drying represents a much higher throughput option for encapsulation, but can often result in large and widely dispersed powder sizes. Preliminary data presented in this study indicates that a novel 3-fluid nozzle design can successfully produce powders of zein

and sodium caseinate with small (< 10 µm) particle diameters and relatively narrow distributions, which makes this technology an ideal candidate for an encapsulation study where controlled release kinetics and/or targeted release is of high importance.

Bioactive compounds that have been successfully encapsulated in zein include antimicrobial agents such as nisin and thymol [10, 11], flavor compounds such as eugenol [12], and other polyphenolic antioxidant compounds such as resveratrol [13]. Zein encapsulates have also been modified via the use of several different surfactants. Among these compounds, sodium caseinate represents an economical and conventional ingredient that has been used both as a stand-alone shell compound as well as a surfactant modifying several different shell materials, including zein.

The objective of this study was to encapsulate quercetin within a zein and sodium caseinate shell via the proposed novel 3-fluid nozzle technology in a bench-top spray-drying application, and to study the effect of contact time within the nozzle on the physicochemical characteristics of the spray-dried powder. The hypothesis was that contact time will have a significant effect on the properties of resultant powder, with longer contact times yielding larger particles and encapsulation efficiency and shorter contact times yielding smaller particles with less total quercetin encapsulated in each particle.

6.3 Materials and Methods

6.2.1 Materials

Zein was procured from MilliporeSigma (Merck KGaA, Burlington, MA). 200 proof ethanol was supplied Decon Laboratories (DLI, Chester, PA) and was diluted to the appropriate concentration with de-ionized water from an in-house filtering system.

Casein sodium salt from bovine milk as well as DPPH (2,2-diphenyl-1-picrylhydrazyl) was also obtained from Millipore Sigma (Merck KGaA, Burlington, MA). Hydrochloric acid with a stated purity between 36.5 – 38% was obtained from Fisher Scientific (TFS, Waltham, MA). Dimethyl sulfoxide (DMSO) was supplied by the UIUC SCS chemical stockroom. De-ionized water for the continuous phase was obtained from an in-house filtration system.

Two Model 1000X syringe pumps (NEPS Inc., Farmingdale, NJ) were used to deliver the dispersed phase to the spray-dryer. The spray-dryer used for all experiments was a Buchi B-290 Mini Spray-Dryer (Buchi AG, Switzerland). Inlet air was treated through a Buchi B-296 Dehumidifier and expelled through an outlet filter, both of which were also procured from Buchi. Nitrogen was used as the atomizing gas via compressed gas cylinders provided by AirGas (Air Liquide S.A., Paris, France). The continuous phase was fed to the dryer via the peristaltic pump mounted on and controlled by the Buchi B-290 spray-dryer. The pH of both phases was measured with an Orion 8157BNUMD pH probe attached to a Orion VersaStar Advanced ElectroChemistry Meter.

Three stainless-steel nozzle “collars” were fabricated by the University of Illinois at Urbana Champaign Electrical and Computer Engineering Machine Shop and fit to thread into the body of the stock 3-fluid nozzle provided by Buchi in order to vary contact time between the dispersed and continuous phases. Figure 6.1 illustrates these modifications of the stock 3-fluid nozzle, and Table 6.1 summarizes the different collar lengths and corresponding contact times.

6.3.2 Methods

6.3.2.1 Stock Solution Preparation for Spray-Drying

Stock solutions of zein and sodium caseinate in ethanol (the dispersed phase) were prepared by first weighing out 200 mL of 70% v/v ethanol. For all trials, 4% w/w zein was weighed, along with the corresponding 0.25:1 mass ratio of sodium caseinate to be dissolved in the dispersed phase. The zein was added to the ethanol solution first, followed by the slow addition of sodium caseinate to the zein-ethanol solution on a stir plate set to ~500 rpm. An initial pH adjustment of 3.0 mL of 1.0 M HCl was added to reach a pH of between 2.9 – 3.1 Quercetin at a ratio of 1:20 w/w quercetin to zein was then weighed and added to the stirred solution, and the stirring speed increased to ~700 rpm. The beaker was covered to prevent excess light from degrading the quercetin and the sample was hydrated overnight.

For stock solutions of sodium caseinate (the continuous phase), first 800 mL of de-ionized water was measured in a large beaker. The beaker was placed on a stir-plate set to ~350 rpm and an initial pH adjustment was accomplished via the addition of 7.0 mL of 1.0 M HCl. The pH was between 2.9 and 3.1 after the initial adjustment. The appropriate mass of sodium caseinate, based on the zein and caseinate masses in the dispersed phase, was added to the beaker. The stirring speed increased to ~450 rpm and the sample was allowed to hydrate overnight. Both dispersed and continuous phases were checked for pH the following day and more 1.0 M HCl was added if necessary to reach pH 3.0.

6.3.2.2 Spray-Drying to Produce Encapsulated Quercetin Powder

The spray-dryer was assembled in a similar way to that described in Chapter 5. Briefly, the spray-dryer and humidification unit were both turned on and the spray-dryer allowed to warm up to a set inlet temperature until the outlet temperature had stabilized. During this time, the zein/sodium caseinate/quercetin stock solution was loaded into two separate 50 mL BD syringes and placed in the syringe pumps. The syringe pumps were programmed with the correct diameter (26.67 mm) of syringe and the flow rate for the trial. These syringes were connected to the inner liquid nozzle channel that was elevated above the nozzle body by one of the three fabricated collar extensions. The sodium caseinate stock solution as the continuous phase was pumped into the outer liquid nozzle channel using the peristaltic pump mounted on the spray-dryer. Atomizing air pressure and flow-rate were kept constant at 40 psi and 40% on the rotameter for all trials. The aspirating fan was set to 90% power and the outlet temperature was maintained at ~ 70 degrees Celsius for all trials by adjusting the inlet temperature accordingly.

The nozzle collar length and total flow rates were the two variables explored in this study. Table 6.2 shows the experimental design used, and also summarizes the contact time between two phases at each treatment level. Spray-drying continued until 100 mL of the dispersed phase had been pumped through the nozzle. At that point the dryer was shut down and allowed to cool for ~10-15 minutes before the powder was collected. The powder was immediately weighed, along with the remaining dispersed and continuous phases. The powder samples were kept in 50 mL opaque Falcon tubes for further analysis and storage. The spray-dryer and nozzle assembly were thoroughly cleaned between each run and the outlet filter was changed.

6.3.2.3 Powder Yield Calculations

Yield was calculated with the same method as described in Chapter 5. Briefly, the total solids for both dispersed and continuous phases were calculated based on the solids weight compared to the overall phase weight. The theoretical maximum powder mass was calculated using these total solids numbers multiplied by the total mass of each phase sprayed, and the resultant powder yield was calculated as the actual collected powder weight divided by the maximum theoretical powder weight and expressed as a percentage.

6.3.2.4 Particle Size and Distribution

Particle size and distribution were determined using the same method as described in Chapter 5. Powders produced were analyzed via a Shimadzu SALD 2300 Laser Diffraction particle size analyzer (Shimadzu Co., Kyoto, Japan). Powder samples were imaged with a FEI Quanta FEG 450 Environmental Scanning Electron Microscope (FEI Co., Hillsboro, OR) at the Beckman Institute for Advanced Science and Technology in Urbana, IL with the assistance of the Imaging Technology Group. Median particle size (LD,50) is reported for each treatment combination, and the particle size interquartile range (IQR) was used to estimate the width of each size distribution. The particle size IQR has been defined as the particle diameter under which 25% of the population falls subtracted from the particle diameter under which 75% of the population falls.

6.3.2.5 Scanning Electron Microscopy

Powder samples were first mounted on double sided carbon tape and coated with a ~ 1 nm thick layer of gold/platinum (Au/Pd) with a Desk II Turbo Sputter Coater (Denton Vacuum, Moorestown, NJ). Samples were imaged with a FEI Quanta FEG 450

Environmental Scanning Electron Microscope (FEI Co., Hillsboro, OR) at the Beckman Institute for Advanced Science and Technology in Urbana, IL.

6.3.2.6 Encapsulation Efficiency

Encapsulation efficiency is a standardized means of not only estimating how much of the core material was successfully complexed within the shell material, but also comparing the efficacy of the different treatment groups for encapsulating the core material. Initially, 0.1 g of each powder sample was placed in a 50 mL Falcon tube; 10 mL of 20% v/v ethanol was then pipetted on top of the sample in each tube. Each sample was then mixed on the vortex meter for about 10s followed by a centrifugation in an IEC Centra CL2 procured from TFS at 4000 RPM for 15 minutes.

After centrifugation, 0.5 mL of the supernatant from each tube was pipetted into 4.5 mL of 20% v/v ethanol. Each sample solution was then briefly swirled to mix and absorbance was measured at 380 nm (the excitation wavelength for quercetin) in a Spectronic Genesys5 spectrophotometer purchased from TFS. The absorbance of each sample was used to calculate the quercetin concentration in the supernatant based on a standard curve of pure quercetin in 20% ethanol also generated at 380 nm. Encapsulation efficiency is then calculated based on the amount of moles of quercetin that were “washed off” in the first step of the procedure; it is assumed that the washed quercetin was either present as unencapsulated or only loosely associated with the microcapsule surfaces. Figure 6.2 shows the standard curve for quercetin in 20% ethanol, and Equations 9 through 13 show the calculation steps for encapsulation efficiency.

$$Q_{Loading} = \left[\frac{\left(\frac{M_Q}{M_{DP}}\right) * M_{Spray}}{M_{Max}}\right] * P_Q \quad [9]$$

$$Q_{mol,sample} = \frac{Q_{mass,sample} \times Q_{Loading}}{MW_Q} \quad [10]$$

$$Q_{conc} = \frac{Abs - b}{m} \quad [11]$$

$$Q_{mol,super} = \frac{Q_{conc}}{V_{dilution}} \quad [12]$$

$$Encapsulation\ Efficiency = \frac{Q_{mol,sample} - Q_{mol,super}}{Q_{mol,sample}} \times 100\% \quad [13]$$

Where , $Q_{Loading}$is the mass ratio of quercetin in the spray-dried powder, $M_Q$is the total mass of quercetin added to the dispersed phase, M_{DP} is the total mass of the dispersed phase, M_{Spray} is the mass of dispersed phase spray-dried, M_{Max} is the theoretical maximum mass of spray-dried powder, P_Q is the purity of quercetin, $Q_{mol,sample}$ is the moles of quercetin in the powder sample, $Q_{mass,sample}$ is the mass of the powder sample used, MW_Q is the molecular weight of quercetin (302.236 g/mol), Q_{conc} is the concentration of quercetin in the supernatant after centrifugation, Abs is the absorbance of the sample at 380 nm, b is the intercept of the standard curve, m is the slope of the standard curve, $Q_{mol,super}$ is the moles of quercetin in the supernatant, and $V_{dilution}$ is the volume of the dilution used.

6.3.2.7 Antioxidant Capacity

Due to quercetin being both a heat and light sensitive compound, it was critical to verify that the form and function of quercetin through the microencapsulation and spray-

drying process. First, 0.02 g of each powder sample was fully dissolved in 5 mL of DMSO. DMSO was chosen as a solvent for this test due to the limited solubility of zein in 100% ethanol and the limited solubility of DPPH in aqueous systems. While the samples were placed in a dark enclosure to fully dissolve, a stock solution of 0.2 mM DPPH was prepared by adding 0.00076 g of DPPH to 100 mL of DMSO in a volumetric flask. This flask was wrapped in tin foil to prevent light infiltration and then sonicated for 10 minutes to ensure complete dissolution of DPPH.

Once the DPPH stock solution was prepared, samples were prepared by adding 2 mL of the dissolved powder sample to 2 mL of DPPH stock solution in a separate test tube. A negative control consisting of 2 mL DPPH in 2 mL DMSO was also prepared. The remaining 3 mL of each dissolved powder sample was used as positive control blanks. All prepared samples were then incubated for 30 minutes in the dark and then the absorbance was measured at 517 nm (the excitation wavelength for DPPH) in the same spectrophotometer used for encapsulation efficiency. Antioxidant capacity was then expressed as percent inhibition (%I), the calculation for which is shown in Equation 14 below:

$$\%I = \left[A_0 - \frac{(A - A_b)}{A_0}\right] \times 100\% \quad [14]$$

Where A_0 is the absorbance of DPPH in the negative control, A is the absorbance of the sample mixed with DPPH, and $A_b$is the absorbance of the blank sample in the absence of DPPH.

It was also imperative to determine antioxidant capacity of the treatments relative to an internal quercetin standard. To do this, samples with different weights from the

treatment group that had the lowest calculated %I (Medium Collar, Low Flow) were taken. Each of these samples was then dissolved in 5 mL of DMSO, resulting in a range of quercetin concentrations from the treatment group chosen. A pure quercetin stock solution was created by adding 0.01 g of quercetin to 100 mL of DMSO; a set of 5 more 2 mL dilutions was prepared using 0.2 – 1.2 mL of the quercetin stock solution added to a balance of DMSO. Table 6.3 outlines the dilutions and concentrations for both the powder samples and quercetin control.

Then, 2 mL of each sample was pipetted into 2 mL of 0.2 mM DPPH, incubated in the dark for 30 minutes before the reading of absorbance at 517 nm. The IC50 is then defined as the concentration of quercetin required to neutralize 50% of the DPPH radical and used to compare the antioxidant capacity with the quercetin control. Figure 6.3 and 6.4 shows the resultant absorbance vs. concentration curves for both the powder samples and quercetin control.

6.3.2.8 Circular Dichroism

Table 6.6 summarizes the α-helix, β-sheet, and random coil percentages found in each sample. Microcapsules produced with a short contact time (~3 seconds) appears to have more similar α- helix content to zein from the manufacturer, while microcapsules produced with a long contact time (~19 seconds) have a much higher α-helix content. Similarly, microcapsules that were produced via high-shear emulsification and spray-dried with a 2-fluid nozzle also have much higher α-helix content, indicating that contact time may drastically impact the level interaction between zein and sodium caseinate. The higher percentage of α-helix content (and correspondingly lower percentage of β-sheet content) could be a mechanism for the prevention of zein agglomeration via the

addition of a surfactant; the β-sheet structures in zein tend to have higher molecular interactions due to the exposed surfaces of the glutamine “turns”, which have hydrogen bonding characteristics [4]. It is possible that by reducing the percentage of β-sheets in the tertiary structure of zein, surfactants allow for less intermolecular interactions between zein particles.

6.3.2.9 Statistics

Statistical analyses were conducted with the R programming language in an RStudio environment. ANOVA was used to evaluate mean differences between treatment groups; the Shapiro-Wilkes test was used to confirm normality of residuals and the Levene-Forsythe test was used to confirm homogeneity of variance prior to ANOVA being conducted. All *post-hoc* mean separation tests were conducted using Tukey’s HSD within R. All statistical plots were generated in R via the “ggplot” package of data visualization functions. Raw statistical outputs have been included in section 6.7 of this chapter.

6.4 Results and Discussion

6.4.1 Percent Powder Yield

No significant effect of either nozzle collar length or total flow rate was found on the powder yield; moreover, no significant differences exist between individual treatment groups. Percent powder yields were in line with expectations based on the experimental results described in Chapter 5; Table 6.4 summarizes the powder yield for each sample, and Figures 6.5 and 6.6 illustrate the powder yield for each treatment group and the 95% confidence interval for yield, respectively.

Given that the yields all fall within the 60-70% range predominantly, the novel 3-fluid nozzle appears to not detrimentally effect total powder throughput. This is an

important consideration when scaling up operations as even if all other physicochemical properties of the powder are in line with what a manufacturer requires, low powder yield across the board for the technology limits its use in economies of scale. These experiments indicate that yield should not be a limiting factor for the proposed 3-fluid nozzle technology when considering the potential scale-up to large spray-drying operations.

It should be noted that moisture content analysis was not done for powder samples; therefore, the yield calculations assume a 0% moisture content. Actual yields would be <2% lower than reported assuming moisture contents of between 2-3%, which does not bring any reported yields under an acceptable level.

6.4.2 Particle Size

No significant effect of either nozzle collar length or total flow rate was found on the resultant median particle size. No individual treatment was found to be significantly different from any other treatment as well. Table 6.4 summarizes the median particle diameter for each sample and Figures 6.7 and 6.8 illustrate the particle size across each treatment group and the 95% confidence interval for particle size, respectively.

Particle sizes seemed mostly centered around the approximately 5 micron range. These are in-line with what was found in the studies detailed in both Chapters 4 and 5, implying that the addition of quercetin to the system does not meaningfully effect overall particle size, a potentially positive sign that encapsulation and/or complexation has been achieved. The overall small magnitude of median particle size seen is also positive from a controlled release standpoint, as smaller particles have a larger surface area to volume ratio, mitigating high variability in release kinetics from individual

particles. Table 6.5 shows SEM images of representative powder samples which seems to confirm the size ranges reported from the LD particle sizer.

Notably, it appears that once again the spray-drying operation by far a larger force for driving particle size than the particle assembly method. At the spray-drying and contact time parameters tested, no difference was found in particle size across any treatment group. It is possible that two narrow a range of contact times were studied to observe a significant effect or interaction, and future work should prioritize large differences between contact times to try to tease apart any potential differences. However, given the dynamic nature of spray-drying, it also may be more pertinent to study the effect of different drying parameters (e.g. temperature, atomizing air pressure, aspirator flow rate, etc.) on the physical characteristics of powder rather than the microcapsule assembly method. It is worth noting that the novel 3-fluid nozzle technology does appear to save a processing step by eliminating the need for a homogenous suspension or emulsion of microcapsules prior to spray-drying, which could be advantageous for manufacturers at large scale.

6.4.3 Particle Size Distribution

No significant effect of either nozzle collar length or total flow rate was observed on the resultant particle size IQR. No significant differences between individual treatment groups was detected either. Table 6.4 summarizes the particle size IQR for each sample, and Figures 6.9 and 6.10 illustrate the particle size IQR across each treatment and the 95% confidence interval for particle size IQR, respectively.

These results are also in line with what was seen in Chapter 5, and the interpretation is generally the same as what it is for particle size. The spray-drying

parameters dominate the microencapsulation method when determining powder particle physical characteristics, at least at the contact times and spray-drying parameters used in this study.

Most importantly, the distributions remain relatively small compared to that of some traditional results seen in spray-drying. This is once again a positive sign for use of the proposed 3-fluid nozzle technology in applications where controlled release is important. Not only does is it save manufacturers a processing step by assembling the microcapsules *in situ* without additional energy input, the resultant powders have small median diameters and narrow distributions, which are of the utmost importance when controlled release kinetics is the goal for a microencapsulated system.

6.4.4 Encapsulation Efficiency

Nozzle collar length was observed to have a significant effect on the encapsulation efficiency of the spray-dried powder samples. The longest collar (7.8 cm) produced powders that had statistically higher encapsulation efficiencies than either the medium or short collars. No significant effect of total flow rate on encapsulation was observed, nor was there an associated significant interaction. No significant difference between individual treatment groups was detected. Table 6.4 summarizes the encapsulation efficiency for each sample, Figure 6.11 illustrates the effect that collar length had on encapsulation efficiency, and Figures 6.12 and 6.13 illustrate the encapsulation efficiency for each treatment level and the 95% confidence interval for encapsulation efficiency, respectively.

SEM images, which can be seen in Table 6.5, indicate that there is no free quercetin in the powder samples, as the defined crystalline structure of quercetin is not

present in the images. This result implies that the quercetin lost in the encapsulation efficiency analysis may be weakly bound on the surface of the microcapsules or located just below the surface of the microcapsules, causing it to solubilize and/or diffuse out during the wash step. It is an encouraging sign for the proposed nozzle technology as it indicates that the core material is successfully interacting with the shell materials during the contact time present in the 3-fluid nozzle body.

Interestingly, there is only an effect of collar length on encapsulation efficiency without any corresponding statistically significant differences observed in contact time. In fact, the two highest encapsulation efficiencies observed were in the longest collar treatments, even though statistically they are not significantly different from the other treatments. One possible explanation for this is that even though the contact times are the same, the longer distance scale that must be travelled in the long collar allows for more time for fully developed flow to occur.

Fully developed flow is defined as the point at which the velocity profile no longer changes with respect to time in the fluid column, and for laminar flow is a function of only the Reynolds number (*Re*) and the pipe diameter. Equations 15-16 below show the calculations for Reynolds number and entrance length ($L_{h,laminar}$,the distance required for fully developed flow) below.

$$Re = \frac{\rho v D}{\mu} \quad [15]$$

$$L_{h,laminar} = 0.05ReD \quad [16]$$

Where ρ is the fluid density in kg/m^3, v is the fluid velocity in m/s, D is the pipe diameter in m, and μ is the fluid viscosity in kg*m^{-1}*s^{-1}.

The *Re* for the 5 mL/min treatment level was 11.46 with a corresponding entrance length of 0.296 cm; the *Re* for the 10 mL/min treatment level was 22.93 with a corresponding entrance length of 0.591 cm. It should be noted that because density and viscosity measurements were not done for the zein/sodium caseinate/quercetin in water/ethanol system, these parameters were estimated using data for pure water, which likely overestimates the Reynold's number due to the uncounted for effect on fluid viscosity. However, these parameters indicate that a larger percentage of the flow contact time exists at fully developed flow in the long collar at low flow rates (~98.5%) than in the short collar with high flow rates (~88%).

Quercetin loading was found to be between 1.9 mg/g – 2.3 mg/g of dry powder. Animal models have indicated that quercetin has an inhibitory effect on cancer cells at concentrations as low as 50 mg/kg of body weight in Wistar rats or 0.5% of total diet in Sprague-Dawley rats; it should be noted that these studies used free quercetin rather than encapsulated quercetin [3]. An *in vitro* study with encapsulated quercetin micelles indicated notably higher improvement over free quercetin with loading of ~14 mg/g of powder [18]. It may therefore be necessary to re-formulate the powder to increase quercetin loading; however, testing with the specific system used should still be carried out to determine if the loading is ineffective or not.

6.4.5 Antioxidant Capacity

No significant effect of either nozzle collar length or total flow rate was observed on antioxidant capacity. No significant difference between treatment groups was detected either. Table 6.4 summarizes the percent inhibition for each sample, and

Figures 6.14 and 6.15 illustrate the percent inhibition across each treatment and the 95% confidence interval for percent inhibition, respectively. The powder sample with the lowest percent inhibition was shown to have ~80% of the total antioxidant capacity as a pure quercetin standard based on the IC50.

The results for the IC50 are extremely positive when considering the application of the proposed nozzle technology for encapsulation. Retaining 80% of the function of the encapsulated quercetin relative to the purified compound indicates that either the nozzle allows for complete enough encapsulation to protect the quercetin from the heat and light of being spray-dried and/or that the spray-drying conditions are mild enough that most of the quercetin remains intact. This has wide-ranging implications for the use of the technology to encapsulate numerous polyphenolic antioxidant compounds that have similar degradation characteristics as quercetin.

The lack of difference in percent inhibition indicates that, if contact time between the two phases is a driver for antioxidant capacity, then an insufficient range of contact times to verify at what point the differences are observable. It is also again possible that spray-drying remains the dominant force for determining physicochemical characteristics of powder.

6.4.6 Circular Dichroism

Table 6.6 summarizes the α-helix, β-sheet, and random coil percentages found in each analyzed sample. Regardless of contact time or preparation method, zein with a surfactant added had a higher percentage of α-helix structures than did unadulterated zein from the manufacturer. This could be a mechanism for the prevention of zein agglomeration via the addition of a surfactant; the β-sheet structures in zein tend to

have higher molecular interactions due to the exposed surfaces of the glutamine “turns”, which have hydrogen bonding characteristics [4]. It is possible that by reducing the percentage of β-sheets in the tertiary structure of zein, surfactants allow for less intermolecular interactions between zein particles.

6.5 Conclusion

The novel 3-fluid nozzle was successfully used to generate spray-dried microcapsules of quercetin in zein and sodium caseinate. Importantly, no prior homogenization was required to ensure microencapsulation, as the self-assembly of zein and sodium caseinate into micelles occurred *in situ*. In general, collar length and flow rate, and correspondingly contact time between the two phases, had little influence on the resultant powder characteristics. Yield was relatively high and not considered detrimental to the scale-up of the technology to industrial levels. Powder size and distribution were both consistently small and relatively uniform relative to typical spray-drying applications.

Encapsulation efficiency appears to significantly higher with longer collar lengths, potentially due to fully developed flow not occurring with the shorter lengths even at higher contact times. Regardless, encapsulation efficiency is considered to be relatively high, indicating that most of the quercetin is insulated against the heat, light, and oxidation that occurs during and post spray-drying. Antioxidant capacity did not very across the samples, and samples retained 80% of the antioxidant capacity of a quercetin control group.

Overall, this technology has shown it has a high level of promise with regards to other potential encapsulation applications. With high yields, low particle sizes and

narrow distributions, and by demonstrating successful encapsulation without core degradation, the novel 3-fluid nozzle could be an important tool for encapsulation at larger scales for the food industry.

6.6 Tables and Figures

Table 6.1 – Summary of Nozzle Collar Lengths and Contact Times

Collar Length	*Contact Time (at 5 mL/min)*	*Contact Time (at 10 mL/min)*
7.8 cm	19.57 s	9.79 s
5.2 cm	13.05 s	6.52 s
3.9 cm	9.79 s	4.89 s

Table 6.2 – Experimental Design and Treatment Codes

	7.8 cm Collar	**5.2 cm Collar**	**3.9 cm Collar**
5 mL / min	*LCLF*	*MCLF*	*SCLF*
10 mL / min	*LCHF*	*MCHF*	*SCHF*

Table 6.3 – Quercetin Concentrations for IC50 Experiments

Concentration of Quercetin from Spray-Dried Powder	Concentration of Quercetin From Control
2.19 x 10^{-5} mol/L	7.60 x 10^{-6} mol/L
8.23 x 10^{-5} mol/L	1.52 x 10^{-5} mol/L
1.25 x 10^{-4} mol/L	2.29 x 10^{-5} mol/L
1.61 x 10^{-4} mol/L	3.04 x 10^{-5} mol/L
N/A	3.80 x 10^{-5} mol/L

Table 6.4 – Analysis Results by Treatment Group

	Yield (%)	LD50 (μm)	Particle Size IQR (μm)	Encapsulation Efficiency (%)	Antioxidant Capacity (%Inhibition)
SCHF	62.9 ± 6.1	5.28 ± 0.17	4.80 ± 0.38	67.8 ± 2.34	16.4± 7.31
MCHF	64.1 ± 5.6	6.04 ± 0.42	5.54 ± 0.68	69.6 ± 2.47	17.7± 0.26
LCHF	67.9 ± 2.3	5.60 ± 0.16	5.47 ± 0.016	73.5 ± 1.93	10.9 ± 2.25
SCLF	64.3 ± 3.7	5.83 ± 0.068	5.59 ± 0.13	76.8 ± 2.41	17.2 ± 1.59
MCLF	68.3 ± 7.6	5.47 ± 0.18	5.46 ± 0.37	70.1 ± 3.57	8.23 ± 1.68
LCLF	61.3 ± 2.9	5.36 ± 0.38	5.25 ± 0.44	78.9 ± 4.22	14.2 ± 7.25

Table 6.5 – Scanning Electron Microscope Images

Zein – Manufacturer – 50 µm view	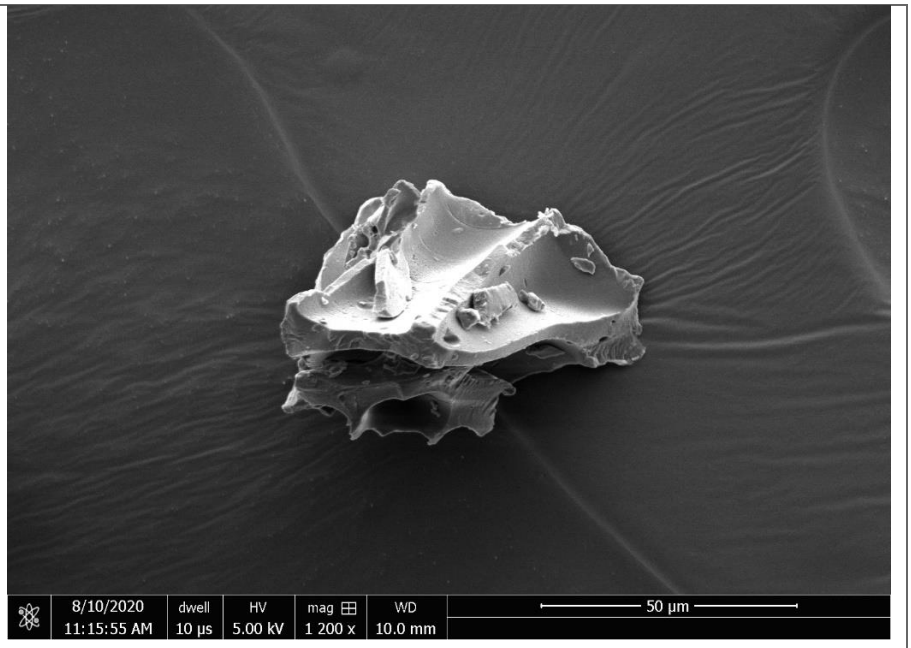
Sodium Caseinate – Manufacturer – 50 µm view	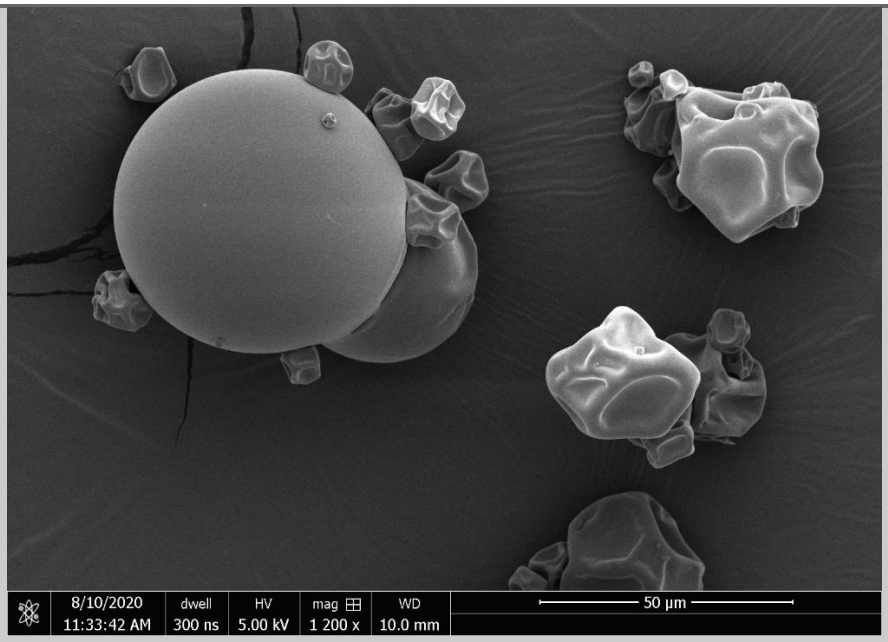

Table 6.5 (cont)

Quercetin – Manufacturer – 50 µm view	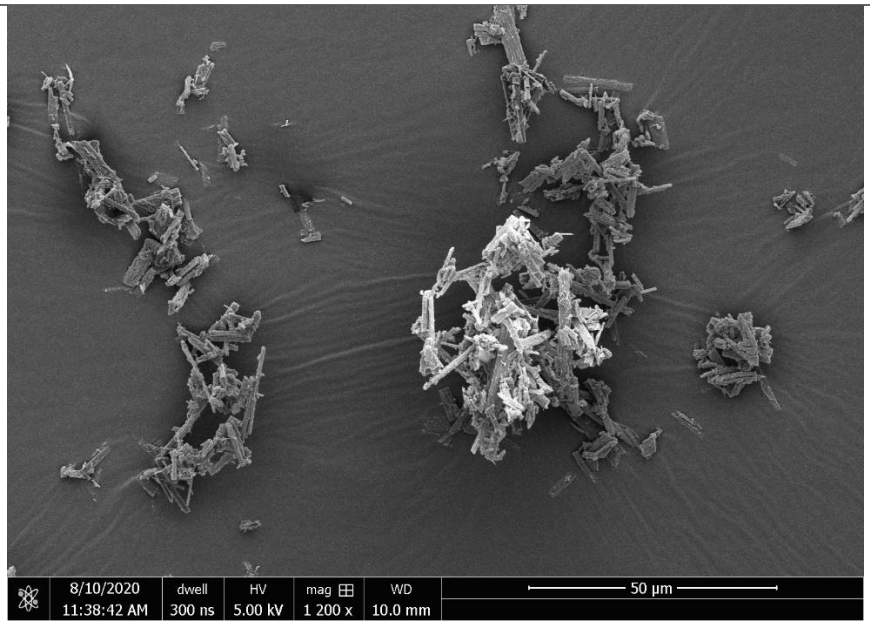
LCLF – 19s contact time – 50 µm view	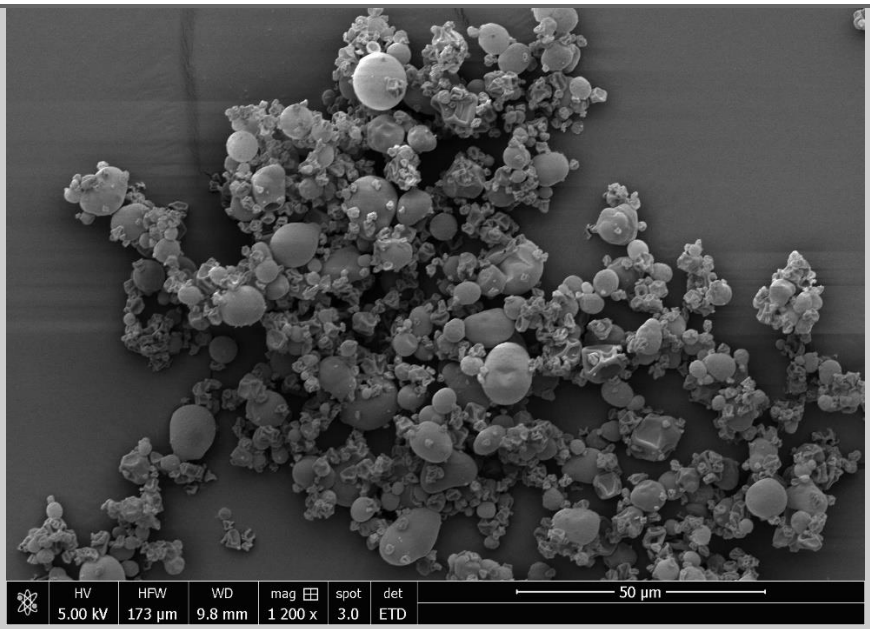

Table 6.5 (cont)

LCLF – 19s contact time – 10 µm view	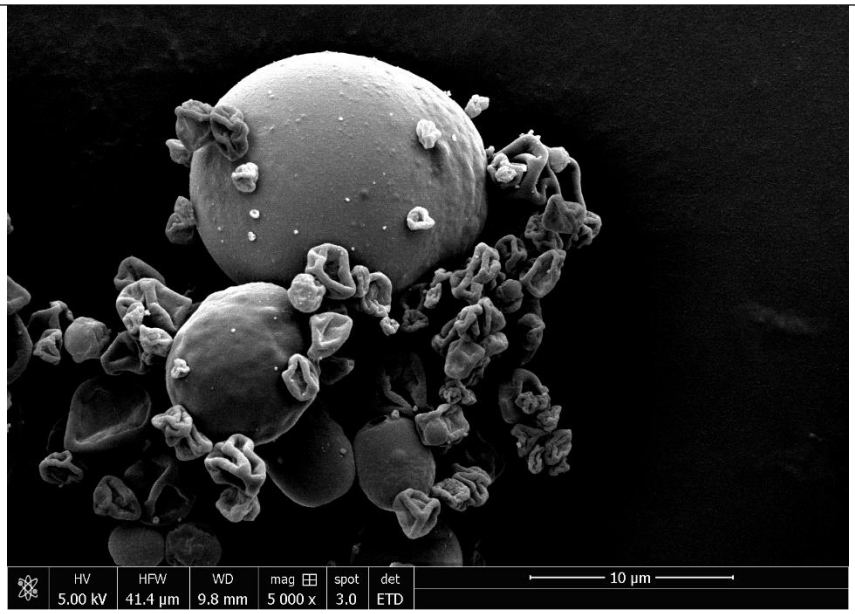
SCHF – 4s contact time – 50 µm view	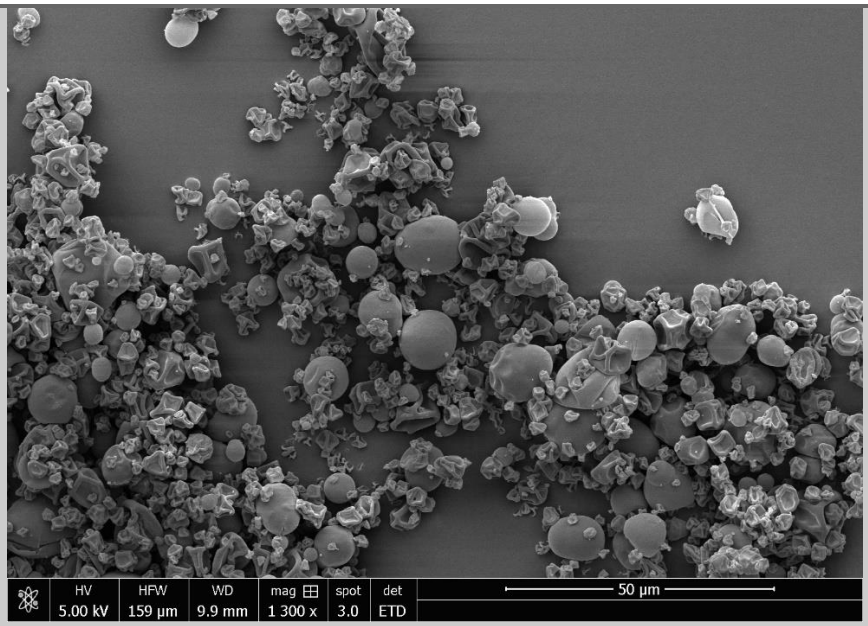

Table 6.5 (cont)

SCHF – 4s contact time – 10 µm view	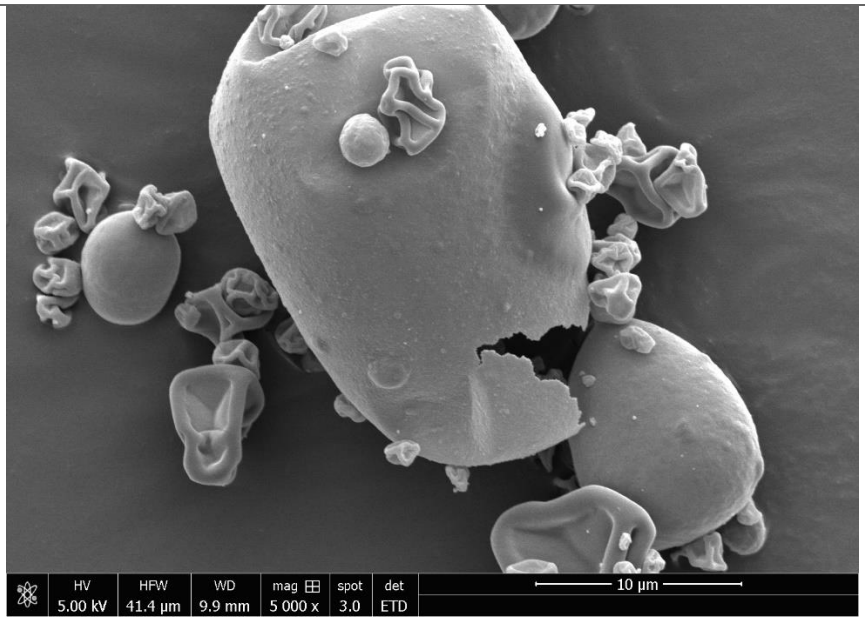

Table 6.6 – Circular Dichroism Analysis

	α-Helix	β-Sheet	Random Coil
Zein – Manufacturer	0.28	0.16	0.55
LCLF	0.44	0.21	0.35
SCHF	0.31	0.10	0.59
High Shear Emulsified/ 2-Fluid Nozzle	0.39	0.19	0.42

Figure 6.1 – Modifications to Stock 3-Fluid Nozzle

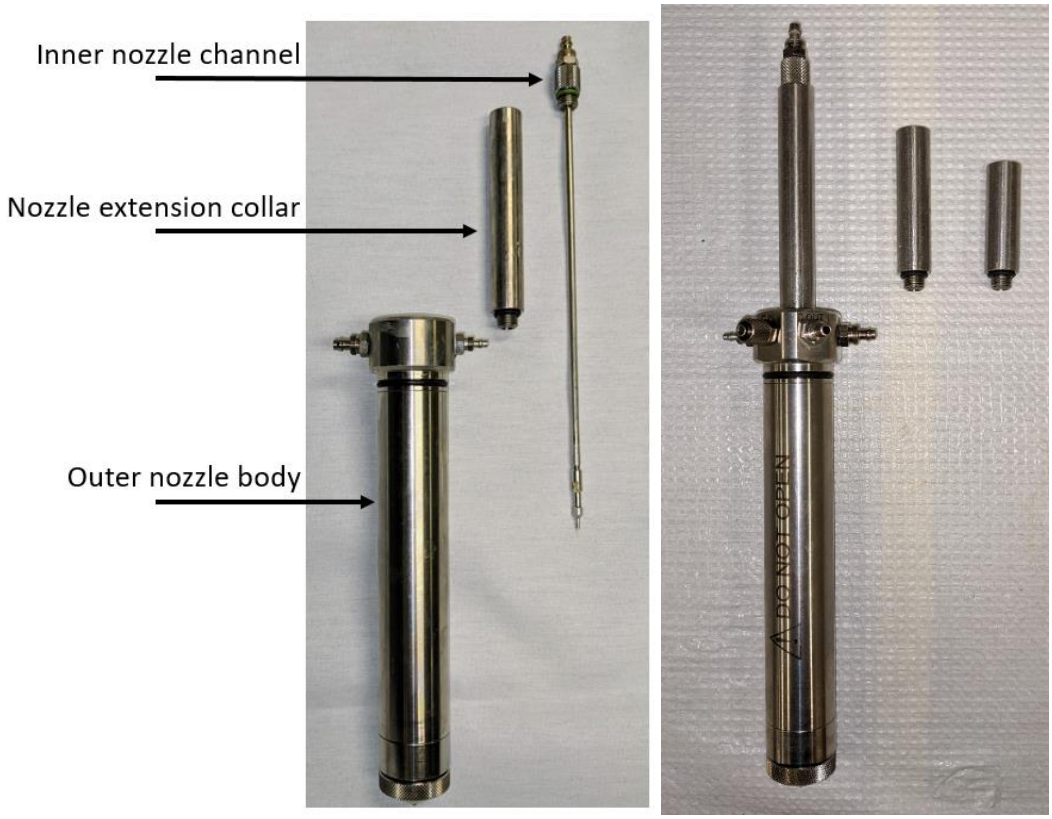

Figure 6.2 – Quercetin/20% Ethanol Standard Curve

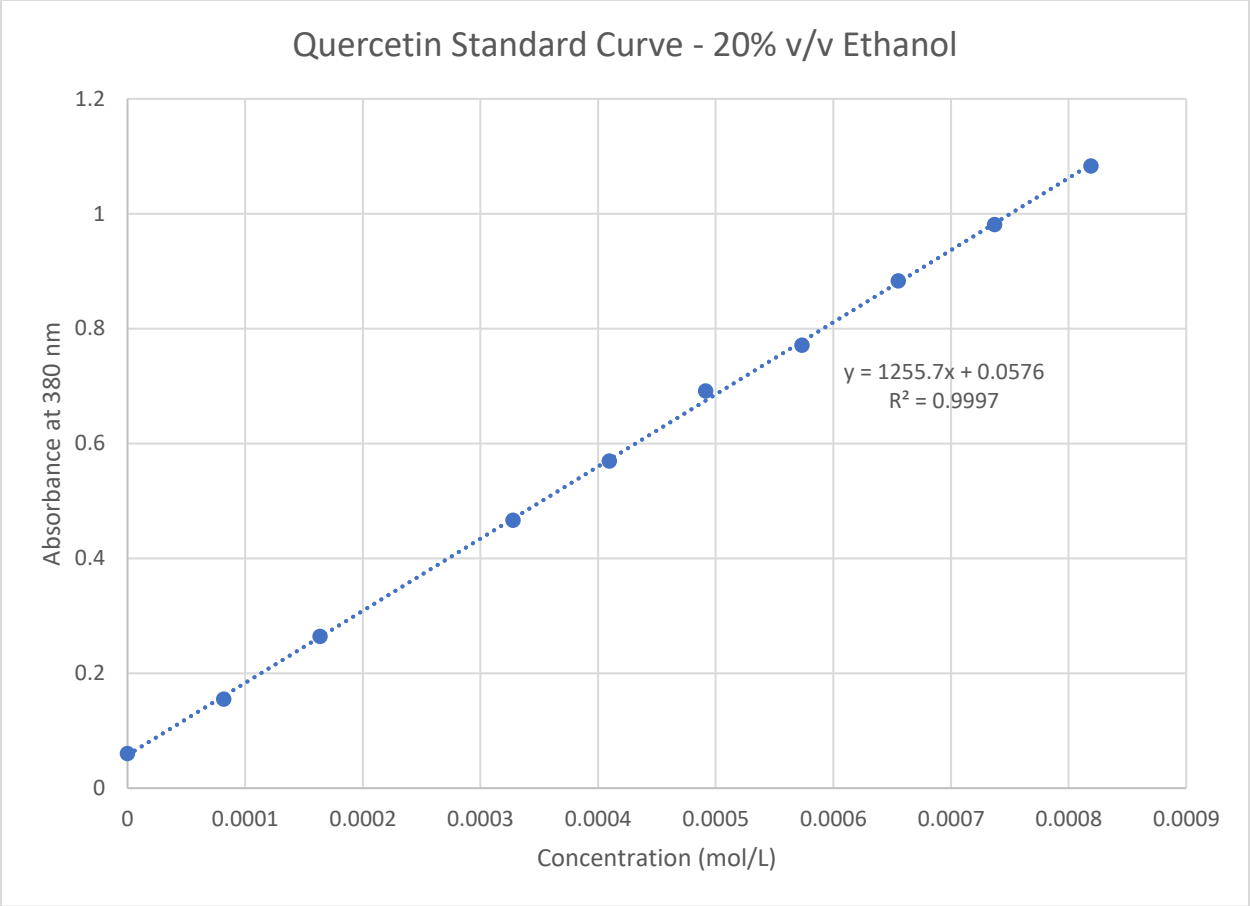

Figure 6.3 – Powder from MCLF Absorbance Curve add axis labels

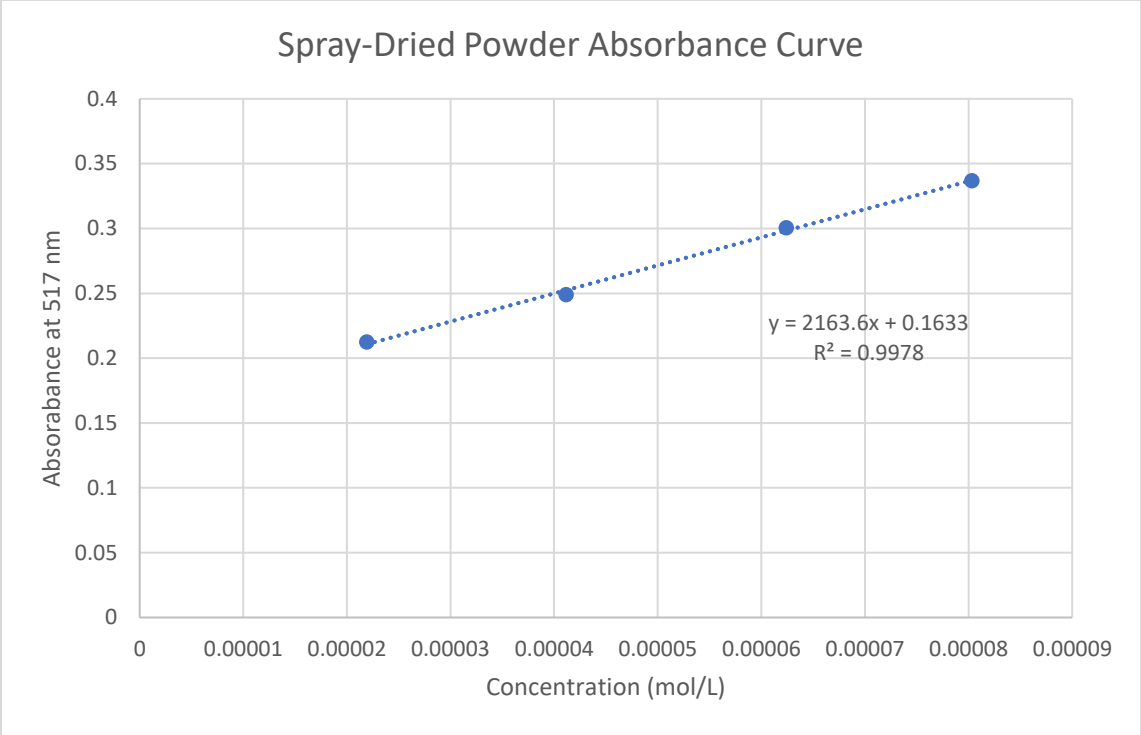

Figure 6.4 – Quercetin Control Absorbance Curve add axis labels

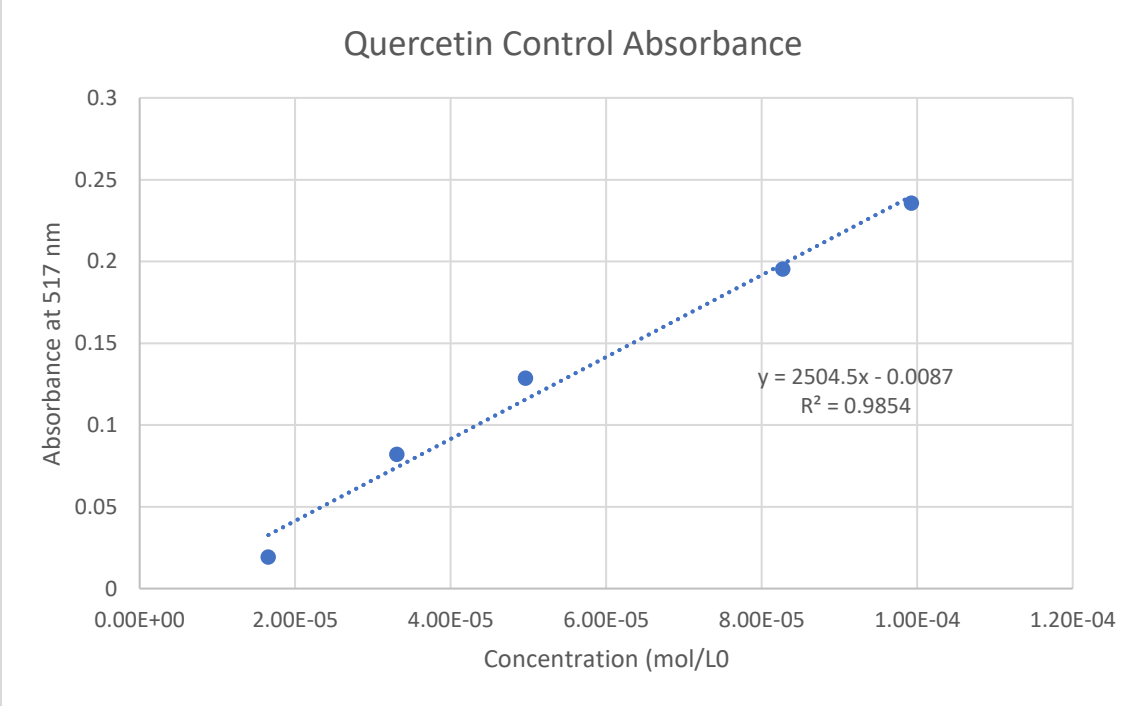

Figure 6.5 – Percent Yield by Treatment

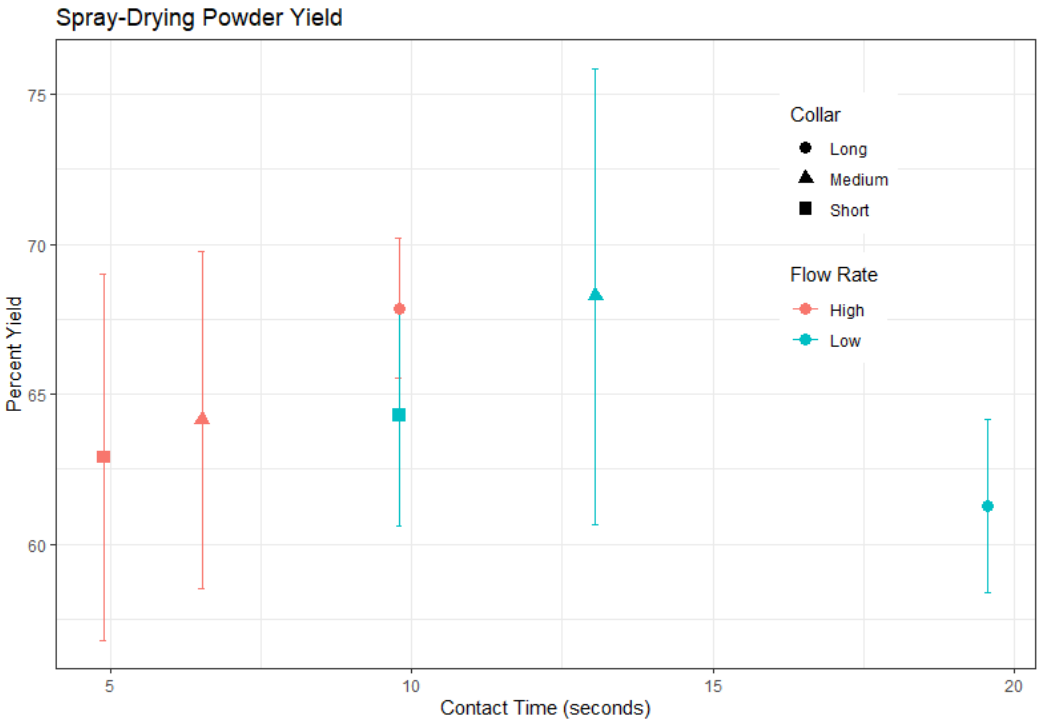

Figure 6.6 – 95% Confidence Interval for Percent Yield by Treatment

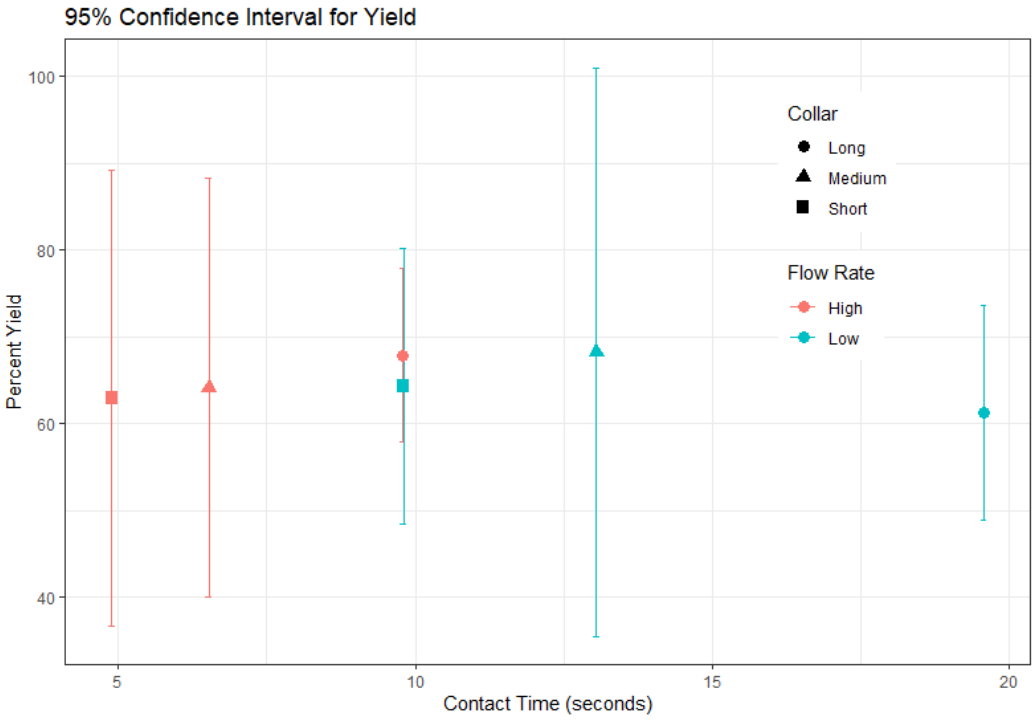

Figure 6.7 – Median Particle Diameter by Treatment

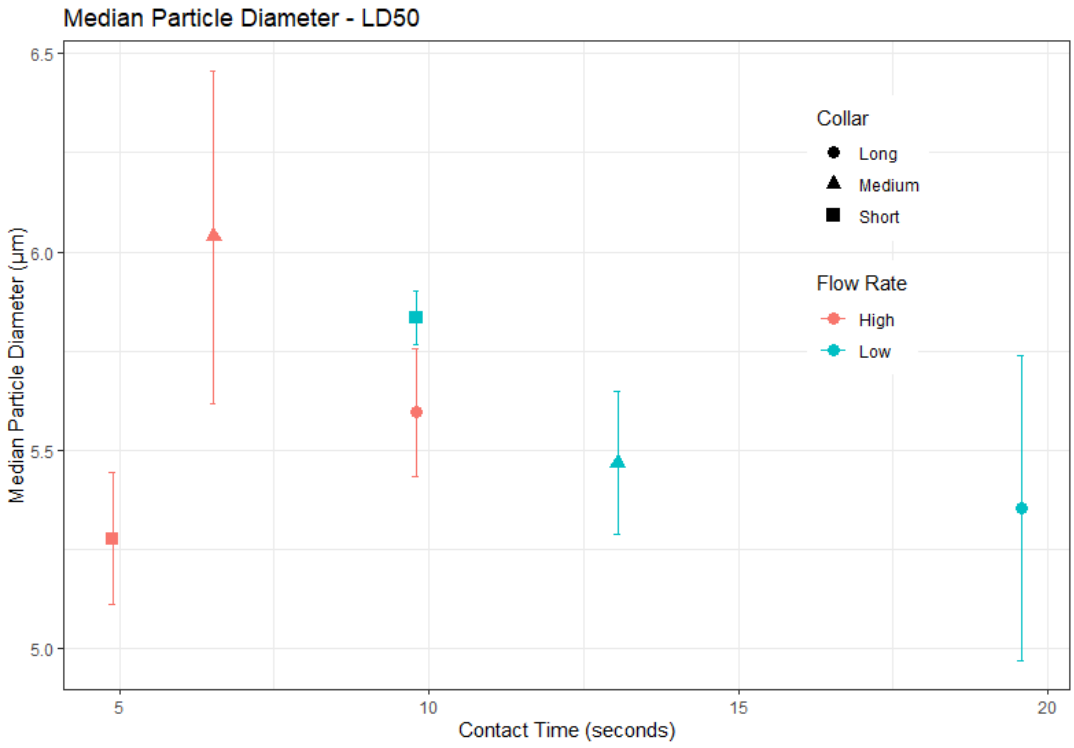

Figure 6.8 – 95% Confidence Interval for Median Particle Diameter

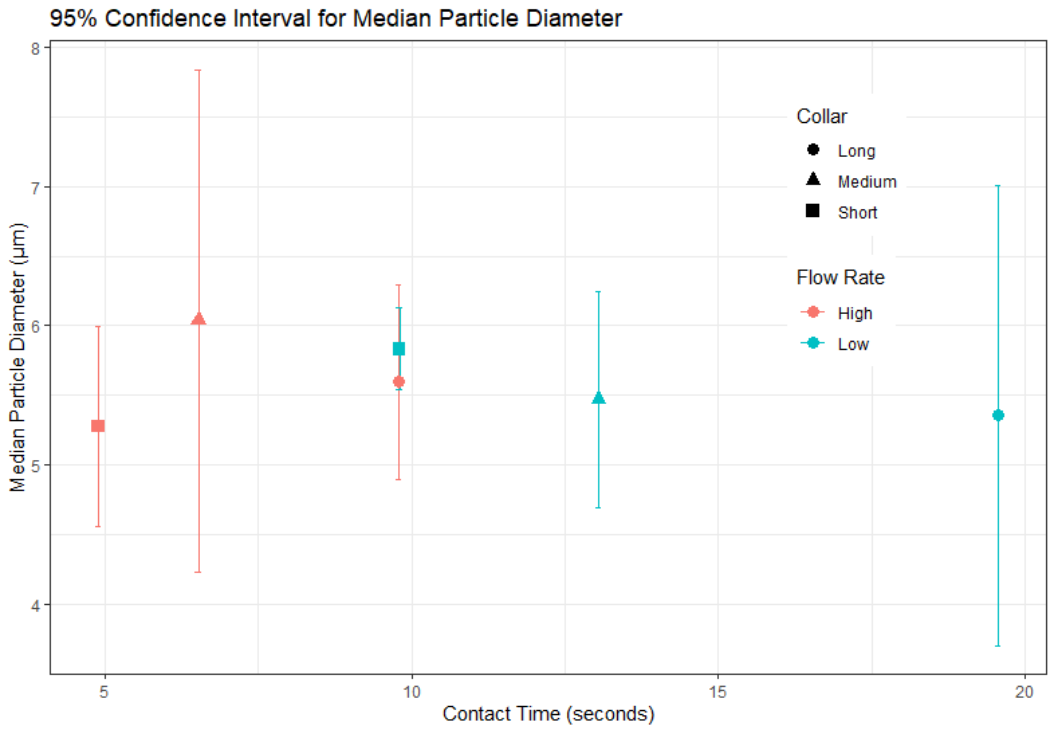

Figure 6.9 – Particle Size IQR by Treatment

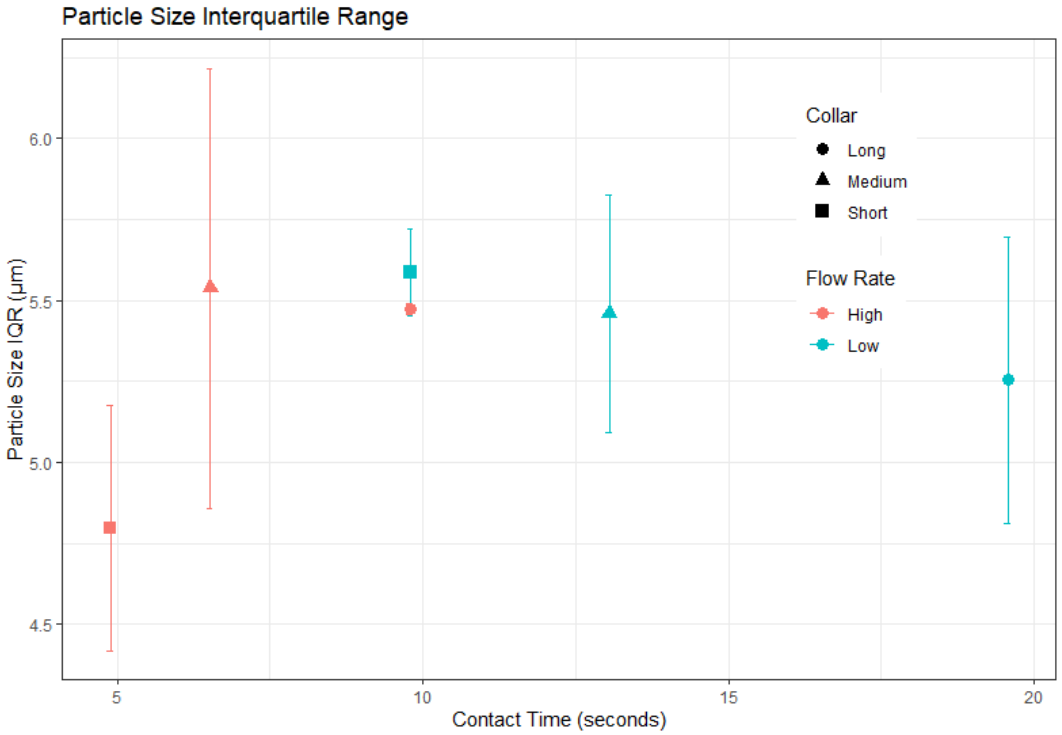

Figure 6.10 – 95% Confidence Interval for Particle Size IQR

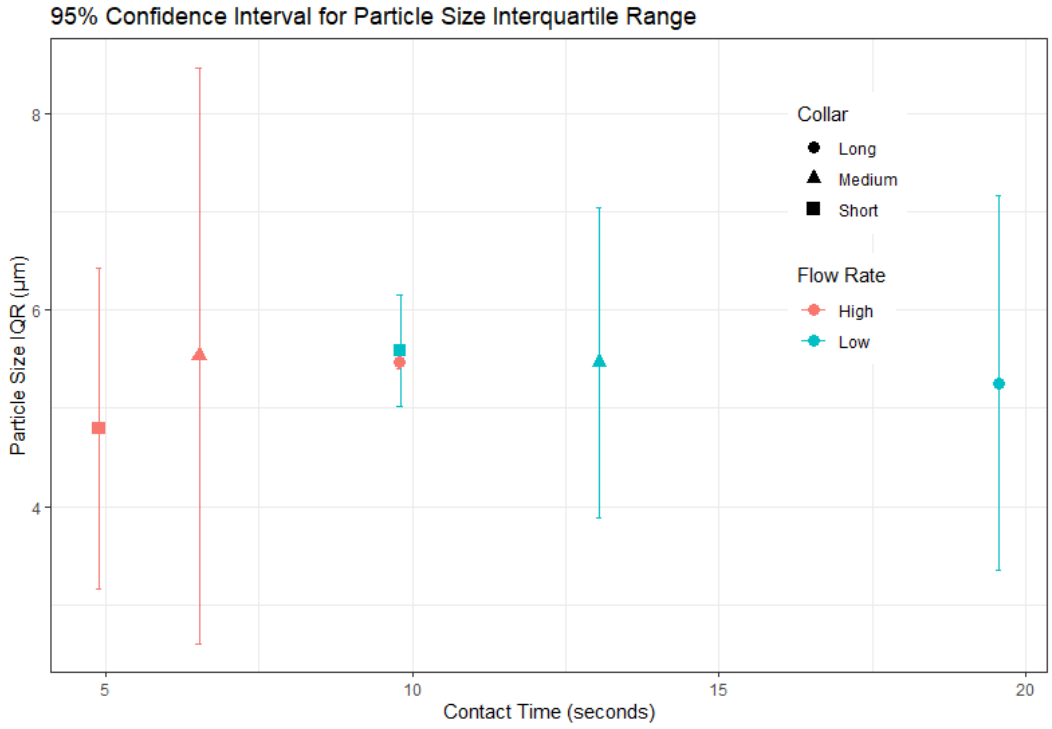

Figure 6.11 – Nozzle Collar Length Effect on Encapsulation Efficiency

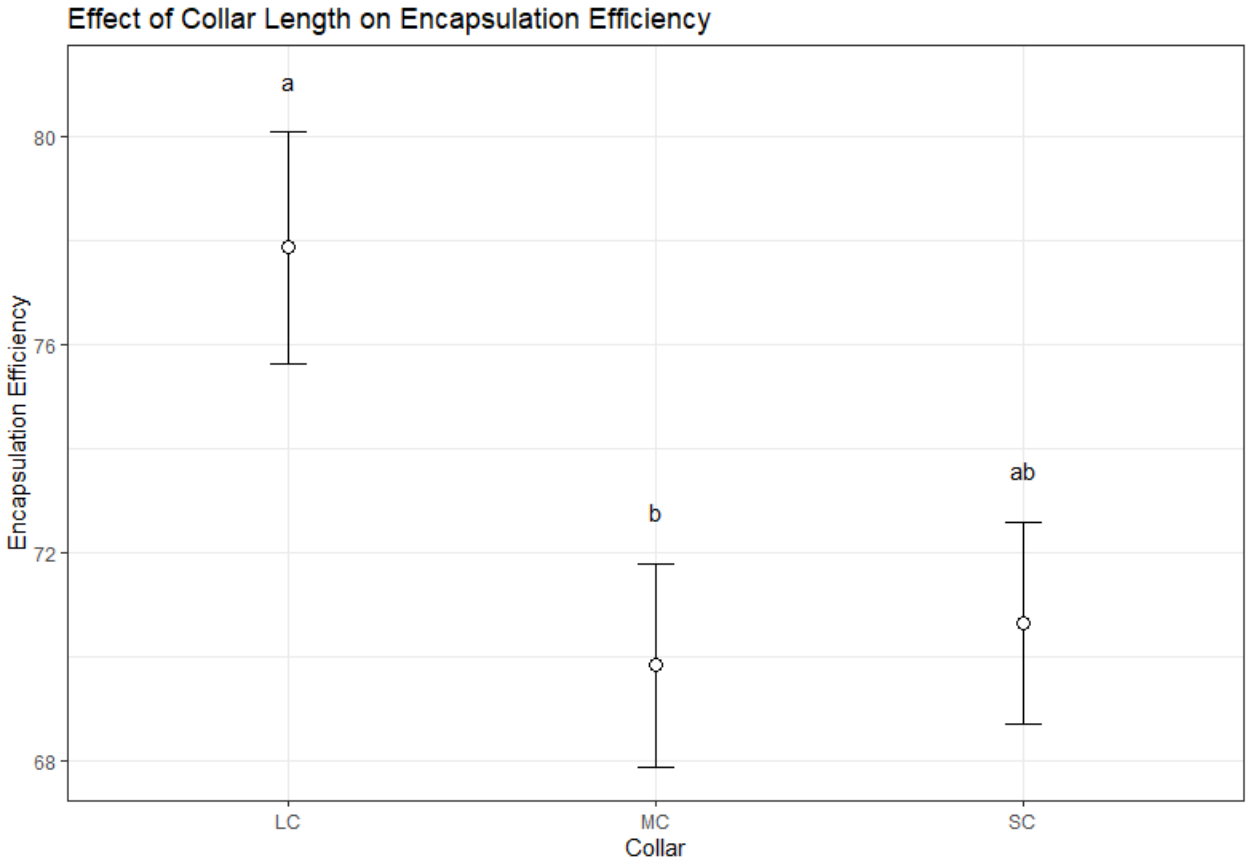

Figure 6.12 – Encapsulation Efficiency by Treatment

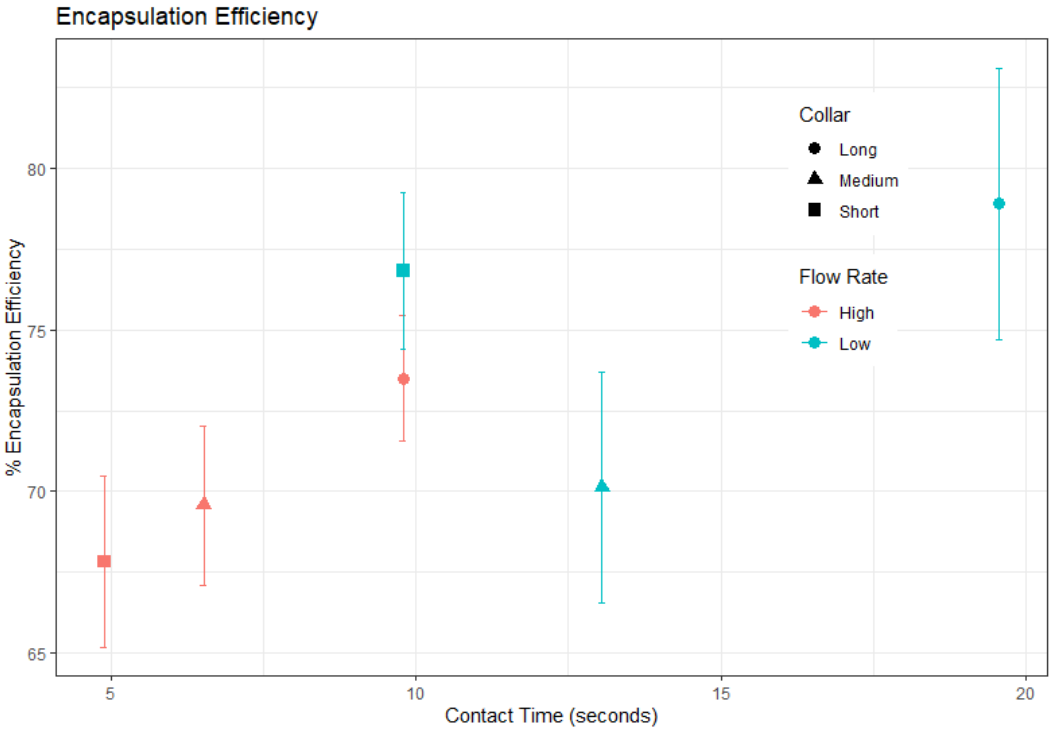

Figure 6.13 – 95% Confidence Interval for Encapsulation Efficiency

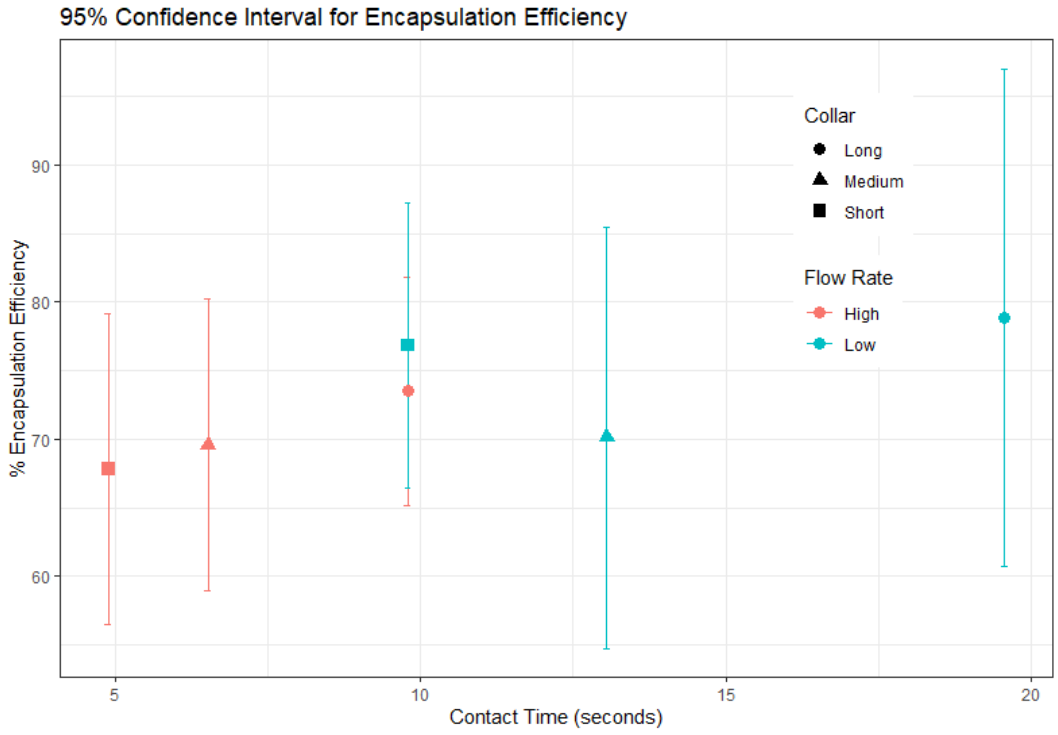

Figure 6.14 – Normalized Antioxidant Capacity by Treatment

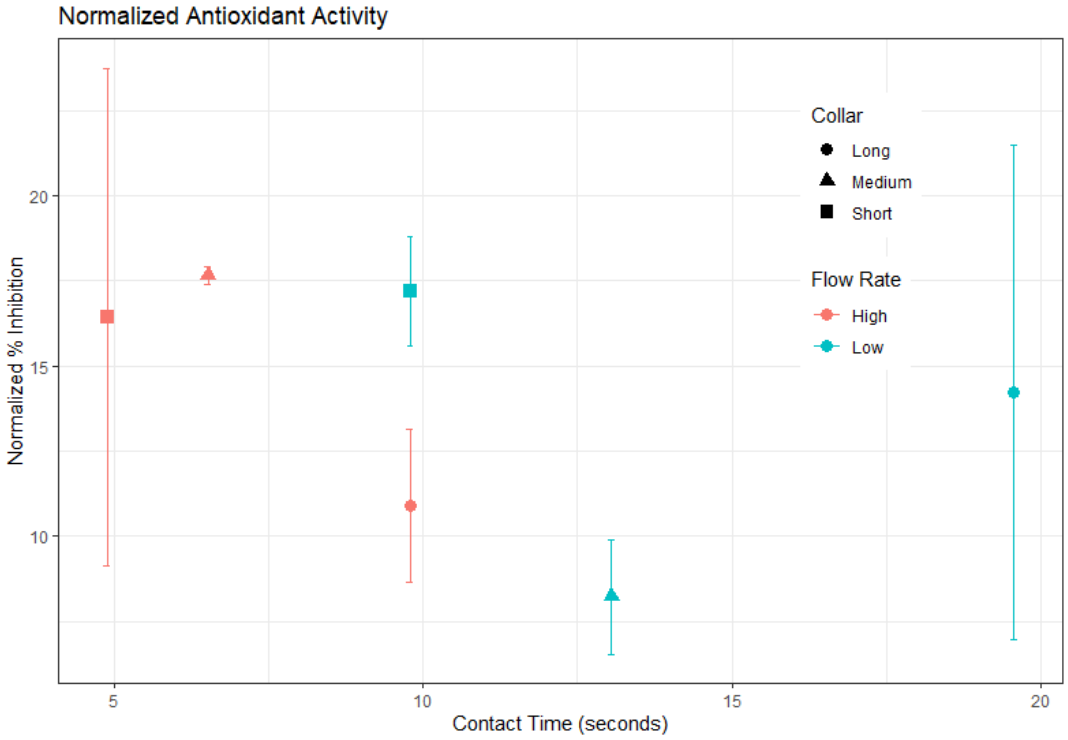

Figure 6.15 – 95% Confidence Interval for Normalized Antioxidant Capacity

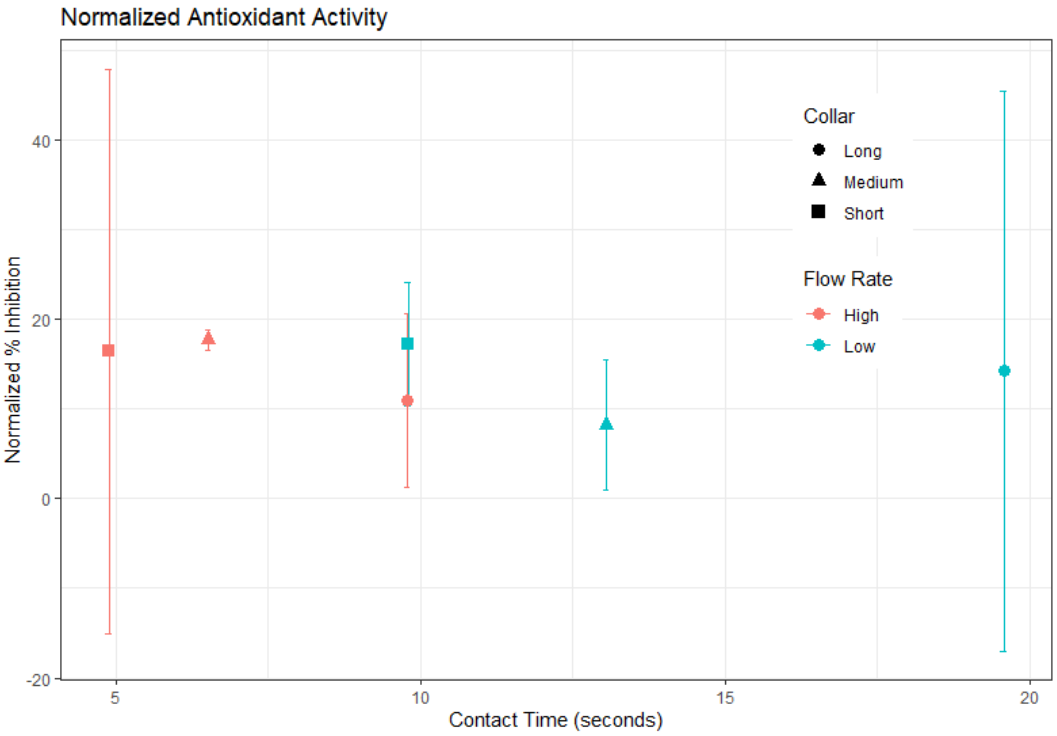

6.7 Raw Statistical Output

6.7.1 – Two-Way ANOVA for Yield

```
Analysis of Variance Table

Response: Yield
            Df Sum Sq Mean Sq F value Pr(>F)
Collar       2  38.20  19.101  0.2482 0.7841
Flow         1  18.40  18.402  0.2391 0.6337
Collar:Flow  2  58.03  29.014  0.3770 0.6937
Residuals   12 923.47  76.956
```

6.7.2 – Two-ANOVA for Yield; No Interaction

```
Analysis of Variance Table

Response: Yield
          Df Sum Sq Mean Sq F value Pr(>F)
Collar     2  38.20  19.101  0.2724 0.7655
Flow       1  18.40  18.402  0.2625 0.6164
Residuals 14 981.49  70.107
```

6.7.3 – One-Way ANOVA for Yield

```
Analysis of Variance Table

Response: Yield
          Df Sum Sq Mean Sq F value Pr(>F)
Treatment  5 114.63  22.926  0.2979 0.9048
Residuals 12 923.47  76.956
```

6.7.4 – Two-Way ANOVA for Median Particle Diameter

```
Analysis of Variance Table

Response: LD50
            Df  Sum Sq Mean Sq F value Pr(>F)
Collar       2 0.30147 0.15073  0.7288 0.5027
Flow         1 0.26523 0.26523  1.2824 0.2796
Collar:Flow  2 0.71614 0.35807  1.7313 0.2185
Residuals   12 2.48183 0.20682
```

6.7.5 – Two-Way ANOVA for Median Particle Diameter; No Interaction

```
Analysis of Variance Table

Response: LD50
          Df Sum Sq Mean Sq F value Pr(>F)
Collar     2 0.3015 0.15073  0.6599 0.5323
Flow       1 0.2652 0.26523  1.1611 0.2994
Residuals 14 3.1980 0.22843
```

6.7.6 – One-Way ANOVA for Median Particle Diameter

```
Analysis of Variance Table

Response: LD50
          Df Sum Sq Mean Sq F value Pr(>F)
Treatment  5 1.2828 0.25657  1.2405 0.3497
Residuals 12 2.4818 0.20682
```

6.7.7 – Two-Way ANOVA for Particle Size Interquartile Range

```
Analysis of Variance Table

Response: LDIQR
            Df Sum Sq Mean Sq F value Pr(>F)
Collar       2 0.4388 0.21941  0.4602 0.6418
Flow         1 0.0352 0.03517  0.0738 0.7905
Collar:Flow  2 0.8265 0.41323  0.8667 0.4451
Residuals   12 5.7212 0.47677
```

6.7.8 – Two-Way ANOVA for Particle Size Interquartile Range; No Interaction

```
Analysis of Variance Table

Response: LDIQR
          Df Sum Sq Mean Sq F value Pr(>F)
Collar     2 0.4388 0.21941  0.4691 0.6350
Flow       1 0.0352 0.03517  0.0752 0.7879
Residuals 14 6.5477 0.46769
```

6.7.9 – One-Way ANOVA for Particle Size Interquartile Range

```
Analysis of Variance Table

Response: LDIQR
          Df Sum Sq Mean Sq F value Pr(>F)
Treatment  5 1.3004 0.26009  0.5455  0.739
Residuals 12 5.7212 0.47677
```

6.7.10 – Two-Way ANOVA for Encapsulation Efficiency

```
Analysis of Variance Table

Response: EE
            Df Sum Sq Mean Sq F value  Pr(>F)
Collar       2 233.55 116.774  4.4122 0.03661 *
Flow         1  36.54  36.540  1.3806 0.26278
Collar:Flow  2  19.95   9.975  0.3769 0.69384
Residuals   12 317.59  26.466
---
Signif. codes:  0 ‘***’ 0.001 ‘**’ 0.01 ‘*’ 0.05 ‘.’ 0.1 ‘ ’ 1
```

6.7.11 – Mean Separation for Collar Effect

```
Results are averaged over the levels of: Flow
Confidence level used: 0.95
Conf-level adjustment: sidak method for 3 estimates

$contrasts
 contrast estimate   SE df t.ratio p.value
 LC - MC     7.533 2.86 14  2.632  0.0487
 LC - SC     6.716 2.86 14  2.347  0.0818
 MC - SC    -0.817 2.83 14 -0.288  0.9554

Results are averaged over the levels of: Flow
P value adjustment: tukey method for comparing a family of 3 estimates
```

6.7.12 – One-Way ANOVA for Encapsulation Efficiency

```
Analysis of Variance Table

Response: EE
          Df Sum Sq Mean Sq F value Pr(>F)
Treatment  5 288.60  57.721  2.1711 0.1259
Residuals 12 319.03  26.586
```

6.7.13 – Two-Way ANOVA for Antioxidant Capacity (%Inhibition)

```
Analysis of Variance Table

Response: AOCMN
            Df Sum Sq Mean Sq F value Pr(>F)
Collar       2  24.74  12.371  0.2122 0.8117
Flow         1 160.80 160.802  2.7589 0.1226
Collar:Flow  2  31.81  15.904  0.2729 0.7658
Residuals   12 699.43  58.286
```

6.7.14 – Two-Way ANOVA for Antioxidant Capacity; No Interaction

```
Analysis of Variance Table

Response: AOCMN
          Df Sum Sq Mean Sq F value Pr(>F)
Collar     2  24.74  12.371  0.2368 0.7922
Flow       1 160.80 160.802  3.0787 0.1012
Residuals 14 731.23  52.231
```

6.7.15 – One-Way ANOVA for Antioxidant Capacity

```
Analysis of Variance Table

Response: AOCMN
          Df Sum Sq Mean Sq F value Pr(>F)
Treatment  5 217.35  43.470  0.7458 0.6044
Residuals 12 699.43  58.286
```

6.8 References

[1] M. Lesjak, I. Beara, N. Simin, D. Pintać, T. Majkić, K. Bekvalac, D. Orčić and N. Mimica-Dukić, "Antioxidant and anti-inflammatory activities of quercetin and its derivatives," *Journal of Functional Foods,* vol. 40, pp. 68-75, 2018.

[2] M. Palma, P. Robert, F. Holgado, J. Velasco and G. Márquez-Ruiz, "Antioxidant Activity and Kinetics Studies of Quercetin, Epicatechin and Naringenin in Bulk Methyl Linoleate," *JAOCS, Journal of the American Oil Chemists' Society,* vol. 94, no. 9, pp. 1189-1196, 1 9 2017.

[3] S. G. Darband, M. Kaviani, B. Yousefi, S. Sadighparvar, F. G. Pakdel, J. A. Attari, I. Mohebbi, S. Naderi and M. Majidinia, *Quercetin: A functional dietary flavonoid with potential chemo-preventive properties in colorectal cancer,* vol. 233, Wiley-Liss Inc., 2018, pp. 6544-6560.

[4] S. G. Darband, S. Sadighparvar, B. Yousefi, M. Kaviani, F. Ghaderi-Pakdel, A. Mihanfar, Y. Rahimi, K. Mobaraki and M. Majidinia, "Quercetin attenuated oxidative DNA damage through NRF2 signaling pathway in rats with DMH induced colon carcinogenesis," *Life Sciences,* vol. 253, p. 117584, 15 7 2020.

[5] Y. Guo and R. S. Bruno, "Endogenous and exogenous mediators of quercetin bioavailability," *Journal of Nutritional Biochemistry,* no. 26, pp. 201-210, 2015.

[6] S. Dall'acqua, G. Miolo, G. Innocenti and S. Caffieri, "The Photodegradation of Quercetin: Relation to Oxidation," *Molecules,* vol. 17, pp. 8898-8907, 2012.

[7] A. Drewnowski and C. Gomez-Carneros, "Bitter taste, phytonutrients, and the consumer: a review," *The American Journal of Clinical Nutrition,* vol. 72, no. 6, pp. 1424-, 2000.

[8] J. Azzi, A. Jraij, L. Auezova, S. Fourmentin and H. El Ene Greige-Gerges, "Novel findings for quercetin encapsulation and preservation with cyclodextrins, liposomes, and drug-in-cyclodextrin-in-liposomes," *Food Hydrocolloids,* no. 81, pp. 328-340, 2018.

[9] H. Li, D. Wang, C. Liu, J. Zhu, M. Fan, X. Sun, T. Wang, Y. Xu and Y. Cao, "Fabrication of stable zein nanoparticles coated with soluble soybean polysaccharide for encapsulation of quercetin," *Food Hydrocolloids,* vol. 87, pp. 342-351, 1 2 2019.

[10] D. Xiao, P. M. Davidson and Q. Zhong, "Spray-Dried Zein Capsules with Coencapsulated Nisin and Thymol as Antimicrobial Delivery System for Enhanced Antilisterial Properties," *Journal of Agricultural and Food Chemistry,* vol. 59, no. 13, pp. 7393-7404, 13 7 2011.

[11] Y. Feng, L. Alberto Ibarra-Sánchez, L. Luu, M. J. Miller and Y. Lee, "Co-assembly of nisin and zein in microfluidics for enhanced antilisterial activity in Queso Fresco," *LWT - Food Science and Technology,* vol. 111, pp. 355-362, 2019.

[12] M. Veneranda, Q. Hu, T. Wang, Y. Luo, K. Castro and J. M. Madariaga, "Formation and characterization of zein-caseinate-pectin complex nanoparticles for encapsulation of eugenol," *LWT - Food Science and Technology,* vol. 89, pp. 596-603, 2017.

[13] F. Zhang, M. Aslam Khan, H. Cheng and L. Liang, "Co-encapsulation of α-tocopherol and resveratrol within zein nanoparticles: Impact on antioxidant activity and stability," *Journal of Food Engineering,* vol. 247, pp. 9-18, 2019.

[14] M. A. Andrade, P. Chacón, J. J. Merelo and F. Morán, "Evaluation of secondary structure of proteins from uv circular dichroism spectra using an unsupervised learning neural network," *Protein Engineering, Design and Selection,* vol. 6, no. 4, pp. 383-390, 6 1993.

[15] L. Whitmore and B. A. Wallace, "DICHROWEB, an online server for protein secondary structure analyses from circular dichroism spectroscopic data".

[16] L. Whitmore and B. A. Wallace, "Protein Secondary Structure Analyses from Circular Dichroism Spectroscopy: Methods and Reference Databases," 2007.

CHAPTER 7 – SUMMARY

The proposed 3-fluid nozzle design successfully produced spray-dried microencapsulated quercetin. The powder samples had consistently small median particle diameter (~5 µm) with a small distribution relative to traditional spray-drying approaches. Quercetin was encapsulated at between 70%-80% efficiency, and retained ~80% of the function of the control. Contact time did not have a meaningful effect on the physicochemical characteristics of the spray-dried microcapsules, at least at the range of contact times tested in this study.

The nozzle simulation chip designed for this study was able to produce nano-scale zein particles (170 nm – 200 nm) with narrow particle size distributions (PDI < 0.2). The operating parameters explored the simulation chip did have a significant effect on the size and distribution of the nanoparticle suspensions, indicating the simulation chip could be a useful tool for high throughput production of encapsulated nanoparticles. The self-assembly properties of zein, especially when stabilized with sodium caseinate, proved to be excellent for encapsulation throughout the entirety of this study.

The work done in these experiments was a preliminary test of a newly proposed design, and represents only a small part of the validation required to determine whether or not the technology can and should be adopted at scale. Repeated experiments with the model system described in this study should be done to ascertain if there is a limit of contact time that does induce alterations to the physical characteristics of the spray-dried powder. Specifically, both no-contact time (no collar) testing with the 3-fluid nozzle

should be done, along with even longer collar trials to determine whether or not the range tested in this study was sufficient or not.

Furthermore, other encapsulated systems should be tested with the same nozzle technology to determine its efficacy with other core/shell systems. Simple and complex coacervation should both be attempted to see if the laminar flow regimes present during the contact time within the nozzle are sufficient for producing microcapsules via these methods. Other macromolecular compounds (starches, lipids) should be tested as wall materials, as zein does represent an ideal case for self-assembly during anti-solvent precipitation conditions.

With regards to the quercetin model system, *in vitro* kinetics test via simulation digestion should be performed to ascertain whether or not quercetin's bioavailability to the colon is actually increased via encapsulation and to what degree, if any, the quercetin loading effects this. If the *in vitro* tests confirm a controlled release profile, animal models with induced oncogenesis in the colon should be considered as well. Spray-dried quercetin microcapsules should also be incorporated into a model food matrix and tested with subsequent consumer sensory tests to validate any difference in liking with encapsulated versus pure quercetin.

Overall, this study confirms that the proposed nozzle design may have implications for food manufacturers interested in encapsulation. There is a potential benefit to the global food system as a result of the increased ability to fortify foods with nutritional or therapeutic ingredients. The ease of adopting the proposed nozzle design into existing spray-drying operations makes it an excellent candidate for further research.